Definition of a Sensitivity Profile for Drug Treatment and Identification on Clinical Biomarkers in Atrial Fibrillation

Universitat Politècnica de València
Programa de Doctorado en
Tecnologías para la Salud y el Bienestar
Tesis Doctoral
Mayo 2022

Autora:
Ana María Sánchez de la Nava

Dirigida por:
Dr. Felipe Atienza Fernández
Dr. Francisco Jesús Fernández-Avilés
Dra. María de la Salud Guillem Sánchez

Agradecimientos

"Have no fear of perfection, you'll never reach it" – Salvador Dalí

Esta tesis no podría haber sido posible la inestimable ayuda del Dr. Fernández-Avilés, el Dr. Atienza y la Dra. Guillem. Me gustaría hacer una mención especial al Dr. Fernández-Avilés y al Dr. Atienza, que además de dirigir y perfilar la tesis, han perfilado el carácter inquieto y curioso con el que entré en el hospital hasta lograr (creo yo) un carácter persistente y paciente al que todavía le queda mucho por aprender.

Una tesis que con la que han tenido que convivir las personas más cercanas a mí, mi red de seguridad. Personas como mis padres y mi hermana, que con amor y paciencia infinitas han avanzado conmigo de la mano, incluso en la más absoluta invisibilidad, para que yo pudiera experimentar la maravilla de hacer las cosas por mí misma pero que, al mínimo atisbo de caída, me han cogido al vuelo. Gracias, gracias y gracias, nunca podré devolveros la mínima parte de lo que habéis hecho, y sé que seguiréis haciendo por mí.

Una tesis que no es solo mía, sino de todos los que, a nivel profesional y personal me han ayudado a que llegase a la meta, que han escuchado pacientemente cuando las cosas iban bien, pero sobre todo cuando ha habido que enfrentar algún que otro fracaso. Gracias Lidia, Ana, Toni, Moni y Gonzalo. I would also like to thank all the people that I have met in conferences and summer courses that have enriched, not only my vision of the research field, but also have contributed to my own personal growth.

Una tesis en la que todavía se atisban los sentimientos de una niña que entendió desde pequeña por qué se necesitaba tanto la investigación. Una niña que vio fortaleza, sufrimiento y tesón en las mujeres de su vida. Una niña que todavía existe y que intenta recordar, siempre que puede, a las tres mujeres más fuertes que ha conocido además de su madre. Abuela Antonia, Abuela Virginia y Tía Izarra, siento no haber llegado a tiempo para que podáis ver la mujer en la que me he convertido hoy. Espero que estéis orgullosas allá dónde estéis.

Resumen

La fibrilación auricular (FA) es una de las arritmias más comunes en la práctica clínica cuyos mecanismos, hasta ahora, no han sido comprendidos en su totalidad. El estudio de dichos mecanismos mediante el estudio de la información clínica, la metodología de estudios computacionales y los algoritmos de inteligencia artificial (IA) que permiten la identificación de nuevos patrones para la personalización de los tratamientos es clave para desvelar las características de la arritmia.

Actualmente, el tratamiento de preferencia para los pacientes con FA que ha presentado mayores ratios de efectividad ha sido la ablación cardiaca. Este procedimiento invasivo utiliza un catéter para quemar el área del tejido cardiaco que es responsable del mantenimiento de la arritmia. Para poder identificar dicha área, es indispensable realizar un estudio electrofisiológico para evaluar las señales eléctricas intracavitarias.

En el campo de las simulaciones por ordenador, varios estudios han presentado abordajes personalizados que intentan establecer una plataforma complementaria para la planificación de la ablación. En este ámbito, la electrocardiografía por imagen se ha utilizado para la estratificación y caracterización previa de pacientes antes del procedimiento de ablación.

Finalmente, los estudios observacionales clínicos permiten la caracterización de la población de FA, ayudando a recoger, no solo datos electrofisiológicos, sino también biomarcadores clínicos directamente relacionados con la prognosis del paciente.

Dada toda la información producida durante este tipo de estudios, la IA se ha introducido paulatinamente en este tipo de estudios con el objetivo de identificar patrones o biomarcadores que permitan caracterizar a estos pacientes incluyendo toda la información recogida. Además, los algoritmos de predicción, que permiten estimar el éxito del tratamiento y la prognosis del paciente, han sido desarrollados. Debido a todas estas razones, estos campos han sido estudiados durante el desarrollo de este trabajo.

En primer lugar, se realizaron simulaciones por ordenador utilizando una población de modelos que permitía evaluar la inducibilidad y mantenimiento de la arritmia en diferentes escenarios. Teniendo en cuenta la gran cantidad de datos derivados de las simulaciones, que incluían la variabilidad introducida en la población y diferentes fármacos, se implementaron algoritmos de IA que extrajeron patrones de los perfiles más proarrítmicos.

En segundo lugar, se realizaron simulaciones personalizadas en una cohorte de pacientes, incluyendo las anatomías de las aurículas y considerando diferentes escenarios arrítmicos. Estos experimentos se realizaron con una carga computacional menor comparado con otros estudios y permitieron identificar un biomarcador obtenido de dichos datos que caracterizaba la actividad en la zona de las venas pulmonares y la comparaba con la evolución del paciente 12 meses tras el procedimiento de ablación.

Finalmente, se analizó el estudio observacional STRATIFY-AF utilizando la información obtenida del ECGi y combinándola con datos clínicos. Como resultado, se obtuvo un *score* electrofisiológico que permite predecir el tratamiento más exitoso para cada paciente.

Los resultados presentados en esta tesis ilustran un claro ejemplo de combinación de diferentes tecnologías, como las simulaciones *in silico*, con datos clínicos y algoritmos de IA, que pueden ser de gran utilidad para investigar los mecanismos de la arritmia cardiaca.

Resum

La fibril·lació auricular (FA) és una de les arítmies més comunes. En la pràctica clínica els mecanismes de la qual, fins ara, no han sigut compresos en la seua totalitat. L'estudi dels dits mecanismes per mitjà de l'estudi de la informació clínica, la metodologia d'estudis computacionals i els algoritmes d'intel·ligència artificial (IA) que permeten la identificació de nous patrons per a la personalització dels tractaments és clau per a desvelar les característiques de l'arítmia.

Actualment, el tractament de preferència per als pacients amb FA que ha presentat majors ràtios d'efectivitat ha sigut l'ablació cardíaca. Este procediment invasiu utilitza un catèter per cremar l'àrea del teixit cardíac que és responsable del manteniment de l'arítmia. Per a poder identificar la dita àrea, és indispensable realitzar un estudi electrofisiologia per a avaluar els senyals elèctrics intracavitarias.

En el camp de les simulacions per ordinador, diversos estudis han presentat abordatges personalitzats que intenten establir una plataforma complementària per a la planificació de l'ablació. En este àmbit, l'electrocardiografia per imatge s'ha utilitzat per a l'estratificació i caracterització prèvia de pacients abans del procediment d'ablació.

Finalment, els estudis observacionals clínics permeten la caracterització de la població de FA, ajudant a arreplegar, no sols dades electrofisiològiques, sinó també biomarcadores clínics directament relacionats amb la prognosi del pacient.

Donada tota la informació produïda durant este tipus d'estudis, la IA s'ha introduït gradualment en este tipus d'estudis amb l'objectiu d'identificar patrons o biomarcadores que permeten caracteritzar estos pacients incloent tota la informació arreplegada. A més, els algoritmes de predicció, que permeten estimar l'èxit del tractament i la prognosi del pacient, han sigut desenrotllats. A causa de totes estes raons, estos camps han sigut estudiats durant el desenrotllament d'este treball.

En primer lloc, es van utilitzar simulacions per ordinador utilitzant una població de models que permetia avaluar la inducibilidad i manteniment de l'arítmia en diferents escenaris. Donada la variabilitat introduïda en la població, en combinació amb diferents fàrmacs, els algoritmes d'IA es van utilitzar per a extraure patrons que identificaven els perfils més proarítmics.

En segon lloc, es van realitzar simulacions personalitzades en una cohort de pacients, incloent les anatomies de les aurícules i considerant diferents escenaris arítmics. Estos experiments es van realitzar amb una

càrrega computacional menor comparat amb altres estudis i van permetre identificar un biomarcador obtingut de les dits dades que caracteritzava l'activitat en la zona de les venes pulmonars i la comparava amb l'evolució del pacient 12 mesos després del procediment d'ablació.

Finalment, l'estudi observacional STRATIFY-AF es va analitzar utilitzant la informació obtinguda de l'ECGi i combinant-la amb dades clíniques. Com resultat, es va obtindre un score electrofisiològic que permet predir el tractament més reeixit per a cada pacient.

Els resultats presentats en esta tesi il·lustren, per tant, que la combinació de les tecnologies in silico, junt amb les dades clíniques i el processament de dades disponibles gràcies als algoritmes d'IA poden ser de gran utilizar per a investigar els mecanismes de l'arítmia cardíaca.

Abstract

Atrial Fibrillation (AF) is one of the most common arrhythmias in clinical practice and thus far, the electrophysiological mechanisms underlying its initiation and maintenance are not fully understood. The study of such mechanism including clinical information, computational models and artificial intelligence (AI) algorithms that enable the identification of new patterns for the personalization of the treatments is key to unveil the characteristics of the arrhythmia.

At the present, the treatment of choice for AF patients with higher effectiveness has proved to be cardiac ablation. This invasive procedure uses a catheter to ablate or burn the area of the cardiac tissue that is responsible for the maintenance of the arrhythmia. In order to find this specific area, it is indispensable to perform an electrophysiological study to evaluate the intracavitary electrical signals.

In the computational field, several studies have presented personalized approaches that aim to stablish a complimentary platform for ablation planning. In this area, electrocardiographic imaging has also been used for the stratification and prior characterization of patients before the ablation procedure.

Finally, observational studies enable the characterization of the AF population, enabling to collect, not only electrophysiological data but clinical biomarkers that can be related with the prognosis of the patients.

Due to all the information produced during this type of studies, AI has been recently incorporated into these studies, with the main objective of identifying patterns or biomarkers that are able to characterize these patients including all the collected information. In addition, prediction algorithms, that allow to estimate the success of the treatment and prognosis of the patient have also been developed. For this purpose, these three fields of study were explored in this thesis.

First, computational simulations using a population of models were performed to evaluate arrhythmia inducibility and maintenance under different scenarios. Due to the variability introduced in the population of models in combination with different drugs, AI algorithms were applied to extract patterns that identified the most proarrhythmic profiles.

Secondly, personalized simulations were performed in a cohort of patients including their anatomical cardiac geometries and considering different arrhythmic scenarios. These experiments were achieved with a lowered computational costs and included the identification of a biomarker extracted

from the simulation analysis that characterized the activity in the pulmonary vein area and evaluating it with the 12-month ablation outcome.

Finally, the STRATIFY-AF observational study was analyzed, using the ECGi information from the patients combined with clinical information. As a results, a stratification score was obtained to predict the most successful treatment for each of the patients.

The results presented in this thesis illustrate that the combination of in silico technologies with clinical data and processing algorithms can be of great utility to further investigate the arrhythmic mechanisms.

List of abbreviations

AF   Atrial Fibrillation

AP   Action Potential

BSPM   Body Surface Potential Mapping

DF   Dominant Frequency

ECG   Electrocardiogram

ECGi   Electrocardiographic imaging

HDF   Highest dominant frequency

LA   Left atrium

MRI   Magnetic Resonance Imaging

PVI   Pulmonary Vein Isolation

SR   Sinus Rhythm

List of Figures

List of Tables

Index

Chapter 1.
Introduction

Digital Health has disrupted the actual panorama by introducing and establishing technology as one of the most useful and rapidly developing tools in the last decade, including a remarkable influence in health applications. These technologies, that are based on computing platforms, connectivity, software and sensors for health care related uses, are giving a more holistic view of patient health through access to data and allowing patients to have more control over their health.

Modern medicine has, therefore, evolved incorporating more and more technologies in analysis, diagnosis and treatment decisions. These incorporations include the merging of clinicians with engineers and basic computational experts, improving data access, reducing costs and incrementing overall efficacy, that will ultimately increase quality and personalisation at medical level.

In the last years, the outbreak of Artificial Intelligence (AI) has helped to include prediction algorithms that assist clinician's decisions, collecting and interpreting relations in digitalized clinical records that can reveal hidden information for the clinician.

Cardiology has been one of the medical fields where digital health applications are playing a crucial role, not only with the use of wearable technologies but also in relation to clinical applications. In this field, electrophysiology has been on the cutting edge of advanced digital technologies for many years (Tarakji et al., 2020). This field has benefited from the use of wireless ECG recordings, implantable loop recorders, cardiac implantable electronic devices with Bluetooth capability and virtual or mixed reality tools at electrophysiology laboratories.

Electrophysiological studies analyzed the electrical activity of the heart, that when presenting abnormalities or disturbances in propagation, originates an arrhythmia. Among all the different arrhythmias, Atrial Fibrillation (AF) is the most frequent arrhythmia with a high prevalence, around 2% of the total adult population. In addition, currently there is no broad consensus on the nature of the mechanisms that initiate and sustain this cardiac arrhythmia. Therefore, the available treatments either pharmacological or interventional do not have the expected success considering the magnitude of this deleterious arrhythmia. In this thesis, two different characterization workflows are evaluated and AI is applied specifically for characterizing, diagnosing and treating AF.

1.1. Motivations

In the last five years, AI has been exponentially implemented and used at clinical level for data analysis, merging and combining information from both clinical records, electrical signals and general characteristics of the patients. In addition, other applications have been found to improve automatized processes management (image processing and segmentation, filtering and denoising of signals, etc).

Since a large amount of data is critical for the accurate performance of these algorithms, efforts have been made to include *in silico* simulations on training sets to reduce or resemble their adjustment patterns.

Moreover, data quality is key for the good performance of these algorithms, therefore different implementations have been tested and limitations have been identified to improve their clinical application.

1.2. Objectives

The driven goal of the present thesis is to explore the application of Artificial Intelligence in Cardiology and, more specifically, in the AF area.

To achieve this goal, the following specific objectives were designed:

1. To study and evaluate the evaluation of AF maintenance under the effect of different drugs, implementing *in silico* models in two different size planes using an electrophysiological model that includes ionic level description..

2. To study and evaluate the pulmonary vein ablation efficacy implementing *in silico* models in 3D personalized geometries using an activation pattern model.

3. To identify a predictive biomarker or a combination of them from the in silico data obtained from the aforementioned objectives that

enable to predict AF maintenance or termination and that relate to clinical scenarios.

4. To evaluate the performance of clinical data from the Stratify-AF study to train clustering algorithms that allow to identify similar groups of patients with similar outcome

5. To assess and define the biomarkers that describe the sensitivity profile by analyzing the overall results of the experiments performed from a translational point of view, that combines in silico computational data and clinical data to explore the electrophysiological biomarkers that characterize AF mechanisms.

1.3. Structure of the thesis

This thesis is structured attending to three fundamental pillars that will guide the reader through the document. These three pillars are the data source for the study, the type of trial design and the artificial intelligence analysis, that when combined, result in the workflow observed in Figure 1.1.

Data Source	Type of Study	Artificial Intelligence
Synthetic data **Clinical data**	**In Silico technology** **Clinical trial**	**Type of algorithm** **Type of application**
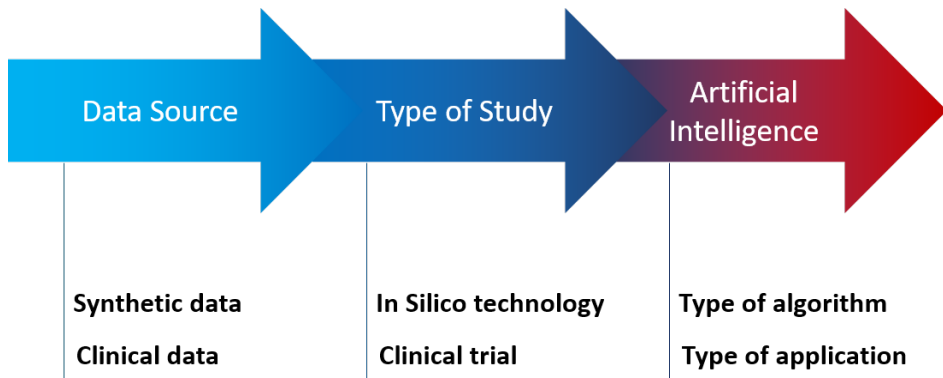
Figure 1.1. Workflow including the three pillars of the dissertation. Data source obtained from synthetic data and clinical trials, In silico technology and clinical trials development and Artificial Intelligence implementation for data analysis and prediction.

Corresponding to the aforementioned pillars, the thesis presents the state of the art, implementation and overall analysis attending to the corresponding chapters:

Chapter 2. State of the art. The three main pillars in which this thesis is based are described in this chapter, with a basic understanding of the Electrophysiology Cardiac field and, specifically AF, together with the fundamental description of artificial intelligence methodology, which are the thesis foundations.

The publication "Artificial intelligence for a personalized diagnosis and treatment of atrial fibrillation" is part of this chapter of the thesis

3

Chapter 3. Study 1: In-silico technology and Artificial Intelligence on a population of models. The aim of this chapter is to describe the first study conducted in this thesis, that covers the implementation of Artificial Intelligence analysis for an *InSilico* Clinical trial based on synthetic data.

Based on the publication "Artificial Intelligence-Driven Algorithm for Drug Effect Prediction on Atrial Fibrillation: An In Silico Population of Models Approach", that is part of this chapter of the thesis

Chapter 4. Study 2: *In-silico* technology and Clinical Images Exploitation. More complex simulations including 3D anatomical data of patients to study arrhythmia complexity are summarized in this chapter.

Based on the publication "Personalized Evaluation of Atrial Complexity of Patients Undergoing Atrial Fibrillation Ablation: A Clinical Computational Study.", that is part of this chapter of the thesis

Chapter 5. Study 3: Stratify-AF: Artificial Intelligence for Treatment Prediction. The Stratify-AF observational study, that aims to characterize and stratify AF patients based on the analysis of the arrhythmia perpetuation mechanisms (NCT04578275), is evaluated in this chapter.

Chapter 6. Discussion and conclusions. The results and main findings introduced in this thesis are discussed and compared with previous works. The conclusions are listed and a guideline for future works is proposed.

Chapter 7. Contributions. The scientific contributions associated to this thesis and derived from the present dissertation are listed in this chapter. The scientific framework in which this thesis is involved is also described.

Chapter 2.
State of the Art

This chapter reviews the fundamentals on the different research fields that are discussed in this thesis. This is a multidisciplinary work that comprises different fields such as cardiology, electrophysiology, algorithm development, computer simulation and artificial intelligence, so abroad introduction for each topic is presented in this chapter.

2.1. Introduction to Cardiac Electrophysiology and Atrial Fibrillation

2.1.1. Cardiac Electrophysiology

The heart is an organ located on the thoracic cavity that pumps blood throughout the body, providing the nutrients and oxygen for the cellular homeostasis to the rest of organs and tissues (How the Heart Pumps Blood).

This organ is formed by four different chambers, the atria and the ventricles, that are divided by different structures: the septum that separates the heart in two identical halves and the atrioventricular valves that separate the atrium from the ventricle (Figure 2.1). This configuration enables blood flow circulation, acting as a pump of the two circulatory circuits present in the system. The complete circuit the starts in the right atrium where blood flows to the right ventricle and directly communicates with the pulmonary circuit to oxygenate blood. Once the blood is oxygenated, it returns to the left side of the heart, entering through the left atrium and later to the left ventricle that distributes the oxygenated blood to the rest of tissues and organs.

Cardiac electrophysiology is the science that studies the electrical activity of the heart and its abnormalities for its diagnosis and treatment (Macdonald, 2008).
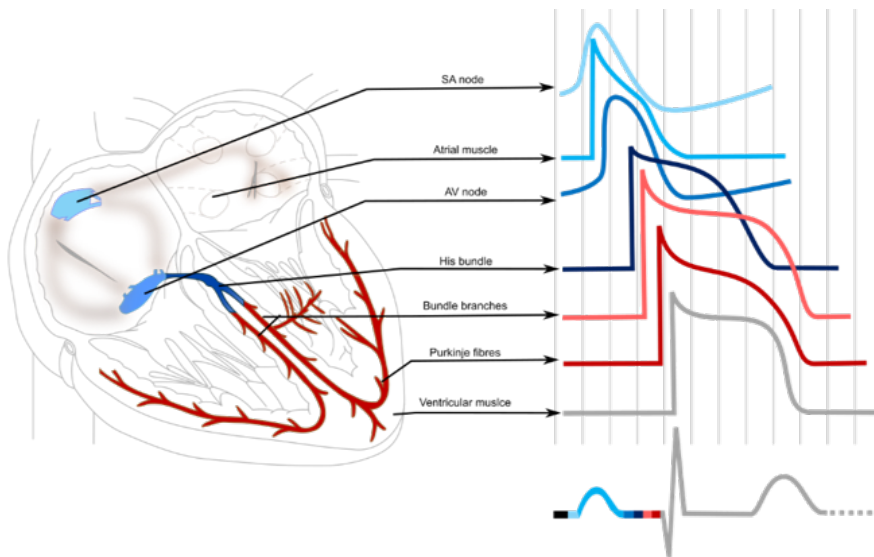
Figure 2.1. Electrical conduction system of the heart. Nodes and bundles propagate the electrical impulse across the heart to perform the contraction that delivers blood to the body (obtained from ECGPedia)

The functional unit of the heart is the cardiac cell, that presents both electrical and contraction forces both at the atrium and the ventricles as shown in the electrical circuit in Figure 2.1. The electrical activity, that is the main topic of this thesis, is governed by the action of different ions and its different concentration inside and outside of the cell. Depending on the influx of these ions, the activation of cardiac cells can be divided into four different phases, that are briefly described and represented in Figure 2.2:

- **Phase 0** corresponds to the depolarization of the cells, driven by an influx of sodium ions that increase the potential of the membrane. Once a given threshold is exceeded, depolarization occurs provoking a sharp upstroke on the action potential morphology.
- During **Phase 1**, sodium channels start to close and outward potassium channels create and early repolarization that tries to bring the cell to its resting state.
- In **Phase 2** or *Plateau Phase*, the repolarization is slowed down by the inward flux of calcium ions, that compensate the outward potassium channels at Phase 1.
- Finally, in **Phase 3** the rapid repolarization returns the membrane potential to its resting state.

The interval of time from which the cell is depolarized in Phase 0 until the repolarization phase finished is called the refractory period. During this period, the cell cannot be depolarized (i.e. return to Phase 0) and this prevent chaotic excitation patterns that would affect the proper functioning of the heart. Finally, after repolarization, **Phase 4** is achieved in which resting the cell becomes excitable.
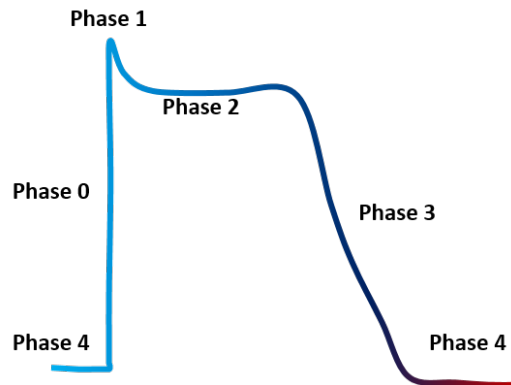
Figure 2.2. Action Potential Activation of Cardiac Cells

In order to propagate this electrical impulse through the cardiac electrical circuit, the sinoatrial node, a specific group of cells, is in charge of initiating the electrical activation and acts as the natural pacemaker of the heart. The normal healthy activation will start with the electrical activation of both atria, followed by the activation of the atrioventricular node and the activation of the ventricles. The consecutive activation of the different areas can be characterized at clinical level to evaluate the correct electrical activation and propagation of the heart and to evaluate, if present, possible abnormalities.

Cardiac Rhythm Disorders

Whenever alterations of the electrical workflow are present, coordination of the electrical propagation is lost. This phenomenon is designated as an arrhythmia (Macfarlane et al., 2011). Depending on the specific characteristics of the arrhythmia, different types are referred in the clinical guidelines. For example, according to location, patients can suffer from atrial or ventricular arrhythmias and according to the rhythm, fast pacing arrhythmias are designated as tachycardia.

These anomalies can be currently characterized with different techniques including wearable technology, conventional electrocardiogram or high-density mapping. A detailed description of the state-of-the-art devices is depicted in the next section.

The target arrhythmia in this thesis is AF, that is further explained in Section 2.1.2.

Cardiac Rhythm Characterization

Electrical cardiac characterization can be performed with different tools depending on the objective of the test. Simple analysis includes interpretation of data registered by wearable devices, that appear as a simple and affordable option for continuous monitoring.

One of the most important tools for characterizing heart rhythm at clinical level is the electrocardiogram (ECG). An ECG is a test that allows measuring the electrical activity of the heartbeat and the complete transmission of the electrical impulse over the heart is represented using 12 leads (Khorovets, 2000), as specified in Figure 2.3. The complete ECG morphology is represented by different waves: the P wave that mainly describes the atrial activity, the QRS complex that represents the ventricular depolarization and the T wave that is associated with the ventricular repolarization. Anomalies in this test enable to characterize patient's rhythm disorders.

Other complementary and more sophisticated techniques could be used to map the electrical activity of the heart, such as Noninvasive Electrocardiographic Imaging (ECGi). ECGi relies on the combination of electrical data obtained from the Body Surface Potential Mapping (BSPM) and imaging techniques that allow for the reconstruction of the torso and its alignment with the heart (Salinet et al., 2021). It makes it possible to detect events and information that could not be obtained in the standard 12-lead ECG. The number of electrodes can vary from 32 to 256 and most study organization strive to position more electrodes on the front of the torso as there are considerably larger potential changes on the front (Rodrigo et al., 2017). By using BSPM, several studies have shown an improved diagnosis (Lefebvre and Hoekstra, 2007) and to characterize different cardiac arrhythmias (Marques et al., 2020). Other applications include the automatic assessment of Electrogram quality (Costoya-Sánchez et al., 2020).
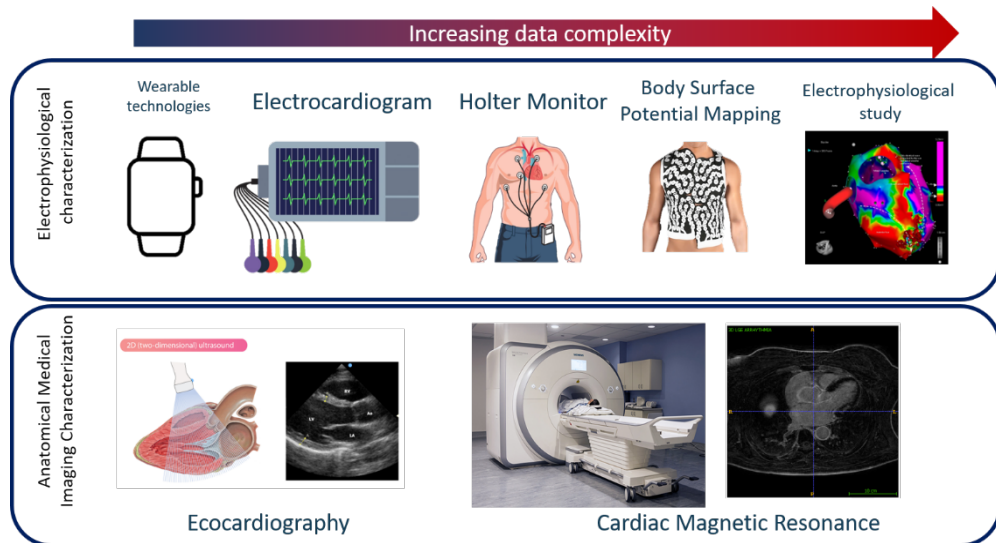
Figure 2.3. Most common electrophysiological characterization techniques present in the clinical practice.

Invasive techniques can also be complementary to the aforementioned characterization techniques. This is the case of the electrophysiological studies. In this

study, an electrophysiologist inserts a catheter through the vasculature and directs it towards the chamber of the heart to be characterized. This catheter usually presents small electrodes that are capable of measuring the electrical activity of the tissue that is in contact with it therefore allowing to register intracardiac signals and even obtaining voltage maps of the area.

Finally, all these techniques can be combined with imaging acquisition systems such as ecochardiography and cardiac magnetic resonance. These two are usually performed to evaluate other characteristics that can influence arrhythmia maintenance such as fibrotic tissue as it was already characterized in the several trials that describe and exemplify the importance of such structural abnormalities in arrhythmic disorders such as the DECAAF trial (Marrouche et al., 2014, 2021).

Body Surface Potential Mapping and ECGi

As previously mentioned (Atienza et al., 2021), ECGi is a non-invasive electrocardiographic system that enables to record de Body Surface Potential Mapping to later estimate the intracardiac electrical activity. To calculate these intracardiac potentials, a transformation matrix is calculated, based on the 3D personalized anatomy of the patient's torso, together with the specific disposition of the patches over it. The intracardiac information is then projected into the atrial anatomy located inside of the torso. This transformation from the BSPM into the intracardiac electrical information is called the inverse problem or ECGi.

Conversely, the calculation of the electrical potentials of the torso (ECG) from the intracardiac recordings of the atria (EGM) is defined as the forward problem (Jalife et al., 2009). The aforementioned forward problem implies a mathematical formulation defined by the biophysical equations and the torso, conductor volume, and this information can be inverted to obtain the epicardial electrical activity from the rest of the known variables (Horáček and Clements, 1997). The ECGi methodology has been experimentally validated under pathological conditions in animal models and human studies (Oster et al., 1997; Ghanem et al., 2005).

ECGi has been widely used in the field of AF that has enabled to identify potential DF areas governing the arrhythmic episodes and, as a consequence, personalized ablation strategies (Haissaguerre et al., 2014; Rodrigo et al., 2014; Pedrón-Torrecilla et al., 2016; Salinet et al., 2021).

2.1.2. Atrial Fibrillation

Atrial fibrillation (AF) is the most common arrhythmia worldwide that is characterized by the rapid and irregular beating of the atrial chambers of the heart. With a prevalence of 2% of the total adult population, AF is associated with an increased risk of stroke, heart failure, and death (Chugh et al., 2014). Diagnostic and treatment strategies for patients with AF are still suboptimal. Current clinical-practice guidelines are based on relatively unspecific clinical criteria, with little room for a personalized approach for managing AF (Hindricks et al., 2020).

Mechanisms underlying Atrial Fibrillation

The mechanisms underlying the initiation and maintenance of AF are complex and still under study. These mechanisms have been analyzed since the first appearance of characterization methods in the twentieth century, giving rise to the theories to explain AF mechanisms: the theory of multiple random sources distributed around the atrium or the existence of propagation in a closed circuit took place (Ref Atienza REC 2006).

This address of the problem remained for this period of time (Rosenblueth and Ramos, 1947; Scherf et al., 1948) and was only updated in the modern age of research by Moe and Abildskoy (Moe and Abildskov, 1959) which contradicted these theories. Moe et al proved that fibrillatory conduction present in AF episodes could be caused by the presence of random wave propagation in inhomogeneous tissue, using computational simulations (Moe et al., 1964). Proposing this new theory, AF was now defined as a self-sustaining process structure independent from ectopic focus that initiated the episode or specific atrial structures that maintained the reentry. This theory was only confirmed with the development of recording techniques that allowed capturing the electrical activity in a sufficiently large number of electrodes simultaneously, 20 years later.

In 1985, the electrical activity of dog hearts was recorded during AF episodes after high frequency stimulation (Morin et al., 2016)*,* obtaining the first in vivo demonstration of multiple wave propagation during AF maintenance.

In parallel, other theories arise such as the focal trigger theory developed by Dr, Hasaguerre. Haisaguerre demonstrated that AF episodes could be initiated by local focal triggers that predominated on the pulmonary vein area and that presented rapid activations (Haïssaguerre et al., 1998).

The mechanisms responsible for AF were evaluated by Jalife et al (Berenfeld et al., 2001; Wellner et al., 2002; Jalife and Berenfeld, 2004) showing that AF maintenance could be identified with rotatory patterns where a single electrical wave turns over a refractory region in a high activation rate, provoking fibrillatory conduction in their surroundings. This theory was based on the occurrence of a functional reentry that is responsible of the maintenance of the fibrillatory activity, due to the presence of a set of abnormal electrophysiological characteristics that are associated with a reduction of the refractory period or a decrease in the conduction velocity (Akar et al., 2000; Wellner et al., 2002).
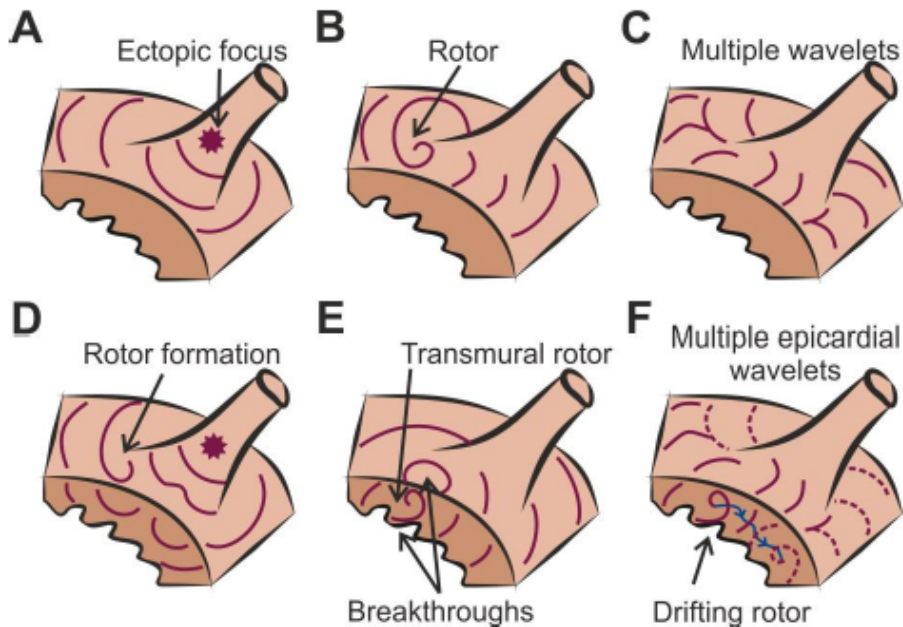
Figure 2.4. AF mechanisms from [Guillem et al Cardiovasc Res]. A) Ectopic focus on the pulmonary veins. B) Rotor in the posterior wall of the left atria. C) Multiple wavelets. D) Rotor formation by an ectopic focus in the pulmonary veins. E) Transmural rotor. F) Multiple epicardial wavelets provoked by transmural drifting rotors.

Therefore, there are two main theories that can be identified to explain fibrillatory patterns:

1) Focal theory

   This theory suggests that AF is caused by the irregularity present on the interaction between the high frequency wavefronts produced by a primary generator (ectopic focus or functional microreentry) and the variable re-fractoriness properties present in the atrial tissue (Leef et al., 2019). Several studies indicate that the pulmonary veins are the most common areas that act as primary generators (Chen et al., 1999), although these have also been found in the superior vena cava, ligament of Marshall, left posterior wall, crista terminalis and coronary sinus (Tsai et al., 2000; Lin et al., 2003).

2) Multiple wave hypothesis

   This theory proposes that the irregular atrial activity is a consequence of a primary arrhythmogenic mechanism (Moe and Abildskov, 1959), wherein the fractionation of the wave fronts propagating through the right atrium results in the self-maintenance of the chaotic activity. Tissue heterogeneity is vital in the explanation of this hypothesis, as it is responsible for the fractionation and perpetuation of the wavefronts. According to this theory, an atrial tissue with wide variability in their refractory period (being quite short) as well as delayed conduction properties has an increased

11

probability of developing sustained AF. This theory is nowadays defended by the existence of transmural conduction that explains the endocardial electrical breakthroughs that otherwise are attributed to focal activity (Eckstein et al., 2013).

Although the two main theories about the maintenance of AF seem to be mutually exclusive, they are closely linked and must be interpreted together. At the case of focal theories, atrial rotors can be initiated by a focal discharge due to a wavefront break (Figure 2.4D), so the focal triggered activity could be acting as an AF initiation mechanism. Moreover, the existence of intramural rotors can be reflected as breakthroughs in the atrial wall and they can be interpreted as endo or epicardial focal sources (Figure 2.4E), thus focal and rotor hyphothesis are not mutually exclusive. Finally, the existence of transmural and drifting rotors can create also multiple epicardial wavelets (Figure 2.4F), so focal and multiple wavelets theories could be compatible.

Atrial Fibrillation Types

From the clinical point of view, there are four main AF types: paroxysmal, persistent, long-term persistent and permanent AF(Atrial fibrillation: Overview, 2017; Hindricks et al., 2020). The type of AF that each patient presents can be classified according to how often AF episodes are present and how it responds to a given treatment.

During **Paroxysmal AF**, episodes that terminate spontaneously or with intervention within 7 days of onset. This type of arrhythmia can happen repeatedly and pharmacological or interventional treatments may be necessary to stop it. In addition, this arrhythmia can be alternated with a heartbeat that is slower than normal, it is called brady-tachy syndrome.

Persistent AF is a condition in which the abnormal heart rhythm lasts for more than a week and where treatment is usually needed to stop it. When this condition lasts for more than a year without disappearing the arrhythmia is called **long-term Persistent AF**.

If the restoring of normal rhythm is not achieved after several attempts nor electrical cardioversion is effective, the arrhythmia is categorized as **Permanent AF**.

2.1.3. Clinical Treatment

AF clinical treatment includes different approaches with pharmacological compounds or with interventional techniques, that are not exclusive, i.e. that can be combined.

Current clinical guidelines discern among two types of strategies depending on the patient current situation and answer that can be subdivided in rate and rhythm control strategies (Figure 2.5 and Figure 2.6) (Hindricks et al., 2020).
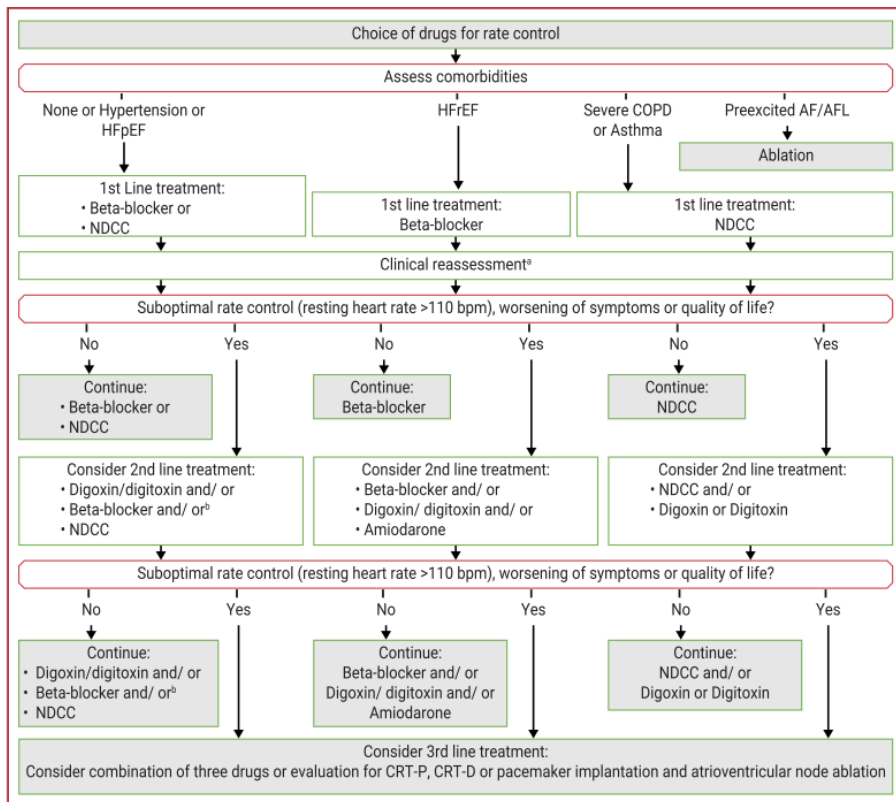
Figure 2.5. Choice of rate control drugs. AF = atrial fibrillation; AFL = atrial flutter; COPD = Chronic obstructive pulmonary disease; CRT-D = cardiac resynchronization therapy defibrillator; CRT-P = cardiac resynchronization therapy pacemaker; HFpEF = heart failure with preserved ejection fraction; HFrEF = heart failure with reduced ejection fraction; NDCC = Non-dihydropyridine calcium channel blocker. [a]Clinical reassessment should be focused on evaluation of resting heart rate, AF/AFL-related symptoms and quality of life. In case suboptimal rate control (resting heart rate >110 bpm), worsening of symptoms or quality of life consider 2nd line and, if necessary, 3rd line treatment options. [b]Careful institution of beta-blocker and NDCC, 24-hour Holter to check for bradycardia. Obtained from (Hindricks et al., 2020).

Rate control is the approach of choice for the first attempt in which pharmacological compounds are used to maintain sinus rhythm (Kirchhof et al., 2020). These compounds include beta blockers such as atenolol and bisoprolol, calcium channel blockers such as amlodipine and verapamil and sodium channel blocker such as flecainide.

If rate control is not possible for a specific patient, the type of arrhythmia is key for further treatment. In case of paroxysmal patients, the strategy of "pill in the pocket" or interventional procedures including catheter ablation are the therapies of choice.

For persistent AF patients, cardioversion is recommended, and posterior catheter ablation or rate control are indicated depending if the patient is in sinus rhythm or in AF.
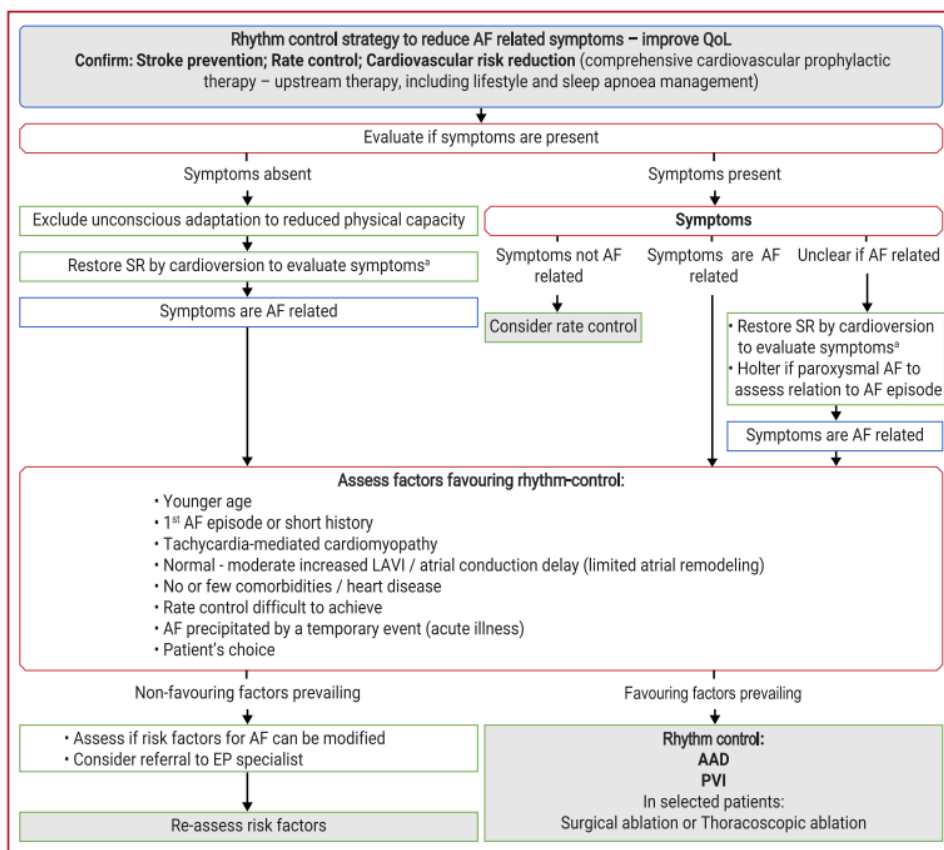
Figure 2.6. Rhythm control strategy. AAD = antiarrhythmic drug; AF = atrial fibrillation; CMP = cardiomyopathy; CV = cardioversion; LAVI = left atrial volume index; PAF = paroxysmal atrial fibrillation; PVI = pulmonary vein isolation; QoL = quality of life; SR = sinus rhythm. ªConsider cardioversion to confirm that the absence of symptoms Is not due to unconscious adaptation to reduced physical and/or mental capacity. Obtained from (Hindricks et al., 2020).

Interventional treatments: Catheter ablation

Catheter ablation is the main interventional treatment used to treat AF. In this procedure, a catheter is inserted through the blood vessels and directed towards the heart. Once the catheter is in the heart, an electrophysiological study is performed in some of the cases in order to obtain more information about the cause of the maintenance of the arrhythmia.

Current approaches include the electrical burning or isolation of the pulmonary veins, as these structures have been identified as ectopic foci in this arrhythmia (Figure 2.7) (Althoff and Mont, 2021). In addition, other areas of the left atrium can also be ablated and current studies point out to the areas with the fastest activation or highest dominant frequency as the objective to be ablated.

Two different strategies can be followed depending on the burning technique: while cryoablation relies on freezing temperatures to eliminate the tissue, radiof-

requency uses high voltage to carry out the task. Each approach presents advantages: cryoablation is anatomical and a fast procedure, while radiofrequency enables a prior electrophysiological study and specific ablation of other atrial sites following pulmonary vein isolation. In the radiofrequency case, several configurations of the catheter can be found in the market depending on the disposition and number of electrodes present in the acquisition part of the catheter. This approach has demonstrated a change in the electrophysiological activity of the atria, that has been extensively quantified (Chua et al., 2021).
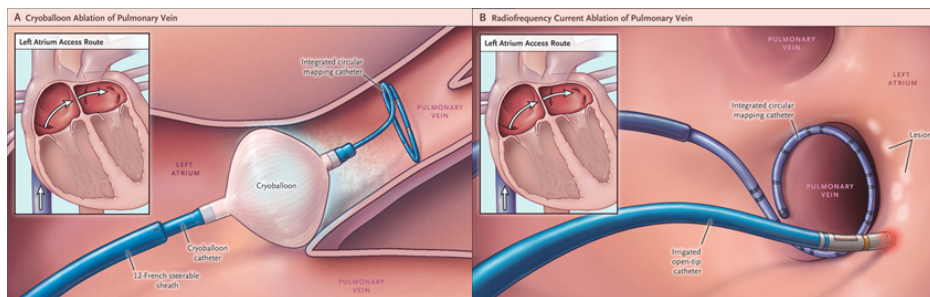
Figure 2.7. A. Cryoablation procedure. B. Radiofrenquency ablation. Image obtained from (Kuck et al., 2016)

Finally, pharmacological treatments are usually combined with interventional procedures the enable long-term sinus rhythm maintenance.

2.2. Atrial Fibrillation Characterization Studies: *In-silico* trials vs. Clinical trials

As shown in Figure 2.8, the process for developing new drugs, testing new treatments, or certifying new devices is constituted by different phases.

The first phase includes the pre-clinical stage, that is principally developed in wet laboratories, mainly consisting of in vitro testing. These experiments are focused on establishing the plausibility for the efficacy of the treatment.

The next stage is focused on in vivo animal models to provide guidance and efficacy on the safety of the product for humans. Depending on the field of application of the product or treatment, animal species can vary.

Once the in vitro and in vivo phases have been successfully completed, the product or treatment can be proposed for certification in human use in a clinical trial (Tenti et al., 2018; Kashoki et al., 2020). A brief description of the clinical trials can be found in Section 2.2.2. secondary effects in human subjects cannot be explored until clinical trial stages are reached, therefore, exponentially limiting the identification of secondary effects in the target population. These late identification of secondary effects can cause the immediate stop of the trial, with the resulting economical and ethical conditions that it implies. Not only secondary effects have been identified at this stages but also lack of efficacy for the general population,

as current approaches are looking for a solution that is both safe and effective in the overall population, rather than considering personalized approaches for each patient.
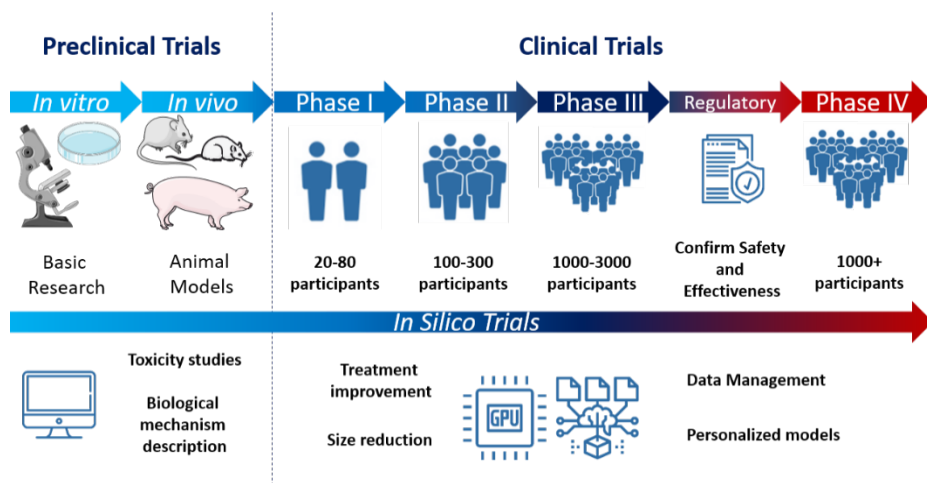
Figure 2.8 Preclinical and Clinical trial description including number of participants and phases

As stated in previous publications (Ávila et al., 2021; Winters et al., 2021), each patient presents a particular condition based on characteristics such as physiology, pathologies present, lifestyle and presence of comorbidities. Other factors that play an important role are therapeutic adherence, and the variability in surgeons' experience and technique during surgical interventions.

2.2.1. *In-Silico* trials

In-Silico trials are based on computer simulations that contain specific information from the patient, enabling personalization of the models (Engineering, 2011; Corral-Acero et al., 2020). The term *in-silico* indicates any use of computers in clinical trials, even if limited to management of clinical information in a database.

This type of computations can be used in the development or regulatory evaluation of a medicinal product (Li et al., 2017; Passini et al., 2017; Patel et al., 2019; Vicente et al., 2019), device or intervention or to characterize and model different diseases (Liberos et al.; Vigmond et al., 2009; Arevalo et al., 2016; Rivera-Juárez et al., 2019). Although this approach presents major limitations that is commented in this chapter (Carro et al., 2017), the combination of the information extracted from the simulations with clinical information can increase the understanding of biological mechanisms (Vicente et al., 2016). Nowadays, these types of trials are currently being validated at in vitro and in vivo levels, as they are expected to have major benefits over current animal trials (Figure 2.9).

In Silico trials soften these biases by using accurate computer models for a specific treatment and its development, including patient characteristics to

broaden the testing scenario to different patient groups and more information. In this sense, the idea of *in silico* trials is to create a virtual twin in the computer that can test all possible treatment, enabling observation through a computer simulation of how the candidate biomedical product performs and whether it produces the intended effect, without inducing adverse effects. Such *in silico* clinical trials could help to apply the 3Rs fundamentals (reduce, refine, and partially replace real clinical trials) by:

1) Reducing size or studying specific groups at clinical level that are identified as risk groups at *in silico* level

2) Adding more detailed information obtained from this type of trials, better understanding interactions, with different groups and long-term effects that clinical trials cannot provide

3) Replacing the pre-clinical phase and preserving the clinical trial for legal requirements

4) Improving unsuccessful treatments or products by providing extra information. Increases innovation, decreases economical costs and exponentially increases understanding of biological processes

5) Avoiding the use of animal models by directly including clinical data and personalized information from the patients. This significantly decreases the overall costs associated to the development of treatments and have proven to be more effective at predicting the behavior of the drug or treatment in large-scale trials and identifying secondary effects, therefore better screening the treatments that progress to Phase III clinical trials.

Modelling Atrial Fibrillation

Computer models include different approaches to describe cardiac electrical activation, propagation and fibrillatory dynamics (Musuamba et al., 2021). A number of models are described in the literature for different cardiac areas such as the atria and the ventricles, and even for different cellular types in the same area, such as the endocardium and the epicardium.

Action Potential Modelling

Action potential modeling started in the 50s when Hodgkin and Huxley first developed a mathematical model that simulated the electrical activity of a cell (Hodgkin and Huxley, 1952). This early model was calibrated with experimental data obtained by patch clamp measurements in the axons of a giant squid. This formulation stated the base for further models and has constituted the initial base for the rest of the models.
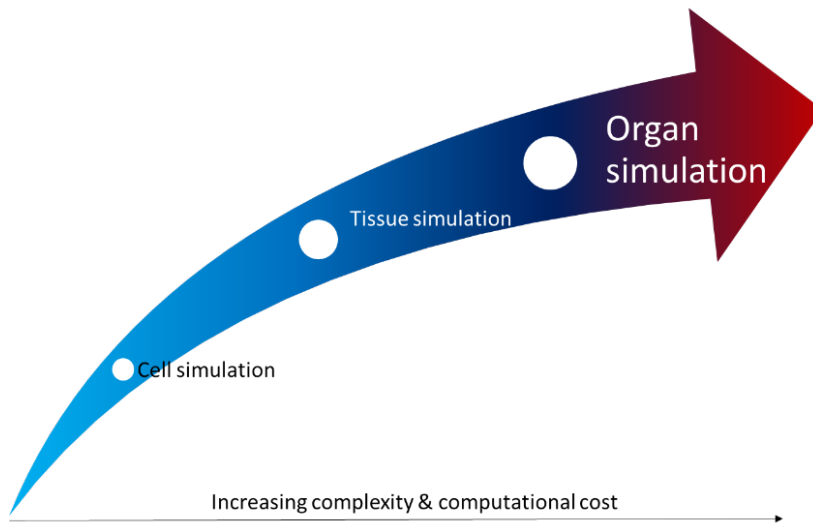
Figure 2.9. Complexity of simulations

This model corresponds to the cell membrane that separates the intracellular and extracellular spaces that are communicated by the ionic channels, as it can be observed in Figure 2.10. For this specific model, internal and external media were characterized as ideal conductors and the cell membrane was characterized as a capacitor (C_m). In total, four ionic channels were modeled, corresponding to sodium, potassium, chloride, and leak currents, as a variable resistance and a resting potential. Once all these elements are particularized, electrical laws can be applied in order to calculate the membrane potential values along time.
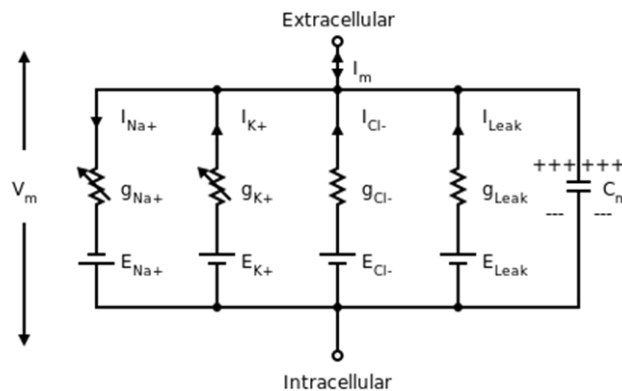
Figure 2.10 Electric circuit from Hodgkin and Huxley for the modeling of the electrical activity.

The development of accurate models implied the need of electrophysiological experiments that enabled to further characterized ionic currents. A high number of patch clamp experiments for the characterization of this currents was needed, performed in isolated cells.

The first mathematical model of cardiac myocytes was done by Denis Noble by implementing and modifying Hodgkin and Huxley's model (Noble, 1962) (Noble, 1962), that combined with posterior experimental data allowed the improvement of the basic cardiac cell model with different currents included (McAllister et al., 1975; DiFrancesco and Noble, 1985). Luo and Rudy continued improving this model to present the first mammalian ventricular myocyte model (Luo and Rudy, 1991), that was later improved by Iyer and ten Tusscher (Iyer et al., 2004; ten Tusscher et al., 2004).

Once the mammalian model was established, human atrial myocyte models started to be developed including several models developed in parallel in the late 90's: Courtemanche's model (Courtemanche et al., 1998) and Nygren's model (Nygren et al., 1998).

Courtemanche and Nygren's models presented some differences in the action potential shape, although both were based in the same experimental data. Posteriorly, Maleckar et al. improved the formulation of some repolarizing currents (Maleckar et al., 2008), Koivumäki et al. included a detailed formulation for the sarcoplasmic reticulum and Ca2+ dynamics (Koivumäki et al., 2011) and Grandi et al. also improved the Ca2+ management (Grandi et al., 2011).

Maleckar and Koivumäki models have been useful for evaluating the effect of electrical and structural remodeling provoked by different arrhythmias, including AF. More specifically, this remodeling has been correlated with a reduction in the action potential duration that is associated with some specific ionic currents (Brundel et al., 2001; Skasa et al., 2001; Workman, 2001; Dössel et al., 2012).

In addition, reduced calcium handling has been associated with reduced intracellular calcium transients that highly affect cell contractility (Schotten et al., 2001). Finally, the electrophysiological effect of the structural remodeling has been mathematically modelled as atrial myocytes electrically linked to cardiac fibroblasts (Maleckar et al., 2009), and by the dilation of atrial cells which results in an increase in the membrane capacitance (Schotten, 2002; Corradi et al., 2012; Koivumäki et al., 2014).

The formulations of the cardiac cell models including remodeling in different ionic channels have enabled the development of specific research lines to study relationships and interactions between different ionic currents and their effect on the electrophysiological behavior of atrial cells and AF progression.

Tissue Modelling

Although cell models have demonstrated important advantages in the study of arrhythmogenic properties, conduction properties of the tissue play a major role in the initiation and maintenance of atrial arrhythmias. To study these properties,

mathematical models that include the connection of cells mimicking the cardiac muscle have been implemented.

Electrical propagation is provoked by differences in electrical potential between neighboring cardiomyocytes, which cause an ionic current through the proteins linking cardiac cells, called gap junctions, and such ionic currents promote the depolarization of the neighboring cells. The behavior of this excitable medium can be modeled by a reaction-diffusion model, which allows computing the currents supplied or received by each atrial myocyte from each of its neighbors. These currents are also modulated by the cardiac media anisotropy, since there is much more electrical connectivity in the direction in which the cells are aligned.

Following this implementation, cardiac propagation can be described as a monodomain or bidomain model. Monodomain models apply the reaction-diffusion equations only to the potential membrane (Clayton and Panfilov, 2008; Dössel et al., 2012) whereas bidomain models include variation of ionic concentrations and electric potentials separately for intracellular and extracellular media (Trayanova, 2006), therefore increasing the complexity of the equations and the computational cost. Monodomain models can reproduce most of the phenomena related with electrical propagation and, therefore, are widely used because of their simplicity (Dössel et al., 2012). Nevertheless, other phenomena like current injections provoked by electrical cardioversion have to be addressed by bidomain models (Trayanova, 2006).

As previously mentioned for cellular simulations, tissue models also present a great advantage for research lines involved in AF initiation and maintenance and the remodeling behind arrhythmia mechanisms

In this respect, several approaches have implemented tissue simulations to characterize the effect of the electrical remodeling on cardiac propagation (Kharche et al., 2008), and the presence of fibrosis (Ashihara et al., 2012) or stretching forces (Yamazaki et al., 2009) in the tissue. These models have been also used to emulate and mimic rotational activity (Wellner et al., 2002; Jalife and Berenfeld, 2004; Clayton et al., 2006) and its evolution in the presence of electrophysiological remodeling (Felipe Atienza et al., 2006; Atienza 2011; Calvo, Deo, Zlochiver, Millet, & Berenfeld, 2014), and 2D plane simulations have played a major role to set the basis for rotor theory (Jalife, 2011, Pandit 2011). Finally, in silico models have also contributed to develop new mapping techniques for (Iyer and Gray, 2001; Narayan et al., 2012) or ablation (Rappel et al., 2015).

Atria Modelling

The development of tissue models that connect the cells allows for further the scaling to complex structures such as the complete atrial anatomical geometry. These simulations enable to realistically reproduce the propagation patterns that have been characterized during arrhythmic episodes. In order to facilitate the description of the atrial geometry, as the atrial wall tends to be slim, the models are

usually represented as single surfaced composed of triangular meshes (van Dam and van Oosterom, 2003; Jacquemet et al., 2006).

Nevertheless, more complex structures including thickness composed by tetrahedrons or cubes have also been applied (Aslanidi et al., 2011; Krueger et al., 2011, 2013). All the information and data comprising the atrial anatomy is usually extracted from imaging characterization techniques such as computer axial tomography (Burdumy et al., 2012) or magnetic resonance (Virag et al., 2002), and they can implement also anisotropic conduction properties (Dössel et al., 2012). Moreover, they can include several atrial regions in which the cellular model takes different electrophysiological properties (Tobón et al., 2010).

Similar to tissue models, atrial models have been used to study the mechanisms that promote and maintain AF episodes. Virag et al. studied the distribution of rotors in presence of anatomical obstacles (Virag et al., 2002), and Blanc et al. studied how the depolarization alternans could be the mechanism responsible for rotor initiation in presence of anatomical obstacles (Blanc et al., 2001). Electrical and structural remodeling has been studied also in anatomical models and their susceptibility to generate functional reentries (Kharche et al., 2008; McDowell et al., 2012; Colman et al., 2013). Finally, detailed anatomical AF models have been used to develop therapies based on catheter ablation (Blanc et al., 2001; Reumann et al., 2008; Tobón et al., 2010) or to evaluate the effect of gaps in ablation lines (Dang et al., 2005; Hwang et al., 2016).

Computational Cost

One of the main drawbacks of in silico simulations is the high computational cost associated to this type of calculations. As the models used included in this field usually imply a high number of differential equations that describe subcellular mechanisms, the computations of whole organ structures in personalized anatomies can last for days. As specified in (Badano, 2021; Heijman et al., 2021), the computational cost has been diminished in the last decade using Graphical Processing Units that enable the parallelization of the computational processes.

2.2.2. Observational Studies and Clinical trials

Observational studies

An observational study evaluates the effect of a risk factor, diagnostic test, treatment, or other intervention, following approved clinical practice, without trying to change who is or is not exposed to it. Cohort studies and case control studies are the two types of observational studies.

Clinical Trials

Clinical trials are research studies performed in patients that are aimed at evaluating a medical, surgical or behavioral intervention (Umscheid et al., 2011). The clinical trial is aimed to evaluate the safety and efficacy of a new treatment,

drug, diet or medical device (for example, a pacemaker) in a patient population with a disease. The basis of a clinical trial is to analyze the effectiveness and safety of the intervention as compared with the standard treatment.

Briefly described four phases of clinical trials as shown in Figure 2.11:

Phase I (20-80 participants) focus on adjusting the safety and dosage of the drug. Approximately 70% of drugs move to the next phase.

Phase II (100-300 participants) focus on evaluating the efficacy and side effects. Approximately 33% of drugs move to the next phase.

Phase III (1000-3000 participants) focus on evaluating the efficacy and monitoring of adverse reactions. Approximately <10% of drugs move to the next phase.

Phase IV (1000+ participants) focus on safety and efficacy of the intervention, after it has been approved.

Figure 2.11 Clinical trial description including phases.

2.3. Artificial Intelligence and Atrial Fibrillation

It is well recognized that clinically determined patterns of AF are unspecific, and they do not correspond to the real epidemiological burden of the disease, rate of complications nor treatment indications (Kirchhof et al., 2013). For example, screening methods for detecting AF show important limitations, and classical clinical and electrophysiological patterns correlate poorly with treatment outcomes (Charitos et al., 2014; Rodrigo et al., 2020; Sanchez de la Nava et al., 2020). Nevertheless, classifying AF as paroxysmal or persistent disease is still the main

basis for patient management. On the other hand, clinical records, electrical signals and medical images provide physicians and researchers with massive amount of information. This opens an opportunity for identifying specific phenotypic, clinical, and outcome patterns that could be useful for tailoring individualized strategies for treatment (Atienza et al., 2021). However large and multidimensional big data are extremely difficult to analyze and interpret with conventional statistical tools. Instead artificial intelligence (AI) algorithms are particularly well suited and are only beginning to be exploited in the field of AF.

2.3.1. Artificial Intelligence vs. Conventional Statistical Methods

Conventional statistical methods are based on the inference principle: hypotheses are stated a priori to deduce the properties of an underlying probability distribution of data (Figure 2.12.A). However, statistical inference requires strict assumptions of data distributions that may limit their applicability and generalization (Krittanawong et al., 2019). Alternative data analysis strategies can overcome the limitations imposed by the number, distribution, and typology of data. AI is a field of computer science that implements algorithms that mimic human behavior through processes, such as the ability to discover meaning, generalize, or learn from past experience. These methods provide investigators with accurate and effective algorithms for data analysis and open completely new opportunities for disease characterization. The combination of powerful computational tools with novel training algorithms increase the accuracy for prediction, pattern identification and task automation in large datasets (Makridakis, 2017; Johnson et al., 2018). AI techniques have been applied in cardiovascular medicine where complex, heterogeneous and multiple rich multimodal datasets (i.e. genome-sequencing, mobile device biometrics, imaging, etc.) are used for diagnosis and treatment (Atienza et al., 2000; Al'Aref et al., 2019; Bello et al., 2019; Krittanawong et al., 2019; Sampedro-Gómez et al., 2020).

A

B
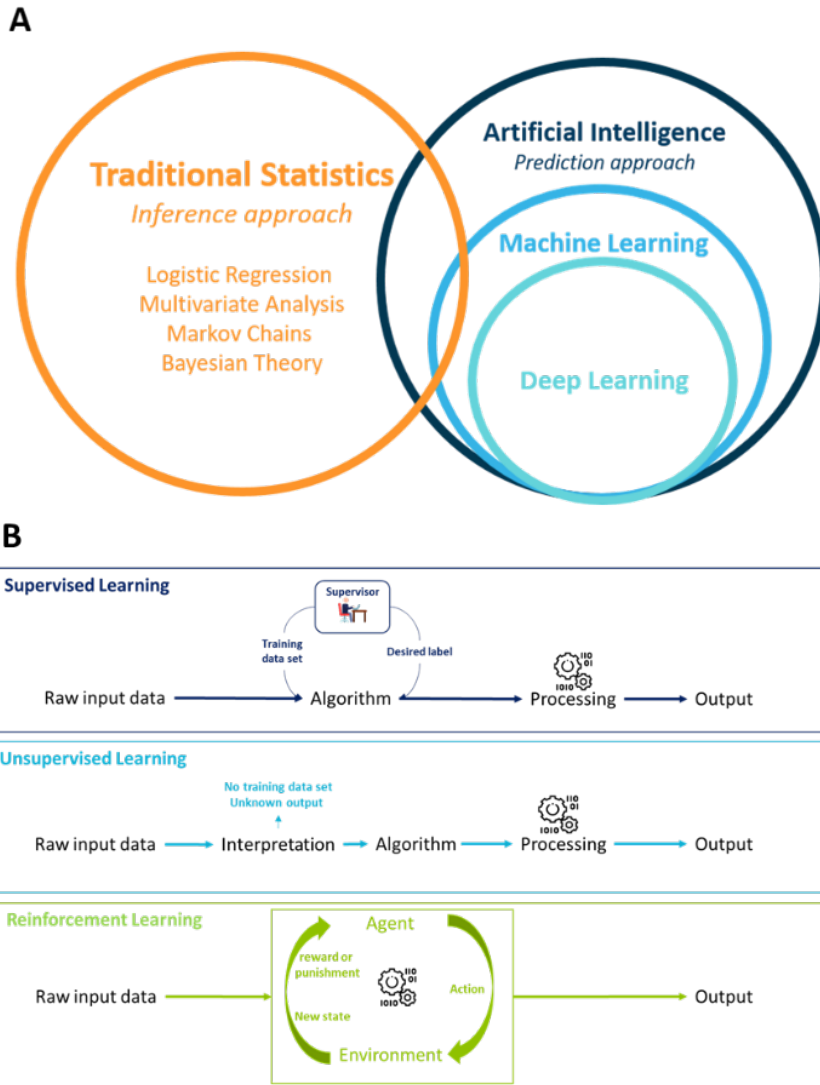
Figure 2.12. A. Description of the hierarchy and relationship of traditional statistics, artificial intelligence, machine learning and deep learning techniques. B. Supervised, unsupervised and reinforcement learning algorithms. Supervised learning presents input of raw data and trains the algorithms by stablishing a linear relation between the training data set and the corresponding label. Unsupervised learning inputs the raw input data and extracts hidden relations in data with an unknown clustering or grouping of the samples. Reinforcement learning works on a system based on reward and punishment towards the objective of finding the cumulative reward.

Machine Learning (ML) is an AI technique based on algorithms that improve automatically through an iterative process of learning from data, identifying patterns and making decisions (Mitchel, 1997) (Figure 2.12). Deep Learning (DL) is

a family of ML methods based on artificial Neural Network (NNs), a more sophisticated mathematical expression for the learning process, capable of extracting higher level features from the raw input (Deng and Yu, 2014). NNs combine a collection of connected computational units, called artificial neurons. Neurons are grouped in layers which are distributed in the input, intermediate (or hidden) and output spaces. As depicted in Figure 2.13, each of these layers, that hold multiple neurons or blocks, are sequentially connected to build the NN. Each neuron is a processing unit with a specific mathematical operation that, in-turn, can receive and feed multiple neurons. The input layer of the NN usually incorporates different type of data (scalars, signals or images) into the net. Intermediate or hidden layers adjust weights during training based on correct or incorrect decisions. Finally, output layers express the predicted value which may be an estimated value (regression problems) or a probability of belonging to a given category (classification problems). These algorithms can be trained using supervised or unsupervised methods (Table 2.1).

Convolutional neural networks (CNNs) are a specific design of NNs that have become the primary choice to make predictions from ECG signals obtained at a single point in time (Xiong et al., 2018; Attia et al., 2019; Hannun et al., 2019). They typically process raw input data from ECG recordings and are also one of the most widely employed architectures for image analysis (Margeta et al., 2017; Vesal et al., 2019; Fahmy et al., 2020). These algorithms are built of consecutive neurons or operational blocks that transform the input information and identify new features for classification. For its correct performance, the number and type of blocks can be adjusted depending on both data and computational power. In addition, each of these layers can be customized by adjusting their variables (hyperparameters), which change and adapt the function or block depending on the input dataset. The standard layers are convolutional layers that rely on convolutional operations, detect and construct feature maps. These feature maps are then processed by the successive layers, creating hierarchical representations of data which are useful for predicting a categorical output. Convolutional layers are usually combined with additional blocks such as batch normalization layers, pooling layers for down sampling feature maps, dropout layers for regularization techniques (i.e. preventing overfitting) and dense or connection layers (Figure 2.13).

Training these algorithms implies two dependent and related processes, defined as forward and backwards propagation (Alpaydin, 2014). During forward propagation, the information flows from the input to the output of the network to make a prediction. Once the prediction is obtained, it is compared to the original label by calculating the difference or *loss*. This loss is used by the network during the backpropagation stage, to adjust the weights of the algorithm in an iterative process with the final goal of minimizing the loss. This principle is based on the gradient descent method and can encounter some difficulties during the training process, especially when a local minimum is found instead of a global minimum
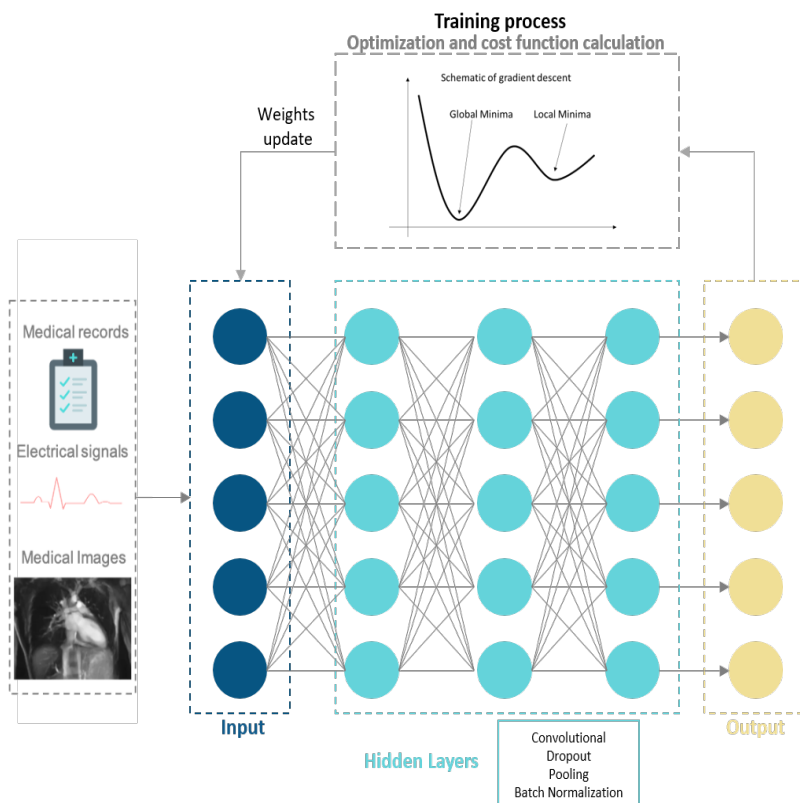
Figure 2.13. Description of a Deep Neural Network for classification including input parameters as medical records, electrical signals and medical images, input layers, hidden layers and output layers. Each of the layers can be customized depending on the mathematical operation that it performs, including convolutional, dropout, pooling and batch normalization.

Different loss functions can be implemented depending on the type of data and network (Deng and Yu, 2014). Root Mean Square Error (RMSE) is one of the most popular loss functions used for NN. However, this function is very complex and as a result, may lead to converging on local minima. Some solutions have been presented to overcome this difficulty such as adding noise to the weights while being updated or the use of momentum which gradually increases the weight adjustment rate.

Recurrent neural networks (RNNs) are NN structures designed to analyze the temporal sequence of data, particularly identifying patterns in long ECG recordings (Faust et al., 2018). This type of architectures is key, for example, for distinguishing AF from other rhythms.

In summary, NNs are associative self-learning algorithms capable of identifying multidimensional relationships in non-linear domains with higher predictive accuracy than linear or traditional regression approaches (6, 42, 61, 76).

2.3.2. AI Learning process: Supervised vs. Unsupervised vs. Reinforcement Learning

AI algorithms are designed to learn from data so, in a second step, prediction or diagnosis can be later performed on a new sample. In this context, three different approaches can be distinguished, depending on the data available for implementation and the final goal, whether it is classification, clustering or learning (Figure 2.12). The main advantages, disadvantages and applications of these algorithms are summarized on Table 2.1.

Supervised learning is designed to predict a label, whether the label is binary (i.e. AF vs. sinus rhythm) or a multidimensional result (i.e. fibrotic tissue presence and location on a MRI image) (Feeny et al., 2020). As depicted in Figure 2.12B, supervised learning methods enter the information directly in the algorithm which is trained adjusting the parameters to match the desired label or prediction. The most critical component of the process relies on feature selection from the dataset (Novig, 1995), as descriptive and high quality biomarkers are key for the success of the algorithm. Moreover, the number classes to predict and the number of samples in each class is critical for the training process, as the algorithm needs to identify enough information to build the patterns required for discriminating different labels. Adequate classification of groups is particularly difficult in medical applications of supervised learning because data is typically imbalanced (each label group has a different number of samples). This imbalanced nature may strongly affect the performance of the Receiver Operating Characteristic (ROC) curve evaluation, which mainly expresses the true and false positive performance, not reflecting the minority class (Davis and Goadrich, 2006). For this purpose, regularization techniques (Reychav et al., 2019) and/or training with synthetic data can be implemented to overcome this problem (Le et al., 2017). Also, other evaluations such as the Precision-Recall (PR) curves (Davis and Goadrich, 2006) can be more informative than ROC in these cases. Some of the most common algorithms used in supervised methods are k-nearest neighbors (k-NN), support vector machines (SVM), Random Forests (RF), Extra Gradient Boosting (XGBoost), Logistic Regression (LR) or NNs (Alpaydin, 2014).

Unsupervised learning is used when the goal is to identify hidden relations and intrinsic structures within the data. Unsupervised learning is based on raw input data and does not take into account features design, label or class (Thrun and Pratt, 1998). Parameter adjustment in unsupervised methods requires less computational power and present results in clusters (i.e. patients with a given set of similar characteristics). Major limitations of unsupervised learning methods are the difficulties in identifying the initial cluster pattern and the requirements for hand coding of some parts of the algorithm. Unsupervised learning is typically used for exploratory analyses (identifying patterns in data) and for reducing dimensionality for further analyses by eliminating redundant features and increasing model efficiency. Dimensionality reduction algorithms are commonly used to reveal new

distribution of samples in space and as noise reduction methods, to apply clustering algorithms based on a second step. Neural networks included in unsupervised learning are mainly represented by autoencoders. Autoencoders (a combination of encoder and decoder blocks), learn a pattern representation from data, distilling the information that better describes the input samples. The final objective of these algorithms is to copy or produce an output holding a similar amount of relevant information than in the input space, but much smaller in terms of dimensions and size.
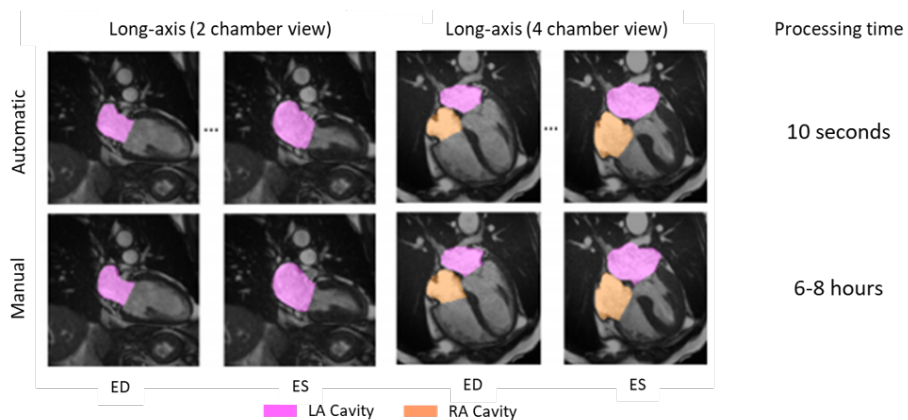
Figure 2.14. Example of automatic and manual segmentation of the atrial cavity during end diastolic (AD) and end systolic (ES) with respective processing time, modified from (Bai et al., 2018). Used with permission.

Reinforcement learning algorithms are trained in an iterative system of incentive and punishment, towards the goal of maximizing the cumulative reward. In this case, the algorithm presents two key figures: the *agent* and the *environment* (Figure 2.12). The agent chooses the response or *action* for a given situation or *state* of the environment, obtaining feedback: a reward in case the response is correct and a punishment in case the response is incorrect. After multiple iterations, the algorithm will learn what is the best action for each tested situation. Although this approach has been scarcely used for healthcare applications, its development in the next years is expected to increase, particularly in observational cohorts with sequential treatments or stages (Gottesman et al., 2019), including AF clinical trials.

2.3.3. Calibration process: Training, validation and test sets

Implementing ML algorithms usually requires calibration based on three different subsets of data: training data, validation data and test data (Alpaydin, 2014). Training data is used to adjust the algorithm to the population sample, validation data are used to refine the parameters or hyperparameters of the algorithm and test data is used as validation to address the performance of the final algorithm on a completely new data set. Typically, the training set usually incudes 60%

of the available data and validation and test data account for 20% each of, although other approaches can be followed depending on the heterogeneity of the population, the complexity of the algorithm to be trained and the number of samples available.
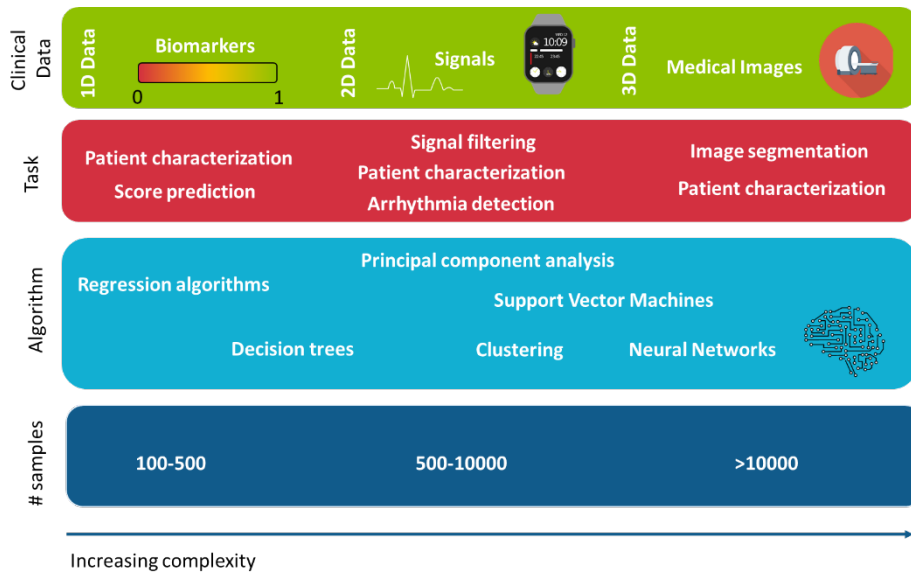
Figure 2.15. Artificial Intelligence in Atrial Fibrillation. Description of the clinical data used, and the tasks performed. Common algorithms used for each type of data and range of estimated number of samples needed for the implementation of each of them.

2.3.4. AI application in AF

AI algorithms are increasingly used in several scenarios related to AF (Feeny et al., 2020) such as diagnosis (Xia et al., 2018), prediction of outcomes (34), characterization of the disease (Xiong et al., 2020), and the evaluation of treatment efficacy (Helms et al., 2014; Dretzke et al., 2019; Mamoshina et al., 2020). These approaches incorporate the advantages described above to process huge amounts of data.

29

Algorithm	Classification problems		Advantages	Disadvantages	Usu app in
k- Nearest Neighbors (k-NN)	Supervised learning	Multiclass classification	Intuitive and simple to code Low number of hyperparameters to adjust Variety of criteria to adjust algorithm	Slow algorithm for increased number of samples Not suitable for large datasets Unbalanced data is a problem Not good at dealing with missing values	Feature ted from
Support Vector Machines (SVM)	Unsupervised learning	Non-linear binary classification	More effective in high dimensional spaces Memory efficient	Not suitable for large datasets	Time a quency bioma
Random Forest (RF)		Non-linear decision tree	Good approach for datasets with low number of variables with a lot of observations Acceptable performance for unbalanced datasets	Overfitting Bad generalization Low control on model performance	Clinical measur sign oma
Extra Gradient Boosting (XGBoost)		Gradient boosted decision trees	Increased speed and performance Allows training very large models Supports parallelization Handling of missing values Can include new samples after first training	Training is slower than RF	Bloc omarke tion pro bioma ECC oma
Logistic Regression (LR)		Categorical or binary data labels	Intuitive and simple to code Efficient to train and fast at classifying No assumptions about distribution of classes	Overfitting present if number of observations < number of classes Assumes linearity relation on data Prediction of discrete data	LA di age,He u
Principal Component Analysis (PCA)		Dimensionality reduction	Removes correlated features Improves algorithm performance Reduces overfitting Improves visualization	Independent variables become less interpretable Data standardization required before use Information loss	Intracan cord

K-means cluster-ing		Explora-tory analy-sis	Simple to implement Scales to large data sets Guarantees convergence Easily adapts to new examples	Hyperparameters to be chosen manually Dependent on initial values Clustering may fail for different size clusters	Heart ra bi
Neural Networks (NNs)	Supervised and unsu-pervised	Different configura-tion de-pending on layers or blocks	Fault tolerance Supports parallelization Ability to train the machine	Hardware dependence Black-box nature	Sig 2D in 3D in (MR

Table 2.1. Description of the main algorithms used in supervised and unsupervised learning, including advanta in atrial fibrillation and other cardiovascular area

31

Chapter 3.

Study 1. *In silico* Trial and Artificial Intelligence

Abstract

Background: Antiarrhythmic drugs are the first-line treatment for atrial fibrillation (AF), but their effect is highly dependent on the characteristics of the patient. Moreover, anatomical variability, and specifically atrial size, have also a strong influence on AF recurrence.

Objective: To perform a proof of concept study using artificial intelligence (AI) that enables to identify proarrhythmic profiles based on pattern identification from *in silico* simulations.

Methods: A population of models consisting on 127 electrophysiological profiles with variation of nine electrophysiological variables (GNa, INaK, GK1, GCaL, GKur, IKCa, [Na]ext,[K]ext and diffusion) was simulated using the Koivumaki atrial model on 2D square planes corresponding to a normal (16 cm^2) and dilated (22.5 cm^2) atrium. The simple pore channel equation was used for drug implementation including three drugs (isoproterenol, flecainide and verapamil). We analyzed the effect of every ionic channel combination to evaluate arrhythmia induction. A Random Forest algorithm was trained using the population of models and AF inducibility as input and output, respectively. The algorithm was trained with 80% of the data (N = 832) and 20% of the data was used for testing with a k-fold cross validation (k = 5).

Results: We found two electrophysiological patterns derived from the AI algorithm that were associated with proarrhythmic behavior in most of the profiles, where GK1 was identified as the most important current for classifying the proarrhythmicity of a given profile. Additionally, we found different effects of the drugs depending on the electrophysiological profile and a higher tendency of the dilated tissue to fibrillate (Small tissue: 80 profiles vs Dilated tissue: 87 profiles).

Conclusions: AI algorithms appear as a novel tool for electrophysiological pattern identification and analysis of the effect of antiarrhythmic drugs on a heterogeneous population of patients with AF.

3.1. Introduction

The first-line treatment for AF are antiarrhythmic drugs, although undesirable proarrhythmic effects have been identified in some cases. The response to these drugs is highly dependent on the specific baseline electrophysiological characteristics of the patient. In this framework, safety pharmacology has emerged as a new field in cardiac arrhythmias with the aim of identifying the drug hazard (Kraushaar et al., 2012; Mirams et al., 2012; Davies et al., 2019) by detecting the probability of triggering an arrhythmia. Different tests have been designed with the objective of determining the proarrhythmicity of a given compound (Falk, 1989; Crumb et al., 2016; Passini et al., 2017).

Variability is, consequently, an important factor to be studied and analyzed to understand its dependency between the specific characteristics of the patient and the effect of the drug. In this scenario, several studies have included and incorporated variability in mathematical approaches by means of a population of models (Britton et al., 2013; Liberos et al., 2016; Muszkiewicz et al., 2016; Bai et al., 2021) to account for the electrophysiological heterogeneity presented in a real population of patients. Other approaches have also been implemented in more recent studies such as the CiPA initiative, that combines in vitro, *in silico* and clinical data to build a platform that can be used for testing new drugs and their potential harmful effects (Stockbridge) in ventricular myocyte models. In addition, studies have also explored electrophysiological variability to identify potential currents involved in AF triggering and maintenance (Ellinwood et al., 2017; Bai et al., 2020). However, these approaches usually focus at unicellular level or present low variability at electrophysiological level in the field of AF.

Anatomical complexity has also been incorporated including *in silico* studies using 2D and 3D structures rather than unicellular approaches to evaluate the proarrhythmicity of anatomical structures (Varela et al., 2016). Within this framework, several studies have identified specific currents or biomarkers that can explain or characterize the proarrhythmicity of a compound. New scenarios considered at this stage the use of sophisticated statistical methods that can, not only identify isolated biomarkers, but groups or clusters that better react to a specific treatment. Although the use of a population of models for the evaluation of proarrhythmicity usually present a broad representation of the electrophysiological characteristics of these patients, other variables that highly influence the arrhythmia induction and

maintenance should be explored. For example, other factors aside from ionic remodeling that can affect AF maintenance can be found in the literature such as the size of the atria, that has been previously identified as an increased probability of triggering an arrhythmia for bigger or dilated tissues. With all these considerations, a new dimension is included in the simulations, introducing anatomical variability into the important factors underlying arrhythmia maintenance (Nattel et al., 2008; Qureshi et al., 2014).

However, and despite the complexity included in all these studies, the identification of new biomarkers or patterns is still challenging and present low accuracy metrics. Our hypothesis is that Artificial Intelligence (AI) can extract patterns or clusters from *in silico* simulations that can help to better predict the effect and risk of antiarrhythmic therapies.

Here, a population of models with AF, including electrophysiological and anatomical variability, was used to study the effect of different drugs on the arrhythmia behavior and was then analyzed by means of AI algorithms. Our research is built on previous studies using population of models (Liberos et al., 2016) showing the importance of specific currents on the drug effect. In addition, previous studies have identified one ionic current or a combination of them (Pandit et al., 2005; Dobrev et al., 2011; Jiang et al., 2017) but none of them have implemented an algorithm that specifies the threshold for each variable of the ionic profile. Our algorithm was developed as a proof of concept of AI applied to population of models guiding the identification of the effect of drug therapy on a heterogeneous population.

3.2. Materials and Methods

3.2.1. Electrophysiological Variation: Description of the Population of Models

To obtain data for the population of models, samples from the right atrial appendages from 149 patients diagnosed with chronic AF in which antiarrhythmic medication was interrupted before the study were available (Wettwer et al., 2013; Sánchez et al., 2014).

Briefly, patch clamp was performed in all the samples obtaining the values for different currents. A total of six biomarkers were used to quantify variability in action potentials (AP) including AP duration at 20, 50 and 90% of repolarization (APD20, APD50, APD90 respectively), AP amplitude (APA), resting membrane potential (RMP) and AP plateau potential at 20% of APD20 (V20). The maximum and minimum values of these biomarkers at a pacing frequency of 1Hz are presented in Supplementary Table 1.

To build the computational population of human AF models, different combinations of ionic currents were generated from the experimental data

described earlier. In further detail, Latin Hypercubic Sampling (LHS) (McKay et al., 1979) and the baseline AF model developed by Koivumaki et al. were used for its generation.

A total of nine parameters were varied from -50% to +100% of their original value: fast Na+ ionic conductance (gNa), Na+- K+ pump (INaK), inward rectified K+ current (gK1), L-type calcium ionic conductance (gCaL), ultrarapid outward ionic conductance (gKur), Ca2+-dependent K+ current (IKCa) and Na+ and K+ extracellular concentration and the diffusion coefficient of the reaction-diffusion equation (Supplementary Figure 2). LHS produced 500 different combinations of these nine parameters from the initial 149 patients. Simulations for these 500 profiles were calculated on 2D planes of 8x256 nodes to evaluate the AP metrics. The models were simulated by pacing at 1Hz (using a 3 ms stimulus duration, twice diastolic threshold amplitude). The APs of three cells along the plane (cells 500, 620 and 748) were analyzed following a train of 15 periodic stimuli and the last 5 periodic stimuli were considered in order to ensure steady state. Only the models that fitted into the experimental constraints (Supplementary Table 1) were considered as representative human electrophysiological models for the final population, resulting in 127 final profiles (Simon et al., 2017).

3.2.2. Chronic Atrial Fibrillation Electrophysiological Cellular Model

Different atrial models have been described at unicellular level to characterize the electrophysiological response. In this study, we implemented the Koivumaki model with Skibsbye modifications (Skibsbye et al., 2016) that includes a reformulation in sodium current to characterize sodium channel inactivation, adjusts transient outward potassium current and L-type Ca+ current, and includes the small conductance calcium-activated potassium current (IKCA). In addition, the model used for simulations included AF remodeling, achieved by modifying the following ionic currents: L-type Ca2+ (ICaL) decreased by a 55%, transient outward current (Ito) decreased by 62%, rapid delayed rectifier potassium channel (IKur) decreased by 38%, inward-rectifier potassium channel (IK1) increased by 62%, Na/Ca exchange current (INCX) increased by 50%, expression of SERCA decreased by 16%, phospholamban to SERCA increased by 18% and sarcopilin to SERCA decreased by 40% as described in (Koivumäki et al., 2014). This model was used for both the calibration of the population of models previously described and the rest of the experiments in the study.
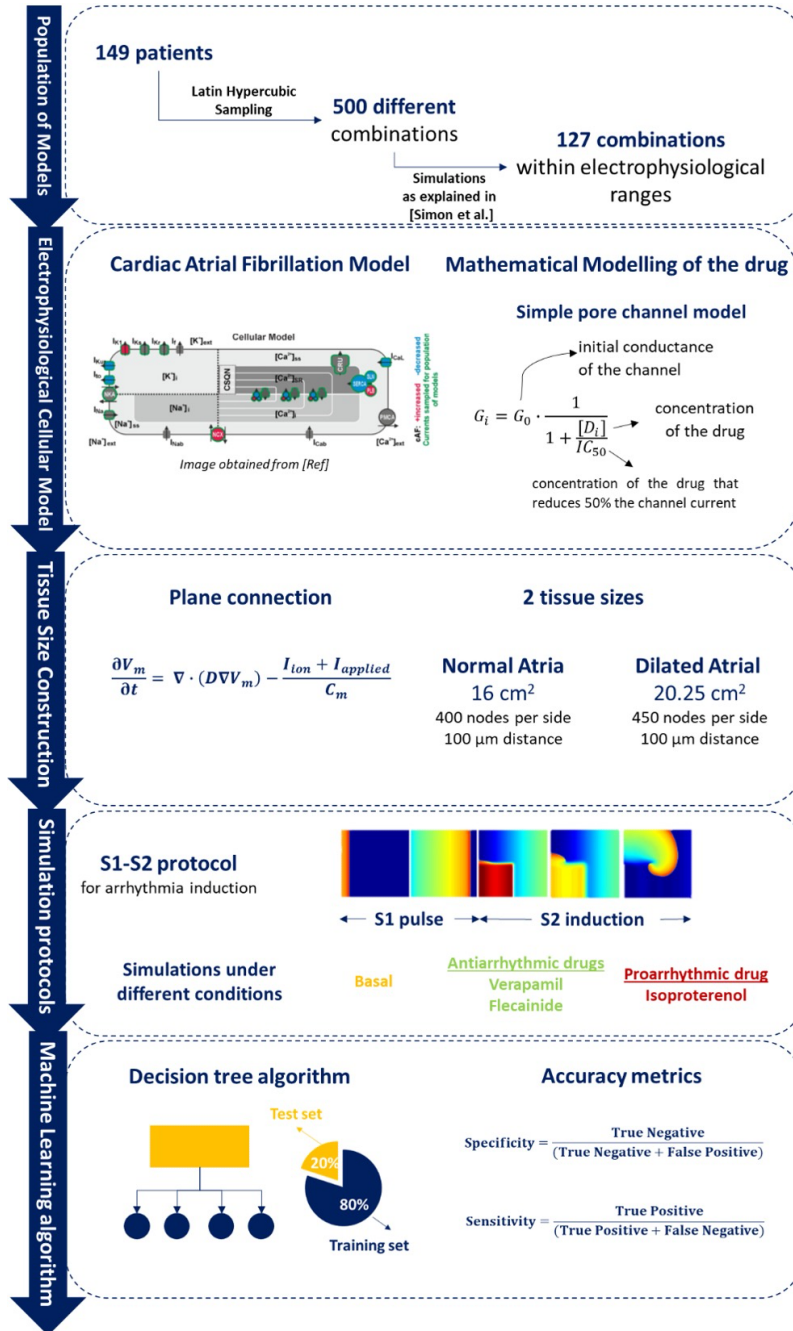
Figure 3.1. Overall methodology description including 1) population of models calibration as described in (Simon et al.). Samples from 149 patietns were obtained to evaluate 500 different ionic combinations that resulted in a final pool of 127 electrophysiological profiles that composed the population of models 2) brief description of the Koivumaki electrophysiological model used and the mathematical modelling of the drug as described 3) connection between different cells for plane simulations and tissue size

used for each for the of the 2D planes used 4) S1-S2 arrhythmia induction protocol simulation and pharmacological compounds simulated during the experiments 5) Artificial Intelligence algorithm training (80% of data) and testing division (20% of data) for the identification of proarrhythmic profiles.

3.2.3. Anatomical Characterization: Monodomain Equation and Tissue Size

Simulations were performed on 2D planes mimicking a sheet of cardiac tissue. Two different tissue sizes were implemented for this study: one square plane corresponding to a normal atrium (16 cm^2, 400x400 nodes) and another square plane corresponding to a dilated atrium (20.25 cm^2, 450x450 nodes) (Kou et al., 2014).

To connect the cells within the plane, the monodomain reaction-diffusion equation was implemented, assuming that tissue behaves as a functional syncytium where membrane voltage is propagated smoothly (Clayton and Panfilov, 2008):

$$\frac{\partial V_m}{\partial t} = \nabla \cdot (D\nabla V_m) - \frac{I_{ion} + I_{applied}}{C_m} \qquad (3.1)$$

Where the ∇ corresponds to the gradient operator and D a diffusion coefficient with units distance2 time -1. By using this monodomain simplification, the tissue is considered to have an unlimited extracellular medium, so the extracellular resistivity can be neglected. The extracellular medium is isopotential an equal to cero for simplicity. Consequently, the membrane potential is the same as the intracellular potential. Planes were fully connected as shown in Figure 3.1, not including structures such as the pulmonary veins. The value of the diffusion constant, referred as D in the above equation, was varied among the different profiles as part of the variability included in the population of models.

3.2.4. Mathematical modelling of the drug

Both antiarrhythmic and proarrhythmic drugs were evaluated in the electrophysiological population of models in order to characterize the effect according to tissue size and ionic currents. Three different drugs were studied presenting different mechanisms and effect: verapamil, flecainide and isoproterenol. Briefly, verapamil is an antiarrhythmic drug that acts as a calcium blocker, flecainide is an antiarrhythmic drug that acts as a sodium blocker and isoproterenol is a proarrhythmic agent (β receptor agonist) that increases intracellular calcium. All three drugs are currently used in clinical

practice and its effect, although established as proarrhythmic or antiarrhythmic, can vary from patient to patient (Bassett et al., 1997). Simple pore channel equation was used for drug implementation at computational level including three channels for each drug that was modelled according to experimental IC50 values to calculate the block of the channel (Dempsey et al., 2014). The model used is described as follows:

$$G_i = G_0 * \frac{1}{1 + \dfrac{[D_i]}{IC_{50}}} \qquad (3.2)$$

Where the G0 represents the initial conductance of the channel for each of the profiles in the population of modes, [Di] corresponds to the concentration of the drug and IC50 is the concentration of the drug that reduces by 50% the channel current. For verapamil and flecainide, values from (Crumb et al., 2016) were implemented. Isoproterenol was modelled increasing the permeability of the calcium current as stated in (Vescovo et al., 1989). The numerical values for each modeled drug can be observed in Table 3.1, including the concentration at which the drug was modelled.

Table 3.1. Parameters for modelling the drug effect including drug concentration, IC50 for the three specific channels modelled. *Corresponds to EC50.

	Drug Concentration (mM)	Nav1.5-peak	hERG	Cav1.2
Flecainide	2.0 e-04	6.7	0.7	20
Verapamil	5.0 e-04	1.0	0.7	0.1
Isoproterenol	8.0 e-02	-	-	20*

3.2.5. Simulation protocols

Simulations were performed implementing differential equations computed with a time step of 1 microsecond for Euler method using in-house software written in C++ with CUDA parallelization and solved with a NVIDIA TESLA C2057 GPU. Rush Larsen method was developed for cell models as it offers stability to the problem by calculating the exact solution for the gating variables. Since all the equations governing the gating variables have a similar structure, the method uses the following expression to solve them:

$$w_i^{j+1} = e^{ai(v)h}\left(w_i^j + \frac{b_i(V)}{a(V)}\right) - \frac{b_i(V)}{a(V)} \qquad (3.3)$$

Consequently, all equations for gating variables were solved by the previous expression whereas the rest of equations were solved by the forward Euler Method.

2D planes were simulated for a total of three impulses (S1) at 1 Hz followed by a fourth one (S2) for arrhythmia initiation. S2 was induced in the cells of the inferior left section of the plane, producing reentry in part of the models. For a given combination of ionic channels in the population of models, an arrhythmia was induced when >1 complete rotational activity followed the S1-S2 induction protocol. In addition, rotor tracking was studied for two specific profiles that is discussed in the result section. The methodology for rotor tracking has already been described in previous publications of the group (Rodrigo et al., 2014). Briefly, phase maps of the simulations were calculated by using Hilbert transform from which singularity points were calculated. A Singularity Point (SP) is defined as the point in a phase map that is surrounded by phases from 0 to 2π. Only those singularity points that were present for the duration of at least 1 full rotation were considered, as described in (Rodrigo et al., 2014). Rotor tracking was defined as the connection between SPs across spherical layers at a given time. Only filaments that completed at least 1 rotation on the outermost surface were considered.

Random Forest Algorithm for AF maintenance prediction

A total of 1016 simulations were computed in this study corresponding to all different combinations of the population of models (127 profiles) simulated in different tissue sizes (2 tissue sizes) and four different conditions (baseline conditions, two antiarrhythmic drugs and one proarrhythmic drug), creating a database with different ionic conductance combinations and tissue size.

Random Forest, which is a decision algorithm consisting on a multitude of decision trees at training time, was implemented to output two possible outcomes: induced or non-inducible AF. This algorithm was trained including the eight variables of the population of models as an input and the presence of AF form simulations as an output to evaluate patterns that may lead to AF maintenance. The algorithm was trained with 80% of the data (N = 832) and 20% of the data was used for testing with a 5k fold cross validation.

3.3. Results

3.3.1. AF induction on the Population of Models

Table 3.2. Profiles maintaining rotational activity for different drug and tissue size. For each tissue size and basal/drug condition, the table specifies the number of profiles with A inducibility. Percentage of the profiles with reentry is specified in parenthesis for every 127 profiles simulated in each case.

		Atrial Fibrillation	Sinus Rhythm
Small	Basal	80 (63.00%)	47 (37.00%)
	Flecainide	37 (29.13%)	90 (70.87%)
	Verapamil	37 (29.13%)	90 (70.87%)
	Isoproterenol	88 (69.29%)	39 (30.71%)
Dilated	Basal	87 (68.50%)	40 (31.50%)
	Flecainide	63 (49.61%)	64 (50.39%)
	Verapamil	64 (50.39%)	63 (49.61%)
	Isoproterenol	94 (74.02%)	33 (25.98%)

From the complete population consisting on 127 different electrophysiological profiles, 80 profiles maintained the reentrant activity at baseline conditions in the normal tissue size and 87 in the dilated atrium. Complete quantification of the profiles maintaining reentry can be observed in Table 3.2, including the effect of the three simulated drugs. As shown, dilated tissue increased the number of profiles maintaining reentry in all cases, independently of the presence and type of drug.
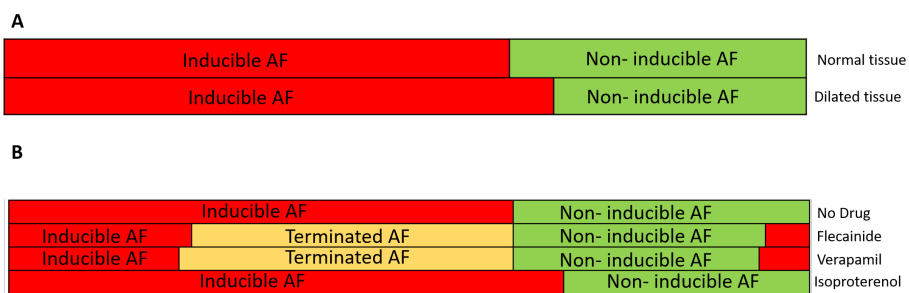
Figure 3.2. A. Distribution of the population of models with induced and non-inducible AF for the normal tissue (top) and the dilated tissue (bottom). Red color shows the proportion of the models with inducible AF during simulation and green color shows the proportion fo the models with non-inducible AF. B. Distribution of the population of models for the normal size tissue under the four studied conditions (no drug, flecainide, verapamil and isoproterenol) with proportion of inducible AF (red), non-inducible AF (green) in each of the cases. Terminated AF (yellow) corresponds to the profiles that,

due to the electrophysiological changes induced by the drug, the reentry was not inducible.

The analysis of the simulations resulted in the identification of profiles that responded differently to the arrhythmia induction under the effect of the drug, as it can be observed in arrhythmia induction Figure 3.2. Non-inducibility of the arrhythmia was observed in the majority of the profiles when the antiarrhythmic compounds, verapamil and flecainide were used. However, in some of the profiles that did not induce the arrhythmia at baseline, the addition of one of those drugs induced rotational activity (Figure 3.2B). Specifically, the addition of flecainide gave rise to non-inducibility of the arrhythmia in 51 profiles and induced AF in 7 profiles that were non-inducible at baseline. For verapamil, 53 and 8 profiles were non-inducible and induced the arrhythmia respectively in normal tissue size samples. Interestingly, all the profiles that showed proarrhythmic and antiarrhythmic effect in the flecainide scenario presented the same behavior in the verapamil scenario. Although verapamil and flecainide showed similar results, the overall action potential morphology was significantly different for the same profile under the effect of these drugs, as it can be observed in Figure 3.3 and Figure 3.4, where the curvature of the action potential is modified due to the effect of the drug at ionic level. Isoproterenol showed a proarrhythmic effect increasing the number of AF maintaining profiles in 8 cases.

3.3.2. Antagonistic effects can be observed for the same drug among the population of models

Antagonistic effects of both antiarrhythmic and proarrhythmic drugs were observed on the population of models. Figure 3.3 presents a specific ionic profile simulated for all four conditions (basal and three drugs) in which reentry was maintained over time in the basal scenario. When the simulation was repeated under the effect of verapamil or flecainide, the arrhythmia was not induced. With the addition of isoproterenol, the arrhythmia was, not only induced but rotational activity presented a higher activation frequency.

For another specific profile shown on Figure 3.4, antagonistic effects were observed: for a profile in which arrhythmia was not induced under basal conditions, verapamil and flecainide showed a proarrhythmic effect, meaning that the arrhythmia was induced, while isoproterenol did not induce the reentry for the complete simulation. Furthermore, for these aforementioned profiles, rotor tracking shows lower area and higher complexity on the simulations in which the arrhythmia was maintained over time, exhibiting the stability of the reentry. Flecainide and verapamil terminated AF for the majority of the profiles in which AF was maintained under basal con-

ditions, whereas isoproterenol induced AF in new profiles that were not inducible in basal conditions. Interestingly, a small proportion of models presented AF induction under the effect of verapamil and flecainide (Figure 3.2B) despite the absence of AF induction at baseline.
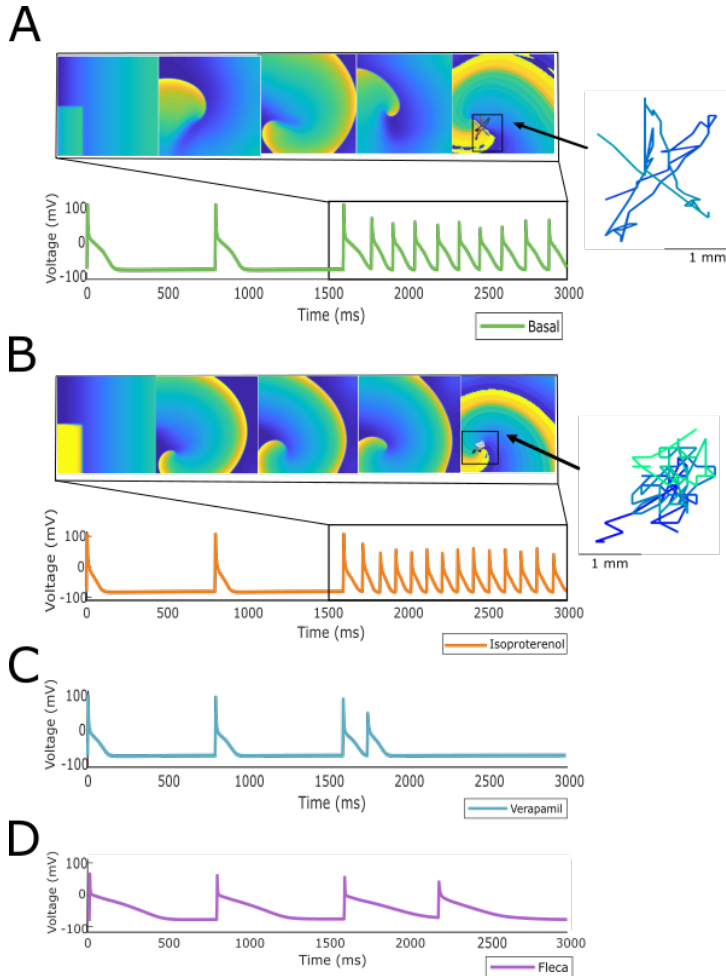
Figure 3.3. Specific profile from the population of models showing: A. Inducible AF after stimulation protocol B. Inducible AF due to effect of isoproterenol, showing and increase on the activation dynamics C. Antiarrhythmic effect of verapamil and D. Antiarrhythmic effect of flecainide. As an example, rotor meandering is shown in panel A and B, exemplifying the effect of isoproterenol in the arrhythmia stabilization.
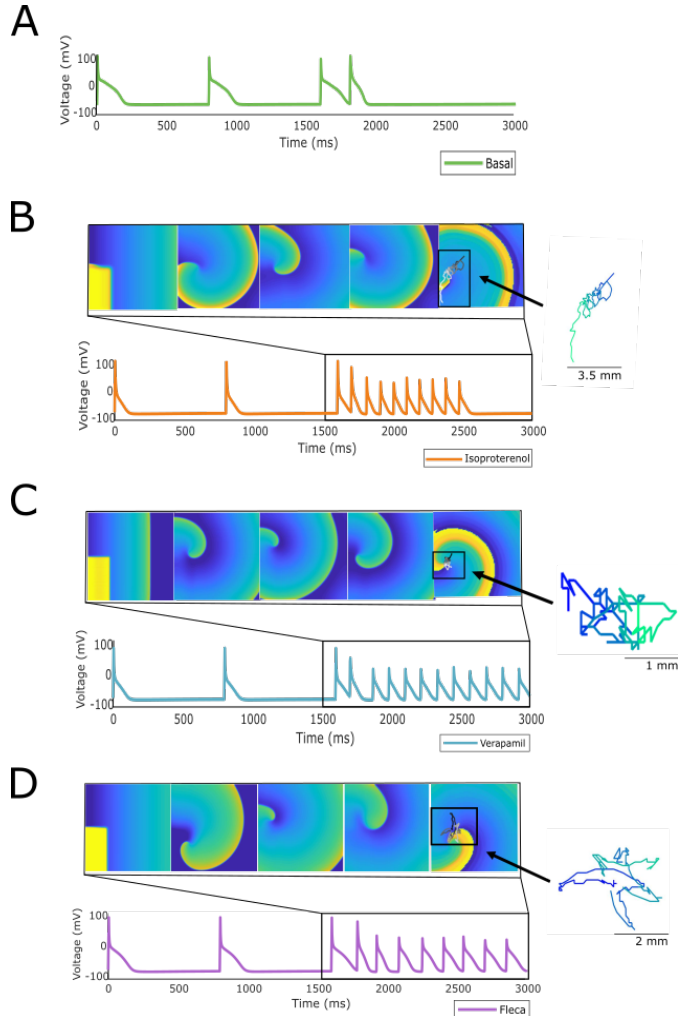
Figure 3.4. Specific profile from the population of models showing: A. No AF induction using the stimulation protocol described. B. Induction but not maintenance of AF when simulation was repeated under the effect of isoproterenol C. Induction and maintenance of AF under the effect of verapamil and D. Induction and maintenance under the effect of flecainide. As an example, rotor meandering is shown in B, C and D panels exemplifying the effect of the drugs in arrhythmia stabilization.

3.3.3. Machine Learning Algorithms Help Understand and Predicts the Ionic Channels Effect

We generated a final database of 1016 simulations that included the basal and drug administration state for both tissue sizes. Therefore, these data represented: 1) the variables of the population of models, 2) the electrophysiologic change conferred by the drug administration; and 3) the changes between normal and dilated tissue size. Then, the database was processed in order to train and calibrate a decision algorithm for drug effect

prediction. As a result, the Random Forest algorithm, shown in Figure 3.5, was obtained. The algorithm had in total seven different consecutive layers, shown in Figure 3.5A that cluster similar profiles together for prediction of AF induction based on the conductance values in the form of a sunburst diagram. In this diagram, each level is represented by a concentric circle containing one or more variables from the population of models, where each level presents threshold values for decision making. To evaluate a specific profile, the decision algorithm starts the clustering process from the most inner circle, that corresponds to the GK1 variable. For each variable, a threshold value has been defined that has to be compared with the value of the variable for the specific profile that is being evaluated. Specific values for each threshold can be consulted in the Supplementary Material Figure 1. For example, in the case of GK1 this value corresponded to 9.12%. If the value of the profile is higher than 9.12%, the next level to be considered will correspond to the right part of the diagram and the next variable (High GK1) to continue the characterization, corresponding to the diffusion variable. In contrast, if the value of the profile is lower than 9.12% for GK1, the next level to be considered will correspond to the left part of the diagram and the next variable, identified as K0. This process should be completed until the last layer or circle of the diagram, finding the path or cluster to which a given profile belongs. Figure 3.5B shows the paths or clusters that have been identified as inducible AF by the algorithm.
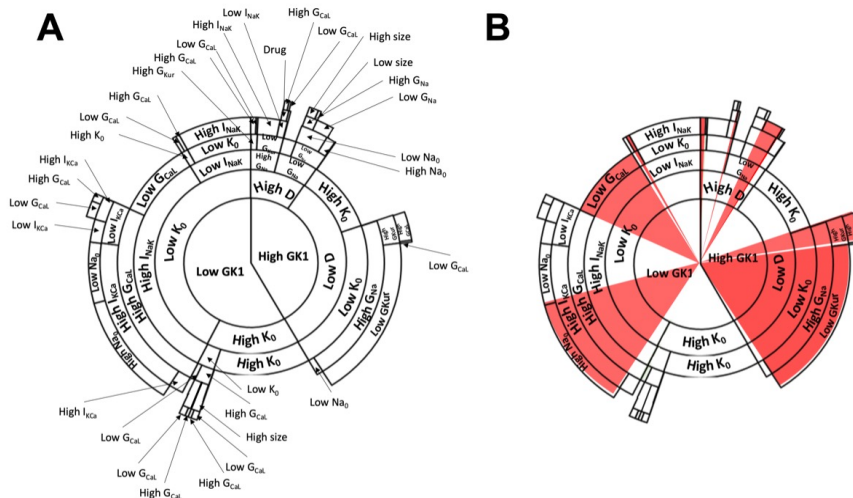
Figure 3.5. A. Decision tree algorithm of the change in conductances based on the population of models with the information of the examples presented in Figures 3.1 and 3.2. The decision tree starts from the center of the circle and continues in an outward trend including all the variables described in the population of models. Specific paths of

the decision algorithm led to induced AF, that are shown in red (inducible AF) in panel B.

Interestingly, if the paths of clusters from the diagram are analyzed, it can be observed that one of the main contributions that lead to AF inducibility is the combination of profiles with high conductance of the inward rectifier K+ channel (K1), low diffusion, high concentration of extracellular potassium, high conductance for the sodium channel and low conductance of the ultra-rapidly activating delayed rectifier current (IKur). Another combination that leads to AF was low conductance value for IK1, low concentration of extracellular potassium, high conductance for the sodium potassium pump, high conductance for the slow calcium channel, high conductance for the calcium-potassium pump and high conductance for the INa channel.

Figure 3.6 shows an example of how the change in conductance of specific channels can affect the final path or cluster to which a specific profile belongs, altering the final outcome of the decision tree algorithm. In this figure, specific pathways of the decision tree are exemplified in each of the panels, highlighting how the change due to the addition of the drug affects specific levels that, depending on the final permeability of the channel, may be fundamental for the induction and maintenance of the rotational activity. Panel A and C highlight changes on calcium channel conductance, that can be affected by the addition of verapamil or isoproterenol, as both drugs were modeled to respectively decrease or increase the permeability of this channel. Specifically, Panel A exemplifies how the increase on permeability of calcium channel, by the addition of isoproterenol, has a proarrhythmic effect. Conversely, a profile that presents high conductance of the calcium channel can be reduced by adding verapamil and changing to a state of non-inducibility of AF. Panel C shows another example in which the decrease of calcium permeability results in AF inducibility and the increase of calcium permeability increases the probability of AF non-inducibility.

Examples for flecainide, which affects sodium channel permeability, are shown in Panel B and D. Specifically, Panel B shows an antiarrhythmic effect of the addition of flecainide, by blocking sodium channel. Panel D shows a level of the decision tree algorithm at which, by changing sodium channel permeability, the probability of AF non-inducibility increases. Thus, the probability of inducing AF is higher for those profiles with lower sodium permeability, showing a proarrhythmic effect of the drug.
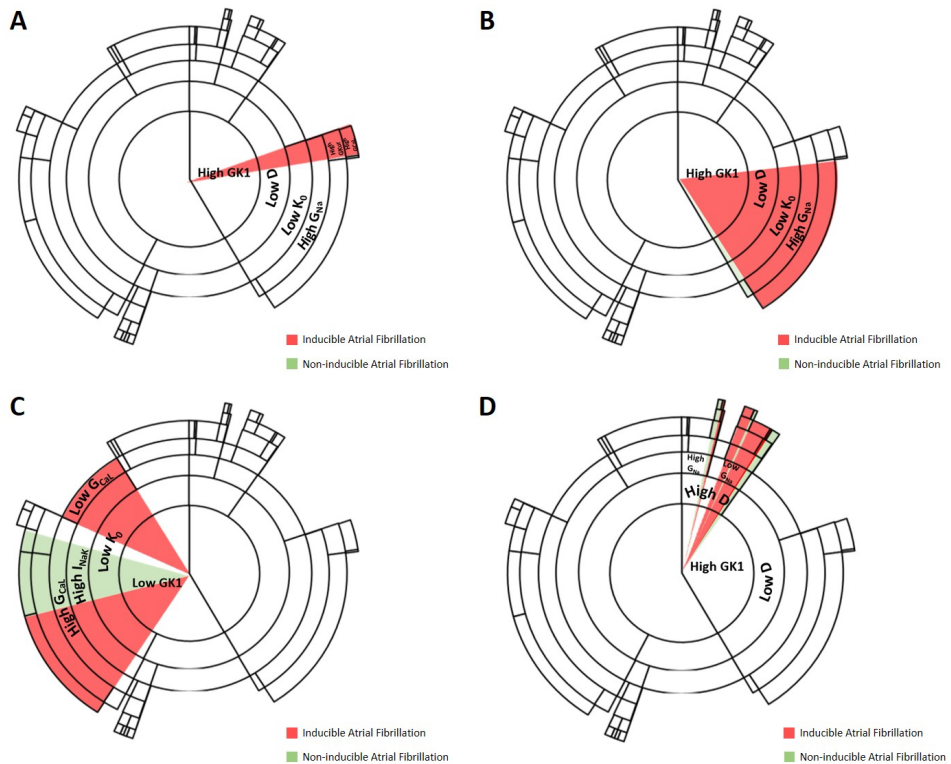
Figure 3.6. Examples of change in channel conductivity that lead to a change in induced/non-inducible AF. A. Level at which increase of calcium channel conductance permeability results in maintenance of AF, example of the proarrhythmicity of isoproterenol. B. Level at which decrease of sodium conductance results in AF non-inducibility, example of antiarrhythmic effect of flecainide. C. Level at which increase or decrease of calcium channel permeability results in AF induction, example of verapamil being anti-arrhythmic and isoproterenol having a proarrhythmic effect. D. Level at which increase of sodium permeability increases the probability of AF inducibility.

3.4. Discussion

In this study we present a new algorithm that identified and clustered the combination of channel conductivities that promoted arrhythmia initiation. The algorithm was calibrated with *in silico* data obtained from 2D simulations in two different size planes simulated on a population of models under the effect of three different drug effects (isoproterenol, verapamil and flecainide) resulting in 1016 different simulations. The main result of the study was the following: first we proved, in a population of models simulation environment, that dilated tissues are more prone to induce AF and that the effect of a given drug can differ from one profile to another depending on the specific expression of the currents. Finally, we also proved that all

this information can be used to train a machine learning algorithm to predict AF inducibility of the tissue.

3.4.1. Variability on AF simulations: Ionic and tissue size variation

The population of models have been widely used in the cardiac electrophysiology field for safety pharmacology, providing new platforms for the assessment of proarrhythmic effects of drugs (Passini et al., 2017; Kügler, 2020). In this study, we have analyzed how variations of the electrophysiological and anatomical characteristics can affect AF inducibility at 2D level. Electrophysiological variability was introduced by using a population of models varying different ionic conductances and extracellular ionic concentrations on a cellular model of chronic AF human atria cardiomyocyte and the anatomical variability was implemented by using models with two different tissue sizes.

This study revealed that simulated dilated atria presented more profiles maintaining reentry, therefore confirming the hypothesis that larger tissues are more prone to fibrillate, effect that has already been shown at clinical level (Zou et al., 2005; Qureshi et al., 2014).

3.4.2. Drug Effect on the Population of Models

The population of models was not only evaluated at basal conditions, but also under the effect of three different cardiovascular drugs: flecainide, verapamil and isoproterenol. Overall pharmacological effects of the implemented drugs matched their clinical characteristics, mainly exhibiting antiarrhythmic effects in the case of flecainide and verapamil (Klein et al., 1979; Echt and Ruskin, 2020). It is interesting to point out that, in the case of dilated tissue experiments, the proportion of non-inducible AF in simulations with flecainide or verapamil was lower than for the smaller tissue size profiles. Furthermore, whereas flecainide and verapamil exhibited mainly an antiarrhythmic effect, isoproterenol exhibited a proarrhythmic effect (Oral et al., 2008). However, some antagonistic effects were observed as exhibited on Figure 3.3 and Figure 3.4, following the same behavior observed at clinical level where undesirable effects of antiarrhythmic compounds have been identified in a minority of patients (Nogales Asensio et al., 2007). This confirms our hypothesis that the effect of the drug can be different depending on the specific expression of the ionic currents. Antagonistic effects of antiarrhythmic drugs have previously been studied (Donnelly, 2004) stating the need of identifying the different factors that can lead to this response such as genetics or drug dynamics, which are not considered in this study. However, none of these approaches analyzed the effects on a population of models of the atria.

Furthermore, we observed that the profiles that changed its behavior when adding a drug were similar in the case of the antiarrhythmic drugs simulated in this study. This suggests that specific groups with similar characteristics have analogous responses.

3.4.3. Artificial Intelligence Algorithms for Arrhythmia Maintenance Prediction

As the number of simulations reached a significant number of samples with an increasing information volume, AI algorithms were applied to reveal patterns in the data. AI application on clinical environments is exponentially increasing and leading towards new diagnostic and treatment techniques (Feeny et al., 2020; Sánchez de la Nava et al., 2021). This trend has also been implemented in the electrophysiology field (Muffoletto et al., 2021; Siontis and Friedman, 2021), in which the use of algorithms has been used for detecting or evaluating proarrhythmicity (Shao et al., 2018; Halfar et al., 2021), classifying different rhythms (Wasserlauf et al., 2019) or automatizing tasks as segmentation (Yang et al., 2017). Moreover, its use in safety pharmacology could be applied to analyze all the data produced by *in silico* simulations. Particularly, Random Forest algorithm grouped similar profiles with the same outcome, therefore implementing an AI-driven algorithm able to predict, based on the ionic combinations of each profile, the probability of AF inducibility with excellent predictive values (Sánchez de la Nava et al., 2021).

Data interpretability in the AI field has demonstrated to be important, especially in the clinical field, where the understanding of the patterns found by algorithms is usually described as a black-box that does not allow to evaluate the biomarker identification and the decision outcome (Nicholson Price, 2018). In this case, the methodology used allowed to analyze high amounts of data and to understand the clinical implications of the characteristics of each cluster. For example, the first variable that initiated the classification on the Random Forest algorithm was found to be the inward rectifier K+ channel that at clinical level has a crucial role in controlling frequency and stability of rotors responsible for AF (Pandit et al., 2005). Moreover, up-regulation of IK1 increased the ability to sustain faster and longer-lasting reentry, predisposing to the development of tachyarrhythmias (Noujaim et al., 2007).

Thus, the identification of this current as the first of the algorithm denotes the importance in the arrhythmia induction and maintenance mechanisms, as overexpression of this repolarization current has been associated with rotor acceleration as a consequence of a reduction in the action potential duration (Atienza et al., 2006; Pandit et al., 2011). The identification of

this variable by the algorithm shows that the patterns are explainable and represent clinical scenarios that can be found in a real-life AF population.

This variable was followed by a succession of combinations resulting as several clusters with similar profiles associated with AF inducibility. Interestingly, from the overall implementation of the AI algorithm, two patterns were identified showing an increase in AF inducibility related to changes in extra and intracellular potassium levels and allowed a clinical interpretability of the results that facilitates the understanding of the patterns found by the algorithm. A first cluster was found showing increased expression and concentration of potassium ions, that can be directly related to hyperkalemia. Another different pattern observed in a group with different profiles presented low values of both ionic expression and ionic concentration of potassium, that can be directly related to hypokalemic conditions (Guo et al., 2009) . At clinical level, these two conditions have been associated with the induction and triggering of different arrhythmias (Pandit et al., 2011; Skogestad and Aronsen, 2018; Rivera-Juárez et al., 2019; Rakisheva et al., 2020). More in detail, studies have shown that hypokalemia is an independent predictor of developing AF (Krijthe et al., 2013) and that specific cases of AF patients have been identified in whom hyperkalemia could induce malignant arrhythmias (Yan et al., 2018).

From the two main identified pathways that led to sustained AF reentry, the first cluster was associated with increased IK1, decreased diffusion, decreased extracellular potassium and overexpression of sodium channels (Figure 3.5). The identified decreased diffusion can be directly related to lower conduction velocity, that has already been reported as a trigger for re-entrant foci and arrhythmia induction (King et al., 2013). Beyond the key role of INa determining excitability (Bezzina et al., 2001), the identification of this first cluster confirms the strong interaction between the molecular correlates of INa and IK1 as part of a common macro-molecular complex, where resting membrane potential hyperpolarization indirectly affect rotor frequency by modifying INa availability (Milstein et al., 2012; Ponce-Balbuena et al., 2018).

In the second cluster, both ionic concentration of potassium and decreased potassium conductivity and extracellular concentration were combined with increased calcium dynamics (Current 1 and Current 2). These currents have a major role during the plateau phase of the action potential and its overexpression contributes to faster repolarization rates, shortening the action potential duration and increasing the risk of early afterdepolarizations which can give rise to initiation of rotors and fibrillation (Cerrone et al., 2007; Nattel and Dobrev, 2012).

3.4.4. Limitations

Results presented in this work were based on a population of models of 149 subjects and further samples and variation ranges should be included to explore a wider population. Besides, simulations on plane do not reflect all proarrhythmic areas present in 3D structures such as pulmonary veins or information including fiber orientation. The use of two different plane sizes did show that the arrhythmia inducibility was higher in bigger tissues but the simplicity of the model presenting constrained borders restricts the overall interpretability of the results, as the real atria contains highly complex structures that play important roles in the initiation and maintenance of AF. In addition, arrhythmia maintenance was considered for 2D planes maintaining rotational activity for more than one cycle, but further analysis should be conducted to evaluate if self-termination occurred in part of the profiles. Moreover, fibrotic tissue is a relevant condition that predispose to AF and should be included in future studies and, if possible, the variables that conform the AI algorithm should be transferable to the clinical practice using metrics such as conduction velocity or rotor dynamic biomarkers. In addition, machine learning algorithms will perform better and will show more robustness with higher number of samples and different concentrations of each of the drugs. Finally, a greater number of drugs could be simulated in order to enlarge the field of application in which the algorithm can be used.

3.4.5. Clinical Implications

The identification of specific groups or ionic characteristics that present proarrhythmic effects can be critical in the understanding of new tools for future pharmacological development. At clinical level, this type of analysis can help to personalize the pharmacological treatments for each of the patients, therefore avoiding possible adverse effects. This study presents, as a result, a new trained algorithm that includes both anatomical and electrophysiological data to evaluate arrhythmia inducibility that is presented as a proof of concept for drug effect evaluation in AF, identifying similar results when compared to the clinic where dilated atria and specific cases of adverse drug effects (Bassett et al., 1997). However, this study includes the implementation of the algorithm based on parameters that are currently difficult to obtain, therefore limiting its current application at the clinical level. New biomarkers describing the ionic characteristics at patient level should be obtained in order to apply this algorithm.

3.5. Conclusions

Safety pharmacology has evolved including *in silico* studies that predict and classify drugs attending to the risk of causing arrhythmias. In this study, we presented a population of models approach in which arrhythmia induction was evaluated by modifications in tissue size and drug administration. Higher probability of induction was observed in larger tissue and, interestingly, antagonistic effects were observed for some of the profiles, showing that for a minority of cases, the drugs may present adverse or non-desired effects. In conclusion, we present an AI algorithm as a novel tool for pattern identification and analysis of the effect of antiarrhythmic drugs on a heterogeneous population of patients with AF.

Supplementary Material

Artificial Intelligence Model
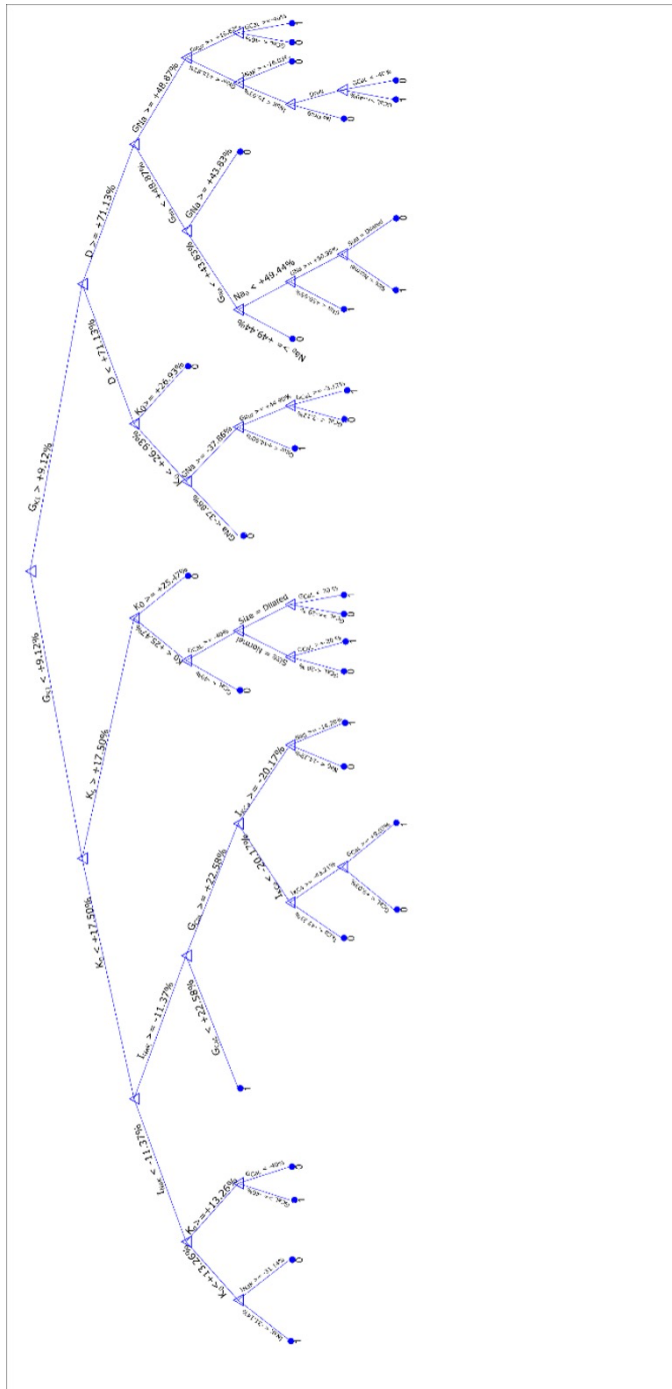
Supplementary Figure 1: Complete decision tree showing variables and threshold decision parameters.

Population of models calibration
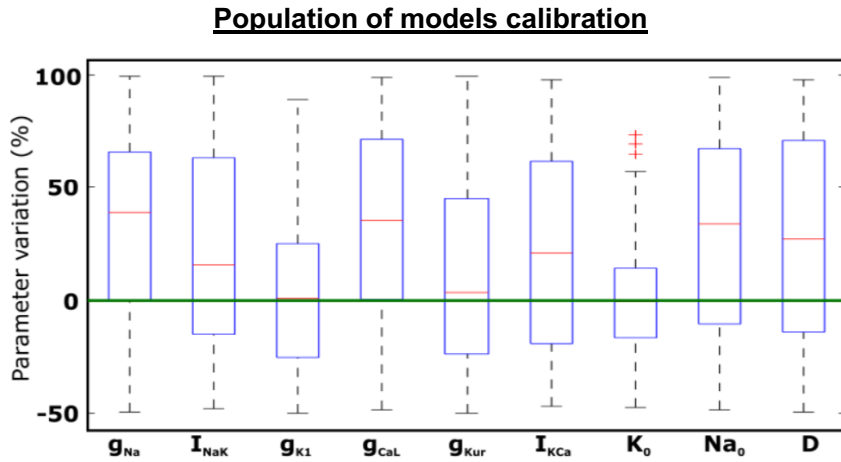
Supplementary Figure 2: Box plot showing the range and mean value of the varied parameters. Edges of the box represent the 1st an 3rd quartiles. The baseline model value is represented by the green line. A wide range of values for the diffusion coefficient, ionic conductances and concentrations is covered, being $[K^+]_0$ the most restrictive parameter. Imaged obtained from (Simon et al., 2017)**.**

	Minimum Value	**Maximum Value**
APD90 (ms)	140	330
APD50 (ms)	30	180
APD20 (ms)	1	75
APA (mV)	80	130
RMP (mV)	-85	-65
V20 (mV)	-30	20

Supplementary Table 1: Human Atrial Action Potential biomarker ranges in AF.

55

Chapter 4. Study 2: *In Silico* Technology and Clinical Data Exploitation

Abstract:

Background: Current clinical guidelines establish Pulmonary Vein (PV) isolation as the indicated treatment for Atrial Fibrillation (AF). However, AF can also be triggered or sustained due to atrial drivers located elsewhere in the atria.

Objective: To design a new simulation workflow based on personalized computer simulations to characterize AF complexity of patients undergoing PV ablation, and to validate it with non-invasive electrocardiographic imaging and evaluated at 1-year post after ablation.

Methods: We included 30 patients using atrial anatomies segmented from MRI and simulated an automata model for the electrical modelling, consisting on three states (resting, excited and refractory). In total, 100 different scenarios were simulated per anatomy varying rotor number and location. The 3 states were calibrated with Koivumaki action potential, entropy maps were obtained from the electrograms and compared with ECGi for each patient to analyze PV isolation outcome.

Results: The completion of the workflow indicated that successful AF ablation occurred in patients with rotors mainly located at the PV antrum, while unsuccessful procedures presented greater number of driving sites outside the PV area. The number of rotors attached to the PV was significantly higher in patients with favorable long-term ablation outcome (1-year freedom from AF: 1.61±0.21 vs. AF recurrence: 1.40±0.20; p-value=0.018).

Conclusions: The presented workflow could improve patient stratification for PV ablation by screening the complexity of the atria.

4.1. Introduction

Atrial Fibrillation (AF) is the most common arrhythmia, affecting a total population of 33.5 million worldwide (Chugh et al., 2014). Circumferential pulmonary vein isolation (CPVI) is considered the standard therapy for symptomatic AF patients (Hindricks et al., 2020). However, non-pulmonary vein drivers located at the posterior wall, superior vena cava, the interatrial septum sites, the terminal crest or the coronary sinus can be found and are responsible in part for the inefficiency of the ablation procedure, especially in persistent AF patients (Lim et al., 2017).

Ablation planning and evaluation of atrial pro-arrhythmic behavior may play a key role toward ablation outcome. For this purpose, the combination of personalized atrial models implemented with electrophysiological and anatomical biomarkers of abnormal behavior, have been integrated in a simulation environment to help identify arrhythmic behavior and improve novel diagnostic (Rodrigo et al., 2014) and treatment strategies (Roney et al.; Ferrer et al., 2015; Muszkiewicz et al., 2016; Aronis et al., 2019; Kim et al., 2020). Computational simulations have emerged in this field as a new tool that can be used for characterization and prediction in different scenarios, from prediction of cardiotoxic compounds (Passini et al., 2017; Yang et al., 2020), targeted ablation (Boyle et al., 2019) or recurrence after ablation (Varela et al., 2017).

In this field, automata models have been used for electrophysiological simulations to achieve simpler approaches with lowered computational time as compared to other models that include ionic level description. A lowered computational cost is translated into faster simulations with a higher number of possibilities to explore (Alonso-Atienza et al., 2005).

Here, we present a novel methodology to predict the efficacy of AF ablation based on computer simulations that included patient anatomy and different arrhythmic scenarios (i.e. different rotor location and number). These simulations were later compared with the clinical results of patients undergoing electrocardiographic imaging (ECGi) maps, CPVI and 1-year ablation outcome.

4.2. Materials and Methods

4.2.1. 4.2.1. Patient Database

We included patients undergoing CPVI for drug-refractory paroxysmal (N=14, 9 female) and persistent AF (N=16, 8 female). Candidates were patients >18-years old, history of symptomatic AF, included if sustained AF was inducible during the electrophysiological study. Patients included in this

study were admitted for ablation of drug-refractory paroxysmal and persistent AF, undergoing circumferential point-by-point ablation (Hindricks et al., 2020). All patients gave informed consent. The protocol was approved by the institutional review board of the Hospital General Universitario Gregorio Marañón.

4.2.2. Atrial Electroanatomical Complexity Evaluation Protocol

Atrial electroanatomical complexity was evaluated analyzing the number and distribution of AF reentrant sites in relation to the anatomic characterization of the atrium. To that purpose: 1) MRI imaging from patients were obtained; 2) computational simulations of cardiac activity in the reconstructed atrium were performed; and 3) the results of simulations were compared with patients´ clinical characteristics, ECGi complexity and outcomes after ablation.

The workflow followed for the evaluation of atrial pro-arrhythmic behavior is explained below and is summarized in Figure 4.1.

4.2.3. Atrial Anatomy

Magnetic Resonance Imaging (MRI) was performed in all patients before ablation procedure. MRI images with a spatial resolution of 0.7x0.7x1.5 mm were acquired 2-3 days prior to the ablation procedure and segmented using ITK-SNAP (Yushkevich et al., 2006). Images were segmented to obtain a 3D mesh of both atrial cavities using growing region automatic segmentation for both atria separately. Later, Meshmixer software was used to combine both left and right atrium. After obtaining the raw anatomies, meshes were resampled to obtain a 200μm resolution for simulations. An example of the final mesh used for simulations, that includes the atrial anatomical complexity present in patients, can be observed in Figure 4.1. Left atrial area (mm2) was measured in every anatomy for further analysis together with the electrophysiological variables obtained from the workflow.

4.2.4. Computational Models of the Atria

Once the atrial anatomies were segmented, simulations were run under AF conditions where rotational activity could be characterized. Overall, for each anatomy, 100 simulations per patient run with different initiation protocols using the corresponding individualized anatomical model for 1000 ms. These simulations had an arbitrary location of rotational activity patterns on the atrial cavity ranging from 1 to 10 rotors simultaneously, ensuring the total coverage of the atria for later evaluation.
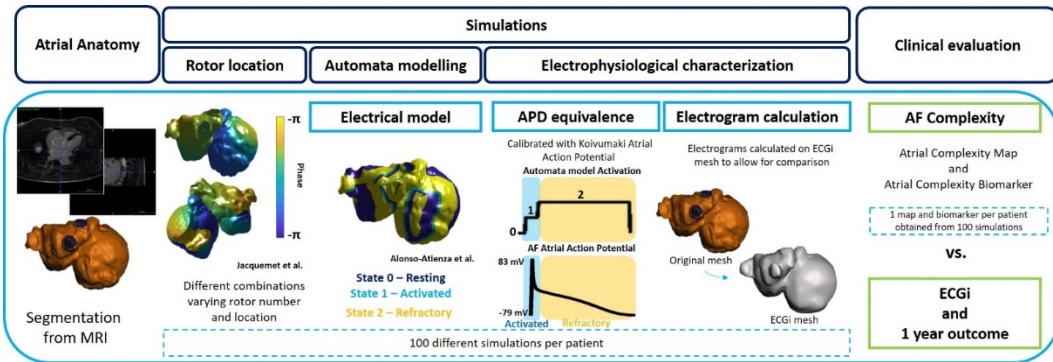
Figure 4.1 Simulation protocol (from left to right): Biatrial anatomy segmentation from MRI. Rotor location with Jacquemet algorithm on atrial anatomy. Simulation with 3-state protocol (Alonso Atienza et al. model) with rotor location obtained from Jacquemet et al protocol. Electrophysiological characterization by translation of the activation pattern into APD equivalence and later electrogram calculation. Evaluation of the simulation by means of new biomarker calculation and validation with rotor histogram.

This protocol was repeated 10 times per geometry to increase the number of simulations, achieving a final number of 100 simulations per anatomical model. First, rotational activity was distributed over both cavities of the atria with different locations each time. After the location of the rotors was obtained (Herlin et al., 2013), the automata model was run to evaluate the evolution of the scenario and posterior characterization. These models, although with simpler formulations, allow the presence of more complex scenarios including location of higher number of rotors. The models for rotor location and activation model are explained in subsequent sections. A brief description of the difference between ionic-level electrophysiological models and automata models showing examples in 2D planes is further discussed in Supplementary Material.

AF Initiation: Automatic Rotor Location

Jacquemet et al. algorithm (Herlin et al., 2013) was implemented for the development of automatic location of the rotational activity. This implementation, based on an eikonal-diffusion solver, allows obtaining computed activation maps similar to those obtained in the mono-domain model, with the option of varying the number of rotors in the model from 1 single rotational foci up to 14 (Herlin and Jacquemet, 2011). The location of the rotational activity was arbitrary and only depended on the curvature of the model. As Jacquemet's algorithm is calibrated in phase, a conversion into the labels for the automata model (3 discrete states) was performed to continue with the workflow.

Automata Model Simulations

An automata model based on activation patterns was implemented to simulate cardiac activity in the atrial cavity. Alonso-Atienza's model (Alonso-Atienza et al., 2005) was implemented to perform simulations with three different states (state 0 or resting, state 1 or activated, and state 2 or refractory period) that depended on the probability equation depicted below, where E represents the excitability of the unit, A the activation and D the distance matrix.

$$P_j^{exc} = E * Q = E * \sum_{I \neq J} \frac{A_i}{D_{ij}^2} \quad (4.1)$$

A more detailed description of this model, including all the equations and variables can be found in the Supplementary material. All nodes in the mesh were simulated following this model, i.e. no differences were implemented for different regions nor fiber orientation. NVIDIA Titan XP was used for all the simulations and posterior analysis of the workflow. Simulations were run in Microsoft Visual Studio 2017 and characterization of the simulations was performed in Matlab. The estimated ionic simulated model cost was 275 minutes vs. automata model: 42 minutes for 1-second simulation during AF, including stabilization and arrhythmia induction for the ionic model.

Electrophysiological Equivalence and Characterization

The evaluation of the electrophysiological properties of the simulations, that included the 3 states of the simulations of the automata, were calibrated using Koviumaki Action Potential Duration (Skibsbye et al., 2016) to translate the automata model into measurable atrial electrophysiological signals. For this purpose, the square pulses that are identified as activations in the automata model, were directly substituted with the atrial APD morphology of an AF model used in previous publications of the group(Sanchez De La Nava et al., 1AD).

Once the electrophysiological information was recovered, electrograms were calculated for each node. More specifically, from each simulation, a uniform mesh of pseudo-unipolar electrograms was calculated under the assumption of a homogeneous, unbounded, and quasi-static medium (Rodrigo et al., 2016). The mesh used for the electrogram calculation was individualized and corresponded to the same mesh used for the ECGi calculation, allowing a direct comparison between both analyses.

In addition, the logarithmic energy entropy, which has been extensively used for the characterization of signals in other disciplines (Aydın et al.) as

well as for cardiac signals (Li and Zhou, 2016), was calculated on the electrograms for each node and normalized for each atrial anatomy. More specifically, this entropy showed similar performance in prediction algorithms in previous studies (Li and Zhou, 2016) as Shannon entropy, widely used in the electrophysiological field. Finally, the mean entropy of the electrograms from all the simulations for a given patient was calculated and evaluated using entropy maps.

The main output of the workflow was produced by means of Atrial Complexity Maps (ACM) and Atrial Complexity Biomarker (ACB). ACM were obtained from the average entropy values of all the simulations from a given patient. ACB was obtained from the quantification of the number of rotors attached to the PV in the sustained simulations for each patient, that were later averaged. A rotor was considered to be attached if rotational activity was maintained around the PV for the complete simulation.

4.2.5. Clinical Evaluation

AF Complexity: Atrial Complexity Map vs. ECGi

We compared the number of AF simulations with maintained reentries (ACM) obtained from the simulation workflow with the histogram of rotors obtained from the ECGi calculation. As explained in previous sections, the entropy maps were calculated with the same anatomies that the ECGi for them to be comparable. The specific protocol for obtaining and calculating ECGi was previously described (Rodrigo et al., 2014, 2020; Guillem et al., 2016). Briefly, a minimum of three segments of at least 1 second duration were selected to calculate the histogram of rotors from ECGi signals. Rotors were obtained by counting the number of rotors in each atrial model node from the ECGi calculations for each of the segments. Finally, all three histograms were averaged and compared with the results of the simulations. Comparison was performed by dividing the complete anatomy by areas as shown in previous studies (McAlpine, 1975) and in Figure 4.2, and evaluating the presence of rotors and high entropy foci per area. This methodology enabled the characterization and evaluation of the complexity of the atria.

AF Complexity and 1-year Ablation Outcome

Evaluation of the simulations was performed attending to the number of sustained simulated AF episodes per patient, rotors attachment to the pulmonary vein (ACB) and left atrial appendage, rotor distribution between both cavities, mean conduction velocity, and maintenance of more complex scenarios. These parameters were evaluated as predictors of ablation efficacy at 1 year. Additionally, AF type (Paroxysmal vs. Persistent) was also compared to reveal possible characterization patterns using the workflow.
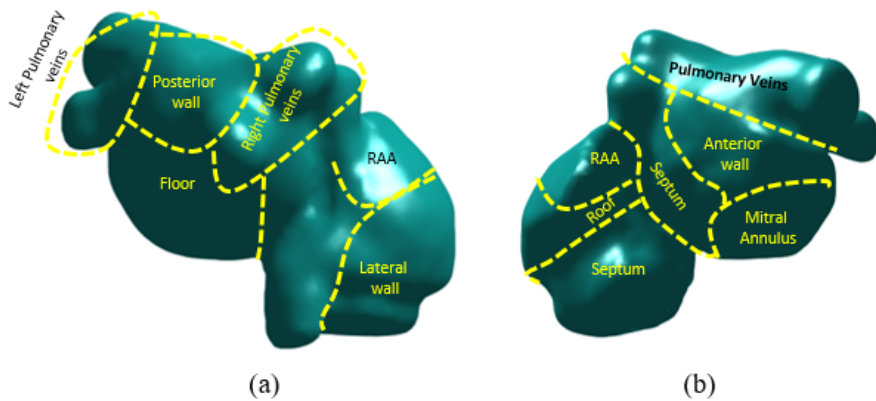
Figure 4.2. Division of the atria for rotor and entropy maps coincidence evaluation

4.2.6. Statistical Analysis

The t-test was used to evaluate the statistical significance between continuous paired or unpaired variables, and statistical significance was considered for $P < 0.05$ for continuous variables. Pearson Chi Independence test was used to evaluate categorical or binary variables, and statistical significance was considered for $P < 0.05$. All data are reported as mean ± SD. In addition, a regression analysis to test the independent predictive value has been conducted including the following parameters: AF type, gender, simulations results and 1-year outcome.

4.3. Results

4.3.1. Cohort Description

In total, 30 patients were included in this retrospective study. The characteristics of patients included in the study are shown in Table 4.1. When patients were compared according to 1-year post-ablation outcome, there were no significant differences in age, height or weight. In contrast, the proportion of persistent AF patients at 1-year was significantly higher on the AF group and the same trend was observed for female patients.

Table 4.1. Patients clinical characteristics and univariate analysis for 1-year outcome after ablation.

Characteristics	Complete Cohort	AF-Freedom Group	AF Group	p-value
Anthropometrics	30 patients	18 patients	12 patients	

Persistent AF	16 (53.3%)	7 (38.89%)	9 (75%)	**<0.001**
Age, yrs	59 ± 14	57 ± 15	62 ± 12	0.38
Female	17 (56.67%)	9 (50%)	8 (66.67%)	**<0.001**
Height (cm)	164.15 ± 9.38	164.87 ± 8.85	163.25 ± 10.33	0.67
Weight (kg)	76.03 ± 16.24	77.80 ± 14.51	73.67 ± 18.68	0.52
Blood samples				
Potassium	4.07 ± 0.40	4.04 ± 0.44	4.12 ± 0.35	0.60
Creatinine	0.91 ± 0.18	0.91 ± 0.17	0.90 ± 0.20	0.90
Hemoglobin	13.83 ± 1.67	13.57 ± 1.93	14.21 ± 1.18	0.32
Leucocytes	7.24 ± 2.29	7.65 ± 2.73	6.65 ± 1.34	0.25
Platelets	206.83 ± 47.90	212.94 ± 54.50	198.17 ± 37.16	0.42
INR	1.25 ± 0.55	1.22 ± 0.55	1.28 ± 0.57	0.80
LVEF	54.42 ± 9.67	53.00 ± 11.21	56.78 ± 6.24	0.37
Atria Size (cm^2)	31.49 ± 7.88	30.71 ± 8.83	32.87 ± 6.05	0.52
Previous diagnostics				
Mitral insufficiency	11 (36.67%)	6 (33.33%)	5 (41.67%)	0.64
Tricuspid Insufficiency	11 (36.67%)	8 (44.44%)	3 (25%)	0.28
Mitral stenosis	6 (20%)	4 (22.22%)	2 (16.67%)	0.71
Medical therapy				
Beta-blockers	18 (60%)	11 (61.11%)	7 (58.33%)	0.88
Flecainide	9 (30%)	7 (38.89%)	2 (16.67%)	0.19
Amiodarone	4 (13.33%)	3 (16.67%)	1 (8.33%)	0.51

4.3.2. Comparison of ACM with ECGi

In Figure 4.3 we show the coincidence between the histograms of rotors recorded in patients ECGi and high entropy areas obtained from the simulation protocol. ACMs were identified as descriptors of the atrial complexity, where the characteristics observed on the histogram of rotors showed a direct correlation with 1-year post ablation outcome. This correlation showed 93.33% similarity in the pulmonary vein area and posterior wall, 80% coincidence in the floor area, 86.67% in the lateral wall and 83.33% in the right atrial appendage. An example of a simple ACM is shown in Figure 4.4A where the entropy foci is mainly located on the left superior PV occurring in a patient that maintained sinus rhythm at 1-year after ablation. Figure 4.4B shows a heterogeneous and complex ACM with multiple high entropy foci, i.e. for electrograms that presented entropy values higher than 0.8*maximum entropy, distributed on both atria, with low rotor attachment to the PV area, that occurred in a patient with AF recurrence during follow-up.

4.3.3. AF Complexity and 1-year Ablation Outcome

Sustained AF Simulation Induction and Rotor Distribution

There was no difference in the number of induced sustained AF episodes during the simulations in relation to 1-year ablation outcome (freedom of AF: 33.00 ± 17.82 vs. AF: 34.90 ± 17.63 simulations; p-value=0.79) (Figure 4.5A). All 30 anatomies presented more than 70% attachment of at least one rotor to the PV area in the simulations, independently of the group (freedom of AF: 86.20±7.06 vs. AF: 81.33±5.97 simulations; p-value=0.10) (Figure 4.5B).

The percentage of patients that presented high entropy values on the pulmonary vein area on the ACM was significantly higher on the freedom of AF group (n=18) than of the AF group (n=12) (freedom of AF: 93.75% vs. AF: 62.5%; p<0.001), supporting the favorable ablation outcome in the former group. Moreover, freedom of AF patients presented lower number of high entropy areas or simpler ACM on the RA than AF patients (freedom of AF: 68.75% vs. AF: 100%; p<0.001).

Patients with freedom of AF at 1-year presented higher values of the ACB (i.e. a higher number of rotors attached to the PV) than patients with AF recurrence during follow-up (freedom of AF:1.61±0.21 vs. AF: 1.40±0.20; p-value=0.018) (Figure 4.4C). Interestingly, the mean number of sustained left atrial appendage rotors tended to be higher on the group of AF Freedom (freedom of AF: 3.52±3.81%; AF:1.50±2.37%; p-value: 0.14) (Figure 4.5E). From the complete set of simulations, the number of rotors was higher on the left atrium (LA) than in the right atrium (RA) for both groups: AF Freedom patients (LA: 2.96±0.35; RA: 2.22±0.34; p-value<0.0001) and AF patients (LA: 2.97 ±0.68; RA: 1.97 ±0.40; p-value<0.0001) (Figure 4.5D).
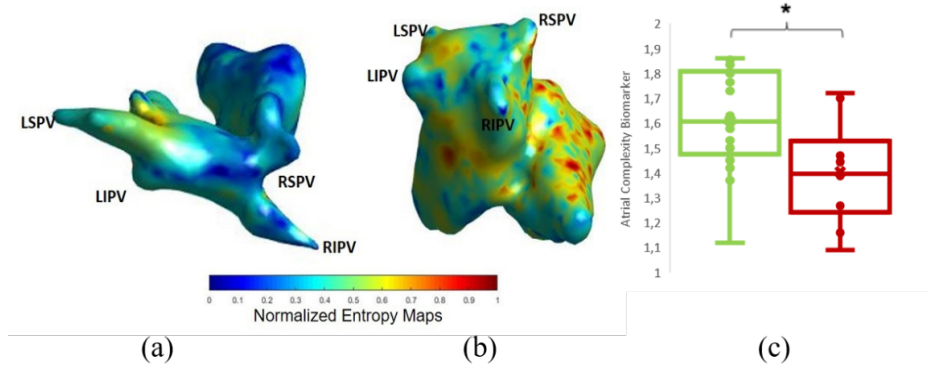
Figure 4.3. Example of normalized entropy maps for (A) Successful and (B) Unsuccessful ablation. A shows higher entropy on the pulmonary vein area while B shows a more diffused distribution of high entropy areas. C showed the mean number of rotors in simulations around the pulmonary vein area for AF freedom (green) and AF cases (red). *p<0.001.
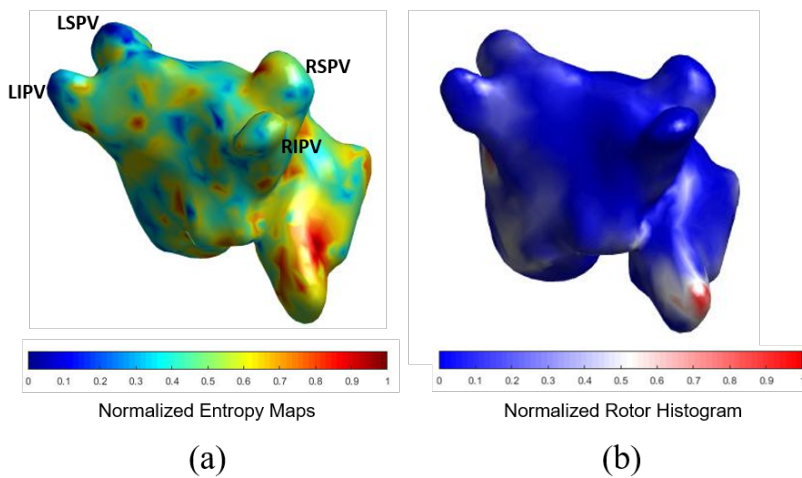
Figure 4.4. Comparison of simulations entropy maps with histogram of rotors in simple case. A shows the results for the computational method. B shows the histogram of rotors computed from the ECGi.

Differences in mean conduction velocity during AF were not significantly different between groups (freedom of AF: 85.91±6.18 vs. AF: 85.73±3.81 cm/s; p-value=0.94) (Figure 4.5C). From all the possible simulated scenarios, some presented more stability in time, that is, a higher percentage of simulations sustained AF during 1000 ms. The relationship between the number of initiated rotors with respect to the number of rotors maintained in the simulations is shown in Supplemental Figure 4.3. In this case, the average number of sustained AF simulations presented a decreasing trend for an increasing number of initiated SP, that is, the arrhythmia was not easily sustained for high number of simulated rotors.
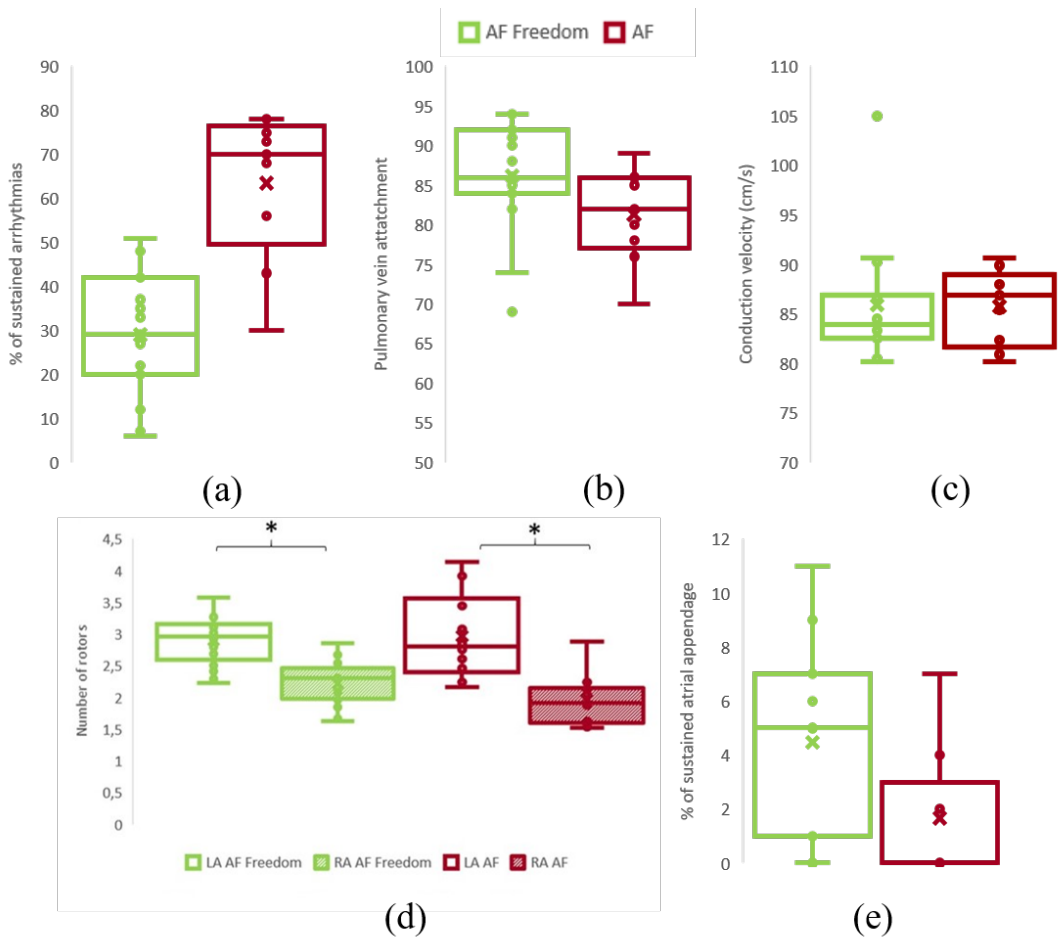
Figure 4.5. Simulation characterization. A. Percentage of sustained F in both groups., B. Percentage of simulations of rotors with pulmonary vein attachment in both groups. C. Conduction velocity of simulated scenarios. D. Number of rotors in the LA and RA for both groups. E. Percentage of rotors with left atrial appendage attachment in both groups.

Furthermore, there were no significant differences between the free-dom of AF and AF group, except for the case in which the number of initi-ated rotors was fixed to two, in which the average number of maintained simulations of AF patients was higher in the AF group (freedom of AF: 3.87±2.17 simulations vs. AF: 5.89±2.09 simulations; p-value=0.035).

Table 4.2. Electrophysiological description of the simulations.

	Complete Cohort	AF-Freedom Group	AF Group	p-value
Simulation characterization	30 patients	18 patients	12 patients	
Sustained simulations (%)	33.70 ± 17.73	33.00 ± 17.82	34.90 ± 17.63	0.79
PV attachment (%)	84.67 ± 6.83	86.20 ± 7.06	81.33 ± 5.97	0.10
Simulations presenting high entropy values in PV (%)	81.25	93.75	62.50	p<0.001
Rotor distribution				
Right Atrium rotors	2.13 ± 0.38	2.22 ± 0.34	1.97 ± 0.40	0.09
Left Atrium rotors	2.97 ± 0.48	2.96 ± 0.35	2.97 ± 0.68	0.99
Left atrial appendage rotors	2.78 ± 3.45	3.52 ± 3.81	1.50 ± 2.37	0.14
Biomarkers from simula-tions				
ACM presenting high entropy areas in RA (%)	81.25	68.75	100	p<0.001
Atrial Complexity Biomarker	1.53 ± 0.23	1.61 ± 0.21	1.40 ± 0.20	0.018

4.3.4. Comparison with AF Type

There were significant differences in long-term outcome after ablation depending on the duration of AF (i.e. AF type) (Table 4.1). Four biomarkers were significantly different when paroxysmal and persistent patients were compared. Paroxysmal AF patients presented a higher number of sustained rotors (Paroxysmal AF:5.30±0.53; Persistent AF: 4.69±0.56; p-value:0.012), especially on the LA (Paroxysmal AF: 3.10±0.41; Persistent AF: 2.65±0.37; p-value:0.01) and the PV antrum (Paroxysmal AF:1.48±0.32; Persistent AF: 1.14±0.18; p-value:0.006), with the number of sustained rotor attachment to the PV being higher on the paroxysmal group (Paroxysmal AF: 1.61 ±0.18; Persistent AF: 1.42±0.25; p-value:0.02). In ad-dition, results did not show any correlation with LA area, (Paroxysmal AF: 31.88 ± 7.20 cm^2; Persistent AF: 30.95 ± 7.56 cm^2; p-value: 0.74).

Regression analysis results show that the ACM biomarker is the only variable with a trend for independently predicting 1-year post ablation outcome (p-value = 0.0752) as compared to other clinical variables such as AF type (p-value: 0.2548) and gender (0.3442).

Table 4.3. Electrophysiological description of the patients attending to AF type.

	Paroxysmal AF	Persistent AF	p-value
	14 patients	16 patients	-
Sustained rotors	5.30 ± 0.53	4.69 ± 0.56	0.012
Left Atrium rotors	3.10 ± 0.41	2.65 ± 0.37	0.01
PV antrum	1.48 ± 0.32	1.14 ± 0.18	0.006
PV attachment	1.61 ± 0.18	1.42 ± 0.25	0.02
LA area	31.88 ± 7.20	30.95 ± 7.56	0.74

4.3.5. Applicability to Clinical Environment

This methodology, and specifically, the ACM and ACB obtained from the workflow, are presented as an estimator of the complexity of the atrial activity. Figure 4.6 shows the rotor maps from three different patients ordered for increasing ACB values. As it can be observed, the higher the ACB, the lower the complexity of the rotor map with more localized the rotors appear on the pulmonary vein area. From left to right, patients with lower ACB presented higher number of rotors than patients with higher ACB. In addition, rotors in patients with low ACB were mainly located in both atria whereas patients with high ACB presented the rotors concentrated on the PV area.

Examples of these cases are present in Figure 4.6, where the left panel, corresponding to an ACB with 1.39, represents a patient in which the ablation was not successful and both the ECGi rotor histogram and the ACM present high activity foci on the right atrium. In contrast, the patient on the right panel represents a case in which the ablation was successful and both the ECGi rotor histogram and the ACM present high activity foci on the right pulmonary veins, accompanied by a higher ACB. Overall, 11 patients (AF Freedom: 2 patients vs. AF: 9 patients) corresponded to an ACB lower than 1.45 and 19 patients (AF Freedom: 16 patients vs. AF: 3 patients) corresponded to an ACB higher than 1.50.

4.4. Discussion

This study presents a new simulation workflow for the personalized electrophysiological evaluation of the atria in a simulation environment. This is a proof-of-concept study that establishes a noninvasive evaluation of atrial electrophysiological complexity by means of two novel biomarkers: ACMs and the ACB to evaluate atrial complexity and predict the efficacy of the ablation. Our results revealed that long-term successful AF ablation occurred in patients with rotors mainly located in the pulmonary veins, while unsuccessful procedures presented greater number of entropy foci outside the PV areas. Paroxysmal AF patients presented a significantly higher number of LA rotors with greater attachment to the PV area and lower density of entropy areas in the RA, as compared to persistent AF patients, explaining the improved long-term clinical outcome in the former group. These results are
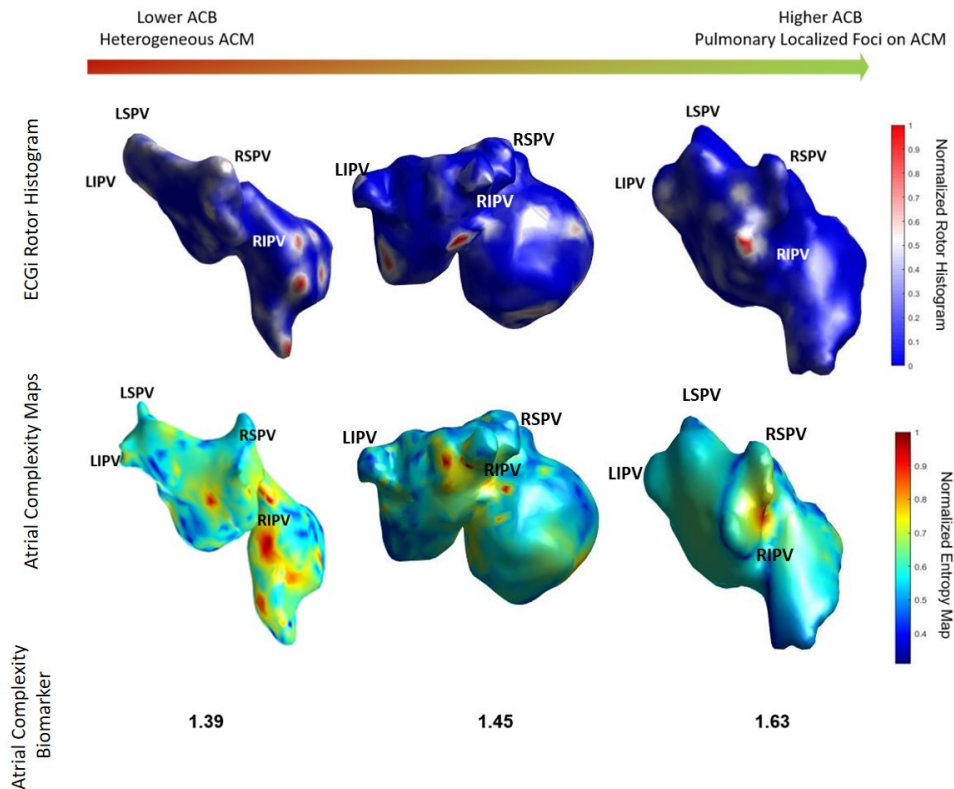
Figure 4.6. Rotor map of three different patients included in the study. Rotor maps with higher complexity are correlated with lower CAN and more heterogeneous ACM while simpler rotor maps are correlated with higher ACB and localized pulmonary foci on the ACM. ACM: Atrial Complexity Maps; ACB: Atrial Complexity Biomarker.

in agreement with clinical studies that consistently report a better outcome of the ablation following PV electrical isolation, while AF recurrences were most common in patients with multiple drivers distributed at extra-PV sites. (Atienza et al., 2009, 2014; Lim et al., 2017; Hindricks et al., 2020; Rodrigo et al., 2020).

4.4.1. Simulation Models

Detailed ionic models for the evaluation of AF induction at different scales include complementary information that may be relevant for the ablation procedure (Arevalo et al., 2016; Passini et al., 2017). These ionic models also appear as a good approach for very specific workflows, such as pharmacological studies, that analyze the playing role of ionic channels and its modification using different drugs. In addition, several studies explore different strategies for the evaluation of the atrial complexity, including specific ablation strategies and targets (Roney et al.), cycle length evaluation (Haissaguerre et al., 2007) and proarrhythmic structures such as the left atrial appendage (Gharaviri et al., 2021). However, they may present significant drawbacks, especially for large-scale simulations, due to the high computational power needed for such specific models, limiting the overall number of scenarios to be studied (Sachetto Oliveira et al., 2018), or the number of structures (i.e. only including left atrium). In contrast, simpler models, such as the automata model used in this study, can be applied for modeling an initiated arrhythmia behavior enabling the analyses of several distributions of rotational foci. Moreover, automata models rely on simpler activation patterns, can be implemented and used on cardiac modeling to obtain similar approaches with a lower computational cost (Alonso-Atienza et al., 2005; Clayton et al., 2010). Therefore, the use of simpler models together with graphical processing units for parallel computation, reduces the total computational time, allowing a potential translation and implementation of this methodology in the clinical environment for patient evaluation.

These simulations are presented, as a workbench for characterizing the proarrhythmicity based on the anatomy and different arrhythmic scenarios. One of the main challenges in computation is the initiation of rotational activity on the desired area. Several approaches have been implemented and described in previous publications in order to tailor arrhythmia initiation by including remodeling such as repolarization alternants, adipose tissue modeling, and cardiac ion channel mutations (Aronis et al., 2019). However, we gave priority to the analysis of scenarios with different combinations of rotational activity that reflect the heterogeneity of the arrhythmias using an algorithm that directly deal with different rotors over the atria, comparing

their different distributions. The inclusion of such a high number of scenarios or combinations of rotational foci (i.e. 100 simulations per anatomy) enables to include all possible areas at which rotors can be maintained, differing from other approaches in which a low number of combinations is analyzed, restricting the arrhythmic simulations to the pulmonary vein area and excluding the arrhythmia initiation on right atrium (Fastl et al., 2018).

Regarding the characterization of the simulations, all simulated atria presented realistic models in which the number of rotors was higher on the left atrium than in the right atrium, with a similar number of maintained simulations per group and high attachment of rotational drivers to the pulmonary vein area, identified as the main proarrhythmic trigger on clinical practice. These results align with previous studies that reflect the dominance of the LA in the rotational activity of AF patients (Atienza et al., 2009, 2014; Narayan et al., 2012; Pandit and Jalife, 2013; Rodrigo et al., 2014; Walters and Kalman, 2015; Zaman et al., 2017), demonstrating the reproduction of a clinical scenario into personalized simulations in a computer.

4.4.2. Clinical Implications

The increasing number of potential candidates for ablation therapies is much higher than the availability of laboratories to perform procedures, but patients are selected based on very simple and unproved selection criteria for efficacy. However, current indiscriminate application of ablative therapies to large, unselected cohorts of patients with AF might dilute the intended treatment benefits and significantly increase the cost. Translation of the mechanistic insights of computational and basic research into clinical management concepts will uncover the full potential of personalized AF management (Atienza et al., 2012). The present approach may help appropriately select patients undergoing invasive therapies by: 1) integrating the workup protocol as shown in Figure 4.7, where anatomical characterization and simulations will be performed 2 days prior to the procedure, to later correlate high entropy areas location in the simulations protocol with ECGi, and help decide the ablation strategy; 2) giving preference for the standard ablation procedures to those patients with favorable predictors for ablation long-term success (low ACM, high ACB) (Kuck et al., 2016); and 3) selecting patients with higher atrial complexity to undergo the elimination of extrapulmonary drivers ablation (Narayan et al., 2012; Haissaguerre et al., 2014; Rodrigo et al., 2020).
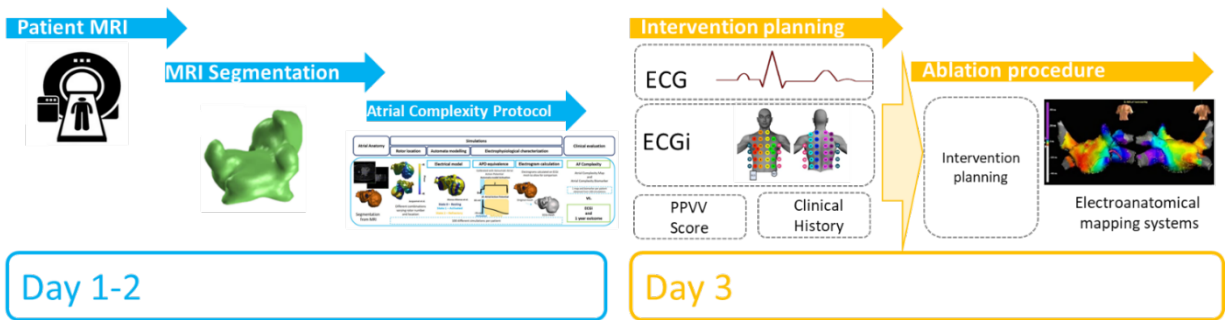
Figure 4.7. Protocol proposal for the integration of the method in a clinical environment.

This protocol is based on a personalized simulation method that could be potentially modified to input other remodeling factors such as fiber orientation to develop more complex fibrotic models, broadening the application to models closer to the clinical setting. Therefore, the integration of image-based computational modeling into treatments for heart rhythm disorders could thus advance personalized approaches to heart disease.

4.4.3. Study Limitations

The main advantage of the model, its simplicity, also constitutes its main limitation, as this model is not as tailored as ionic models. Furthermore, other scenarios such as different conduction velocity areas or fiber orientation should be implemented on the automata model and considered to study a wider population of patients. Second, we were able to demonstrate that all the areas that presented high-frequency activation on the ECGi presented high entropy values, but we were unable to ensure that all the high entropy areas were coregistered with high-frequency areas or rotational activity. Further studies should be conducted to evaluate if this mismatch is due to a lack of more ECGi episodes or if rotors were present only in part of the atrial anatomy.

In addition, other tailored characteristics such as fibrosis distribution over the atria and ionic heterogeneity (Calvo et al., 2014; Palacio et al., 2021; Sánchez et al., 2021) should be considered in further studies to better represent the anatomical and electrical remodeling of the cardiac tissue. Atrial thickness and blood pressure are two important factors that have been demonstrated to affect frequency dynamics and should be further explored to complement the models (Gosai et al., 2015).

Finally, higher attachment to the left atrial appendage was observed on the AF freedom group, which exclusively underwent PV isolation. Further studies should confirm the proarrhythmic behavior of the left atrial appendage in these models (Di Biase et al., 2018).

4.5. Conclusions

This study presents a new method for the evaluation of the pro-arrhythmic areas on atrial anatomies providing ACMs and the ACB as estimators of atrial complexity. This approach, validated using ECGi to measure atrial complexity, was able to identify the set of patients that presented higher atrial complexity.

Supplementary Material

Automata Models: Implementation and Electrophysiological Characteristics

We applied automata models consisting on probabilistic models in which each unit can present different discrete states that change according to simple rules as a function of the previous state and the state of the neighboring cells. Once the simulation is completed, each of the discrete states can be interpolated with an action potential to calibrate the model at electrophysiological level. A brief example on 2D planes is shown in Supplementary Figures 1 and 2, for both sinus rhythm and AF initiation respectively. As it can be observed, propagation along the plane is depicted in the figure along with the electrical activation. Koivumaki et al's model (Skibsbye et al., 2016) was simulated in a plane of 2 cm^2 side to simulate three coordinated impulses on an AF model, obtaining a conduction velocity of 45.45 cm/s and Action Potential Duration at 90% repolarization (APD90) of 193.95 ms. These parameters were later introduced in the automata model used for the study (Alonso-Atienza et al., 2005), to compare both simulations. As it can be observed, similar results were obtained for the propagation of the model and the electrical signal obtained from the automata model is similar to the one obtained in the detailed ionic model.

Automata Model: Alonso-Atienza Model Description

Alonso-Automata model (Alonso-Atienza et al., 2005) relies on three activation states that depend on the following modelling.

State 0 correspond to the resting phase, in which the tissue is relaxed and excitable. The excitation of the tissue, and therefore the depolarization phase, is modelled by the following equation:

$$Pjexc = E*Q = E* \Sigma AiDij2i \neq j$$

Where E stands for excitability, A for activation and D corresponds to the distance matrix. Once the state is the activated one, corresponding to a cell that can is excited and can excite others, the behavior is modelled by the following equation: $APD = APDmin + APDmax*(1 - \exp(-0.5*di))$

Where the APDmin and APDmax correspond to the minimum and maximum values of the APD and the di corresponds to the diastolic interval. State 1 is modeled for the 10% time of the total APD. After this simulation time, State 2, corresponding to the refractory phase in which the tissue is

exited but not able to activate the surrounding tissue, is modelled for 90% of the APD length (partial repolarization).
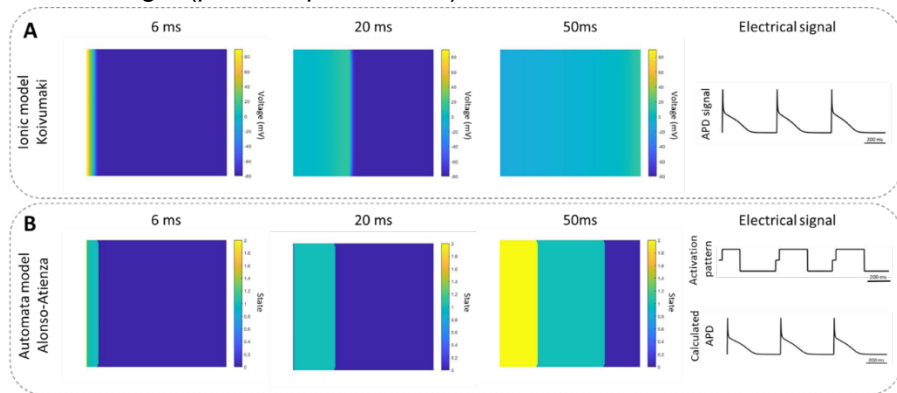
Sup. Figure 1. A. 200x200 simulation for Koivumaki ionic model B. 200x200 simulation for Alonso-Atienza automata model.
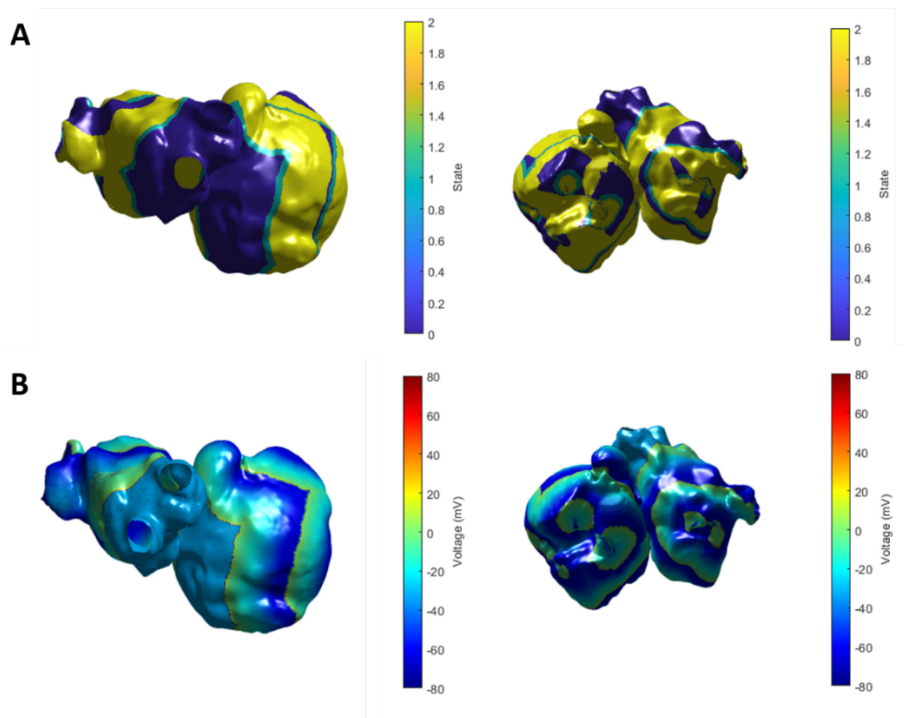
Sup Figure 2. Example of models after Jacquemet implementation A. Complete Atria simulation for Koivumaki ionic model. B. Complete atria simulation for Alonso-Atienza automata model
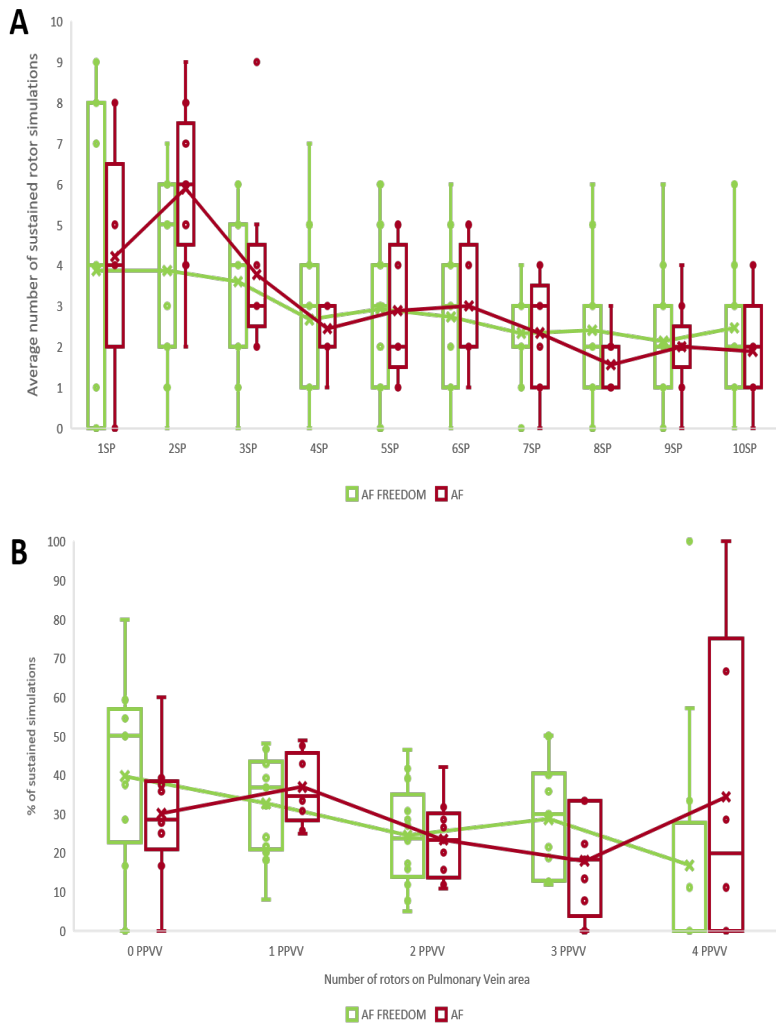
Sup. Figure 3. A. Average number of sustained rotor simulations with respect to the number of initiated singularity points (SP) B. Percentage of sustained simulations with respect to number of rotors in pulmonary veins

Chapter 5. Study 3: STRATIFY-AF. Artificial Intelligence for Treatment Selection

ABSTRACT

Background: Atrial Fibrillation (AF) treatment strategies are suboptimal and clinical predictors of success are limited. Artificial Intelligence (AI) has arisen as a powerful tool for efficacy prediction.

Objective: To develop an AI-driven platform for the stratification of patients prior to ablation based on non-invasive Electrocardiographic Imaging (ECGi) biomarkers and clinical parameters to evaluate and predict optimal patient treatment.

Methods: We evaluated 204 patients from consultation and ablation procedures that were treated according to clinical guidelines and characterized at electrophysiological level using Body Surface Potential Mapping recordings during AF. ECGi signals were calculated to obtain frequency and rotational biomarkers. Baseline clinical characteristics and the treatment followed after inclusion were registered. 80% of the data was used to calibrate an algorithm for prognosis 12 month after inclusion in the study and the 20% remaining was used for testing.

Results: A clustering algorithm was calibrated identifying 3 main variables for prediction. The first variable for prediction was the AF type (paroxysmal or persistent). Secondly, an electrophysiological risk score obtained from the ECGi and formulated using logistic regression including the following parameters: highest dominant frequency, median dominant frequency and mean rotor time. Finally, the type of treatment identified as rhythm control (drugs, AF ablation) or rate control. The performance of the algorithm

revealed 89.99% of success when predicting the outcome, increasing over-all performance with respect to conventional persistent and paroxysmal classification.

Conclusions: We were able to predict 12-month prognosis by using AI algorithms that combined clinical information with ECGi biomarkers and identified the most suitable treatment for each patient, attending to clinical guidelines recommendations.

5.1. Introduction

Atrial Fibrillation (AF) is the most common clinical arrhythmia associated with significant complications and impaired quality of life. Clinical guidelines mainly describe two approaches for AF treatment: medical therapy, that presents limited efficacy, and cardiac ablation, with an associated risks and arrhythmia recurrence in 50% of cases (Hindricks et al., 2020). Multiple observational studies have identified predictors of arrhythmia recurrence.

ECGi studies have already identified potential biomarkers (i.e. activation patterns, atrial frequency) that improve the decision process for treatment selection and potentially help in the design of the ablation procedure, among others (Rodrigo et al., 2014; Cheniti et al., 2019; Molero et al., 2021; Salinet et al., 2021). This technology, in combination with advanced computational calculations such as neural networks and score prediction in combination with clinical baseline characteristics of the patients, enforce the identification of new biomarkers to evaluate AF prognosis (Sánchez de la Nava et al., 2021).

Our hypothesis is that the electrophysiological complexity is determinant for the characterization of AF patients and is helpful to predict treatment success (either pharmacological or interventional). We aimed to evaluate AF complexity using ECGi and to develop a new stratification score to identify and predict which treatment is more suitable for each patient.

5.2. Methods

5.2.1. Data and Study Population

Patients from our center were included in the study from two different cohorts: outpatients who were treated in ambulatory care settings, and patients that were submitted for ablation procedures. Both groups were treated according to the ESC guidelines.

Ablation group patients were classified in two subgroups depending, depending on the ablation strategy performed: Pulmonary Vein Isolation

(PVI) (cryoablation or circumferential radiofrequency ablation), and PVI combined with driver ablation using radiofrequency ablation. In the last case, rotors or high frequency areas were identified by the ECGi technology and the final decision of performing ablation on these sites was decided by the responsible electrophysiologist.

In addition to the ECGi-based electrical characterization of patients, clinical and imaging data was also collected including age, gender, type of treatment and concomitant pathologies of all patients. The protocol was approved by the Institutional Ethics Committee of the institution and all patients gave informed consent.

5.2.2. BSPM recordings

The ECGi methodology used in this study has been previously described in other publications from our group (Rodrigo et al., 2014, 2020; Atienza et al., 2021). Briefly, BSPM signals were recorded from patients during AF episodes including a total of 63 electrodes homogeneously distributed over the torso of the patient (Figure 5.1.). Signals were recorded in resting state in case of the outpatient group or under anesthesia in case of ablation procedure at a sampling frequency of 1kHz. The geometry of the torso was reconstructed from a video to identify the electrode patch location and processed (Atienza et al., 2021; Rodrigo et al., 2014, 2020).
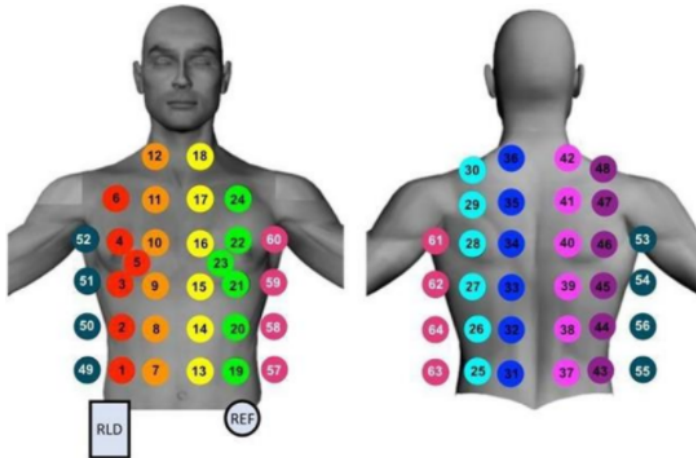
Figure 5.1. Body Surface Electrode configuration including 63 electrodes for the electrical activity registration

5.2.3. Data processing and cleaning

QRS complex was removed from the recorded signals as described in (Rodrigo et al., 2016). After removing QRS, signals from the body surface were filtered eliminating baseline and with a high pass filter (Fc = 20 Hz)

and low pass filter (Fc = 2Hz). Segments of, at least, 4 seconds were selected to calculate the frequency maps and 1 second segments were used to calculate rotor maps. This process was repeated three times per patient and results were averaged. More specifically, for patients belonging to the ablation group, a segment of at least 20 seconds was recorded prior to the ablation and consecutive episodes were obtained thereafter. For the outpatient group, a complete segment of ≥60 seconds was obtained. ECGi was calculated using preselected atrial anatomical models as described in (Rodrigo et al., 2018).

The parameters evaluated from the ECGi were obtained from signals acquired at the moment of inclusion and patients were clinically followed for 12-month after the outpatient visit and/or postablation (Table 5.1). For each recorded segment we obtained two maps, Dominant Frequency (DF) and rotor histogram maps (Figure 5.2). Briefly, DF was defined as the frequency that presented the highest power calculated with a Welch's periodogram to determine the local DFs with a spectral resolution of 0.01Hz (Guillem et al., 2013). Rotor location was carried out by identification of SP (SP) in the phase map obtained with the Hilbert Transform as described in previous publications of the group (Marques et al., 2020). Phase values were obtained along 3 different circles surrounding each evaluated point, and six to twelve points per circle were used for the phase analysis in which the signal was interpolated by a weighted average of the neighboring nodes, being d2 the weight for each node and d the distance between the nodes.

An evaluated point was defined as a SP only when the phases of at least two of these three circles was monotonically increasing or decreasing for a total of 2π. A rotor was defined as the connection between SPs across time. The distance between SPs at consecutive time instants should be less than 1, (electrogram and inverse computed electrogram) or 5 (ECG) to be related and maintain a continuity of rotation. Finally, only long lasting rotors, defined as those that complete at least one rotation were considered as rotors and other SPs were discarded.
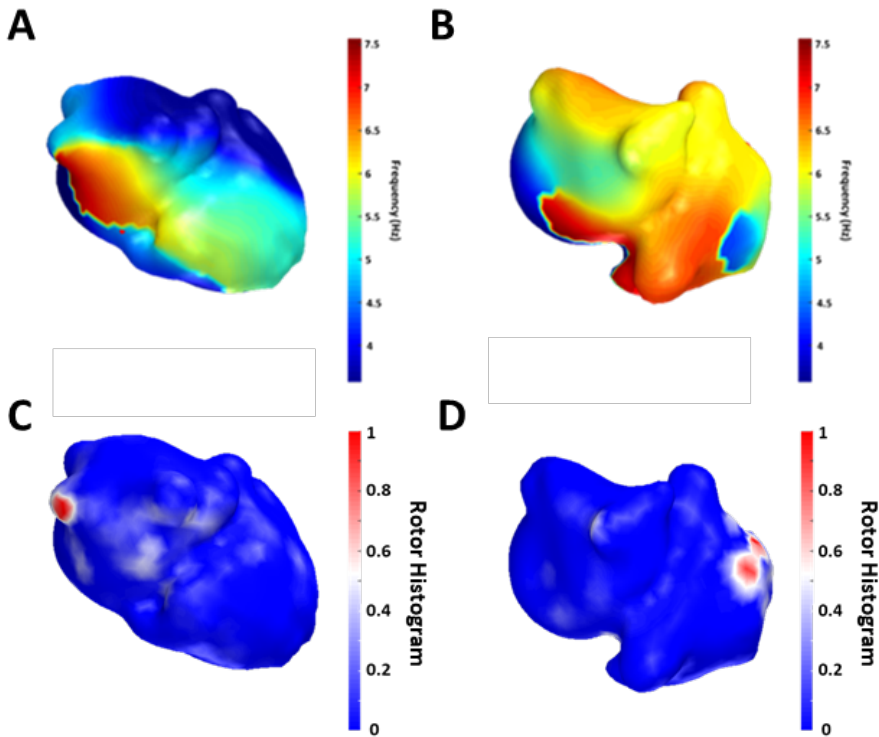
Figure 5.2. A. Patient showing simple and homogeneous distribution of activation frequency associated with low values of the complexity score with localized rotors in the pulmonary vein (panel C) and B. Patient showing a heterogeneous distribution of activation frequency associated with high values of the complexity score showing rotational activity in the right atrium.

The complete list of calculated biomarkers can be consulted in Table 5.1, including all the frequency and rotor biomarkers extracted from the ECGi maps.

Table 5.1. Evaluation metrics obtained from the ECGi

	Outcome Measure	Description
	Dominant Frequency (Hz)	Power spectral density of the ECGi signals
Frequency Biomarkers	Highest Dominant Frequency (Hz)	Highest value of the calculated Dominant Frequencies
	Highest Dominant Frequency Extension (%)	Extension of the Highest Dominant Frequency
	Median Dominant Frequency (Hz)	Median value of the Dominant Frequencies

	Median Dominant Frequency Extension (%)	Extension of the median Dominant Frequency
	Minimum Dominant Frequency (Hz)	Minimum value of the Dominant Frequencies
Rotor Biomarkers	Rotor per second	Number of identified rotors per second
	Mean simultaneous rotor	Number of identified rotors simultaneously
	Mean rotor duration	Mean rotor duration in percentage for the calculated segment
	SP at Highest Dominant Frequency	Singularity points that present the highest dominant frequency
	SP per second	Number of singularity points per second
	Mean rotor time (%)	Percentage of time with rotors
	Entropy	Value of the entropy
	Calculated score	Score for the evaluation of the electrophysiological complexity

5.2.4. Studied cohort

Only patients that met the eligibility criteria were included in the study and were followed for a 12-month period to evaluate rhythm outcome and clinical evolution including changes in treatment. We included ambulatory patients with AF attending the outpatient clinic and/or patients submitted for AF ablation following the ESC guidelines clinical indication. We excluded patients enrolled in another investigational study, patients with implanted pacemaker or Implantable Cardioverter Defibrillator and those with contraindications for AF ablation. Clinical follow-up included Holter recording at 6, 9 and 12 months after the outpatient visit and/or ablation, treatment strategies and drugs doses were also recorded. These changes included redo ablation procedures and/or electrical cardioversion and pharmacological changes, including dose changes and number of antiarrhythmic drugs.

5.2.5. Data analysis

Neural Network for processing BSPM signals

To evaluate and alternative method that enables to extract the biomarkers calculated from the ECGi, a neural network was trained to evaluate the performance of the algorithm. More specifically, filtered BSPM signals as described in Section 5.2.3 were used as input of the neural network, calibrated to output the values of the frequency and rotor biomarkers specified in Table 5.1.

As neural network present complex structures, the amount of data needed for its testing and training process is very demanding. In order to

overcome this limitation, several segments from each patient were used to calibrate and train the network. Specifically, 892 BSMP recordings from 150 patients undergoing ablation were used for the calibration and testing of the net.

For its calibration, 2 second signals during AF episodes were recorded prior to ablation and calculated in 4 second episodes as explained in previous publications of the group (Nava et al., 2021).

The structure of the net included a convolutional layer, followed by a dropout layer, a convolutional layer, a flatten layer and three dense layers as depicted in Figure 5.3. Training was performed with 85% of the data and evaluated by means of mean absolute error. All layers were fully connected.

Due to lack of validation and low number of samples to train this algorithm, the subsequent steps were directly evaluated with the metrics obtained from the ECGi computation.
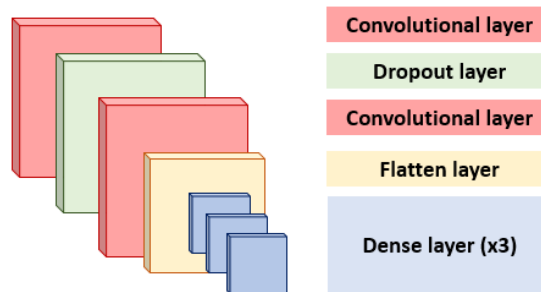
Figure 5.3. Neural Network configuration including four different types of layers**.**

Score identification

The new score was built as follows: First, an electrophysiological score was developed using only the parameters obtained from the ECGi. To develop this score, the 12 variables obtained from the ECGi were evaluated using feature extraction to identify the most important variables for 12-month rhythm outcome evaluation. Three different signal segments were selected for each patient and ECGi was calculated. The average of the results obtained from these three different segments were used to obtain a single measurement for each biomarker per patient. Once the variables were identified, the score was built and trained using 80% of the data and the remaining 20% was used to test its performance. After the score was tested, clinical data was incorporated into the algorithm to evaluate if the addition of clinical variables (AF type and type of treatment) were complementary to this score. We assessed if the proposed method tested in combination with classical clinical guidelines parameters was able to improve

overall performance. For this purpose, a clustering algorithm was built to identify profiles that presented similar profiles. Briefly, clustering algorithms enable to identify patterns in data with similar basal characteristics (such as AF type or electrophysiological profile) and similar outcome (in this case identified by AF or AF Freedom at 1-year after the inclusion in the study).

5.2.6. Statistical Methods

The Student's t-test was used to evaluate the statistical significance between continuous paired or unpaired variables, and Z score was used to calculate p-values of prevalence (percentages) in the population. One-way multivariate analysis of variance was used for multivariate analysis. Statistical significance was considered for $P<0.05$ for continuous or percentage variables. Pearson Chi Independence test was used to evaluate categorical or binary variables, and statistical significance was considered for $P<0.05$. All data are reported as mean ± SD. All ECGi calculations were performed in Matlab and the training of both the neural network and the regression algorithm were programmed in Python.

5.3. Results

5.3.1. Patient Cohort Clinical Description

A total of 204 patients were included in the study from the outpatient clinic (N=84) and ablation (N=120) groups according to their consecutive referral to each group, between June 2018 to December 2019.

Table 5.2 and Table 5.3 show the baseline characteristics of the cohort, including gender, age, type of AF and most important comorbidities studied.

Regarding the outpatient group, no differences were found when gender, AF type or comorbidities when AF Freedom and AF patients were compared. AF patients were significantly older when compared to AF Freedom patients.

Ablation group did not show any clinical differences among AF and AF Freedom patients. Additional information can be found in the supplementary material including all the measured variables and their corresponding significance.

When both subgroups, outpatient and ablation groups were compared, female AF freedom patients was significantly higher on the consultation group (outpatient group: 54.54%; ablation group: 33.75; p-value: 0.04).

Table 5.2. Description of outpatients included in the study.

	All patients	AF Freedom	AF	p-value
	84	33	51	
Gender	32 female	18 female	14 female	0.99
Age (yrs)	65.37 ± 11.00	64.72 ± 12.51	65.80 ± 10.01	0.67
Comorbidities				
Arterial Hypertension	40 (47.62%)	17 (34.34%)	23 (45.10%)	0.79
Obesity	9 (10.71%)	1 (3.03%)	8 (15.69%)	0.07
Ischemic Cardiac Condition	2 (2.38%)	2 (6.06%)	0 (0.0%)	1.00
Cardiac Insufficiency	3 (3.57%)	1 (3.03%)	2 (3.92%)	0.66
Mitral Insufficiency	3 (3.57%)	2 (6.06%)	1 (1.96%)	0.94
Atrial/Ventricular Dilation	2 (2.38%)	1 (3.03%)	1 (1.96%)	0.85
AF Type				
Flutter	6	4	2	
Paroxysmal	24	9	15	0.40
Persistent	53	20	33	

Table 5.3. Distribution of patients undergoing ablation.

	All patients	AF Freedom	AF	p-value
	120	80	40	
Gender	42 female	27 female	15 female	0.417
Age	60.90 ± 9.27	59.13 ± 9.50	64.45 ± 7.77	0.003
Comorbidities				
Arterial Hypertension	34 (28.57%)	24 (30.00%)	10 (25%)	0.78
Obesity	15 (12.5%)	12 (10%)	3 (0.75%)	0.93
Ischemic Cardiac Condition	1 (0.84%)	1 (1.25%)	0 (0.0%)	1.00

Cardiac Insufficiency	2 (1.68%)	2 (2.5%)	0 (0.0%)	1.00
Mitral Insufficiency	2 (1.68%)	1 (1.25%)	1 (2.5%)	0.56
Atrial/Ventricular Dilation	2 (1.68%)	2 (2.5%)	0 (0.0%)	1.00
AF Type				
Flutter	12	8	4	
Paroxysmal	33	26	7	0.20
Persistent	72	44	28	

Interestingly, dyslipidemia was more frequent in outpatient group than in ablation group (Outpatient group: 39.29%; Ablation group: 1.67%; p-value<0.001) and obese patients presented better outcomes in the ablation group than in the outpatient group (Obese AF Freedom in outpatient group: 1.19%; Obese AF Freedom in ablation group: 10%; p-value: 0.01108).

Multivariate analysis revealed that both the AF type and the ablation strategy were significantly associated with the endpoint (AF Freedom/AF) (p<0.001), suggesting that these variables should be included in the final model. Regarding the strategy, ablation strategy did not show statistically significant differences between patients in which PVI was performed compared to the PVI + driver ablation strategy in the overall cohort (PVI AF-Freedom group: 75.51%; PVI + drivers AF-Freedom group: 59.70%; p-value: 0.075) (Figure 5.4). Interestingly, patients in whom a pharmacological change was indicated after the ablation significantly presented better outcomes with respect to patients in whom a second ablation was performed (Pharmacological changes AF-Freedom group:77.8%; Interventional changes AF-Freedom group: 30%; p-value: 0.00014).
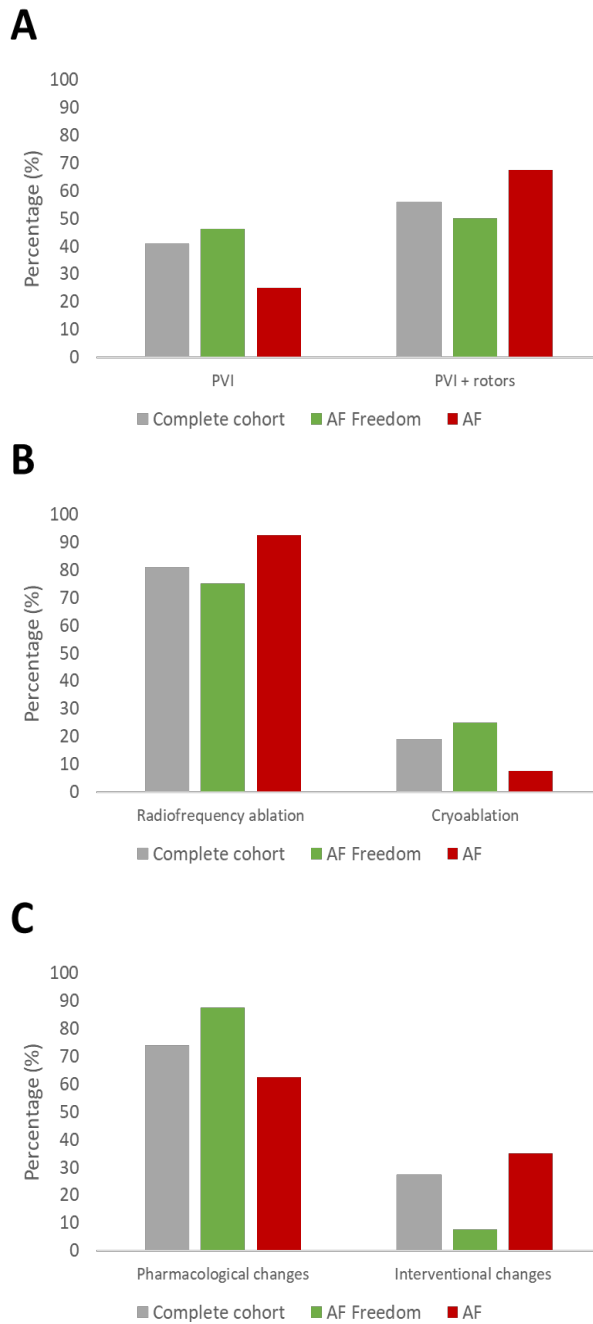
Figure 5.4. A. AF and AF freedom proportion depending on ablation strategy. B. AF and AF freedom proportion depending on ablation type. C. AF and AF freedom proportion depending on the strategy followed after ablation.

5.3.2. Patient Cohort ECGi description

As it can be observed from the graphs (Figure 5.5 and Figure 5.6), there was no significant difference when the ECGi biomarkers were independently used to predict AF outcome. Thus, we decided to evaluate the ability of an outcome score using a composite measure of these biomarkers to predict treatment success.
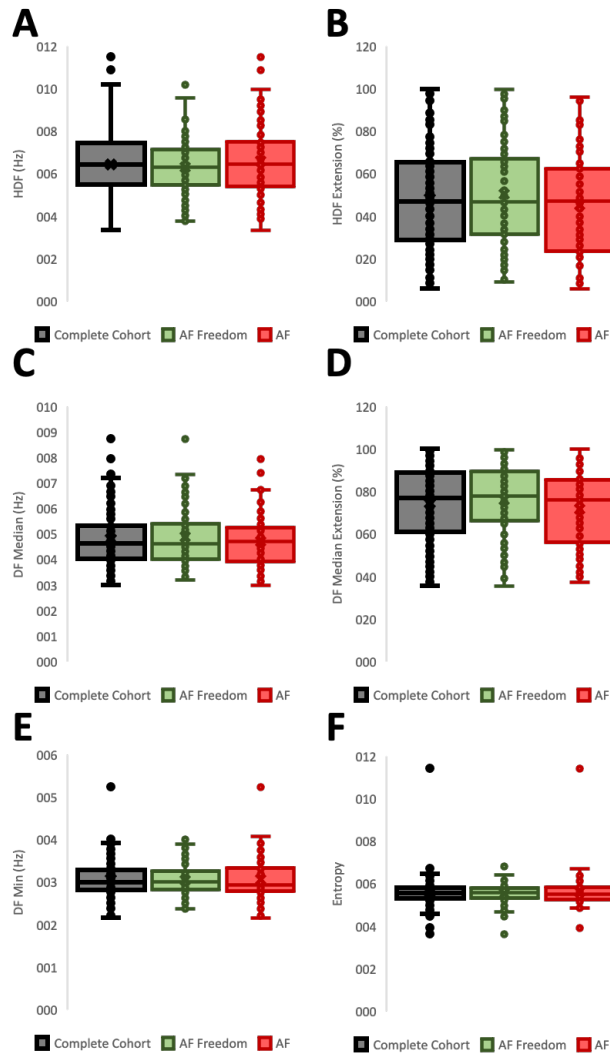
Figure 5.5. Frequency biomarkers and entropy for AF and AF Freedom groups including A. Highest Dominant Frequency, B: Highest Dominant Frequency extension, C. Median Dominant Frequency, D. Median Dominant Frequency Extension, E. Minimum DF and F. Entropy.
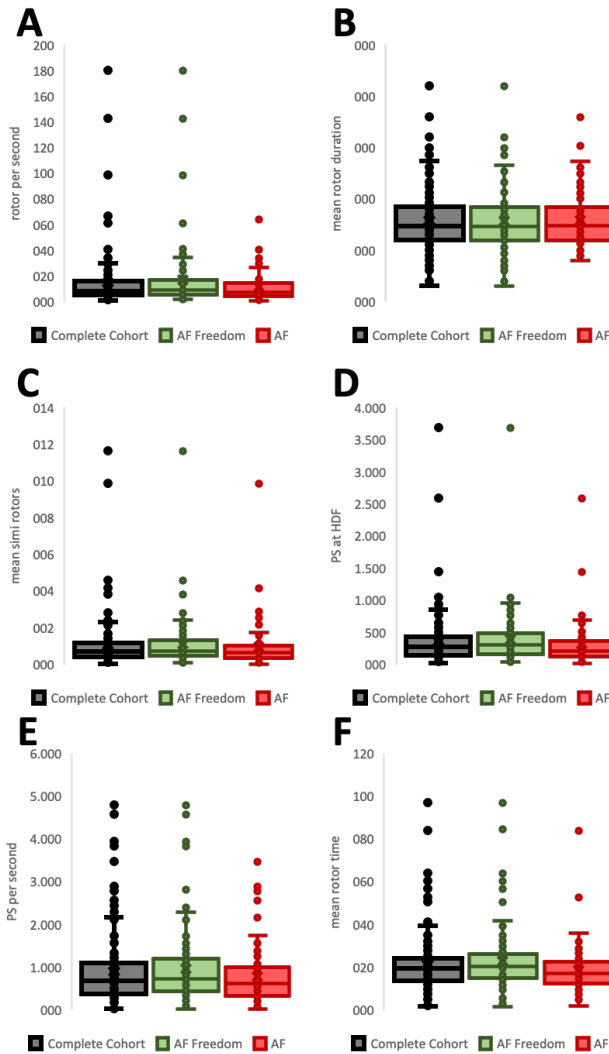
Figure 5.6. Rotor biomarkers obtained from the ECGi for AF and AF Freedom groups including A. rotors per second, B. mean rotor duration, C. mean simultaneous rotors, C. SP at highest dominant frequency, E. SP per second, F mean rotor time.

5.3.3. Neural Network performance

Results from the Neural Network showed that the calculated parameters were calculated with a low error value, as shown in the table below.

Table 5.4. Description of the performance of the neural network for the evaluation of electrophysiological variables.

Biomarker	Mean Absolute Error

Highest Dominant Frequency	0.12
Minimum Dominant Frequency	0.08
Mean Simultaneous rotors	0.01
Mean rotor time (%)	1.04
Median Dominant Frequency	0.11

However, this methodology did not enable to evaluate the location or distribution of the biomarkers, therefore losing the spatial information of the maps.

In addition, the low number of patients and lack of validation revealed the need to include new patients for the electrophysiological estimation and characterization.

5.3.4. ECGi biomarker evaluation for prediction

The calibration of the electrophysiological score resulted in a logistic regression equation that used three parameters for the decision. These three parameters were the Highest Dominant Frequency, the Median DF and the Mean rotor time.

$$P = \frac{1}{1 + e^{-(-0.1117 + 0.3963*HDF - 0.3929*Median\ DF - 0.0386*Mean\ Rotor\ Time)}} \quad (5.1)$$

Following this mathematical formulation, the behavior of the chosen electrophysiological variables can be described in as follows: first, for higher values of the Highest Dominant Frequency, the score will present higher values, meaning that the complexity is also higher. In addition, when considering the Median Dominant Frequency, the score will present lower values, meaning that the complexity is lower. Finally, if the rotor time is studied, the same trend is observed for lower values of the score when higher values of the rotor time are observed.

5.3.5. Effect of clinical variables on global model

The values obtained from the score were directly implemented in the clustering algorithm that revealed five different groups as shown in Figure 5.7.
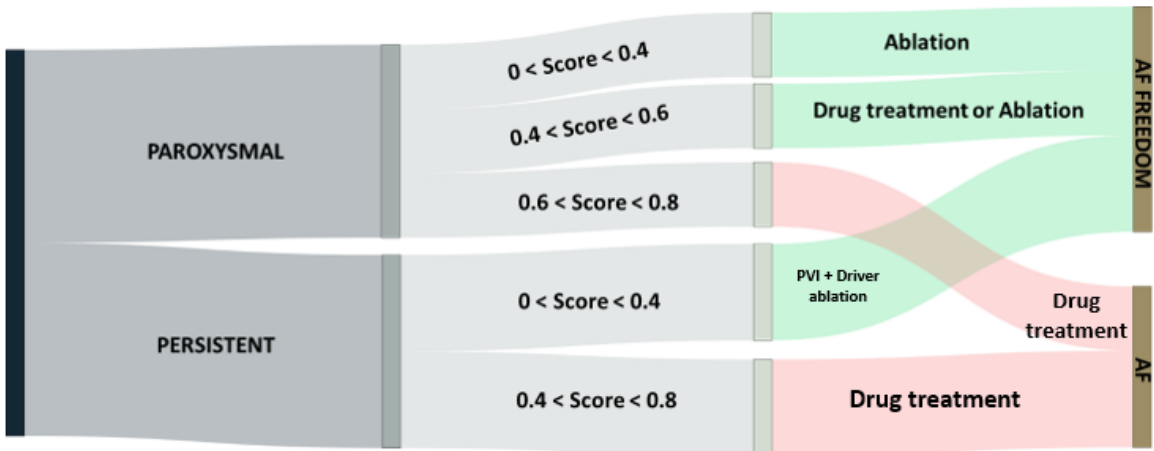
Figure 5.7. Results obtained from the clustering algorithm identifying 5 different groups in three levels. From left to right, the first variable represents AF type (Paroxysmal on top, Persistent on the bottom), score value divided in three subgroups for the paroxysmal patients and in two groups for the persistent patients and type of treatment in the last part of the diagram. Green and red colors represent AF Freedom and AF respectively.

Three different variables were identified as relevant to predict the outcome of the patients, in the following order: AF type (persistent or paroxysmal AF), ECGi electrophysiological complexity variables and type of treatment.

Type of treatment was classified in four different categories: ablation, ablation with drivers, drug treatment or rate control.

This clustering technique revealed five different groups based on the test set that can be described as follows:

The first group, corresponding to paroxysmal patients with low score values, present better outcomes when ablation is performed, independently of the type of ablation. The second group, corresponding to paroxysmal patients with values of the score between 0.4 and 0.6, presented good outcomes independently of the treatment used (pharmacological or interventional). The third group, corresponding to paroxysmal patients with high values of the score, presented bad outcome (AF) independently of the treatment strategy used.

In the case of persistent patients, those with a low score value, presented better outcomes when rotor ablation combined with PVI was performed. Finally, the fifth group, corresponding to persistent patients with high score values, had poor outcome regardless the type of treatment.

92

Table 5.5. Distribution of patients in clusters attending to the developed algorithm divided into cluster treatment and other treatments. Blank spaces correspond to clusters in which a successful treatment was not found.

	Selected and Predicted Treatment		Predicted treatment mismatch	
	AF Freedom	AF	AF Freedom	AF
Cluster #1	14	1	3	6
Cluster #2	18	5	5	3
Cluster #3			1	5
Cluster #4	22	8	10	10
Cluster #5			28	39

For each of the identified clusters, the algorithm identified the most suitable treatment for each case, as shown in Figure 5.7. For example, for paroxysmal patients with low electrophysiological complexity, the pattern identification revealed that the most promising treatment was ablation, without any relevant different among the strategy used (cryoablation, radiofrequency ablation nor driver ablation). Therefore, this diagram depicts the most suitable treatment for each of the five clusters. More in detail, Table 5.5 shows the AF freedom prevalence in each of the clusters attending to the proposed treatment on the test set. Successful treatments are shown in green in Figure 5.7. while the groups showing red color correspond to unsuccessful treatments, also associated with higher electrophysiological complexity.

Figure 5.9 shows one example for each of the clusters and the calculated metrics for each of them. Interestingly, this clustering analysis demonstrates the importance of identifying the AF type for patient outcome. This is specifically important for patients with score between 0.4 and 0.6, as in the case of being paroxysmal patients, suggested treatments can be effective, while in the case of the same patient being persistent, the outcome is not very favorable. Finally, this algorithm was tested on the 20% test set, obtaining 89.99% of success, showing better performance than the conventional paroxysmal vs. persistent classification (Figure 5.8).
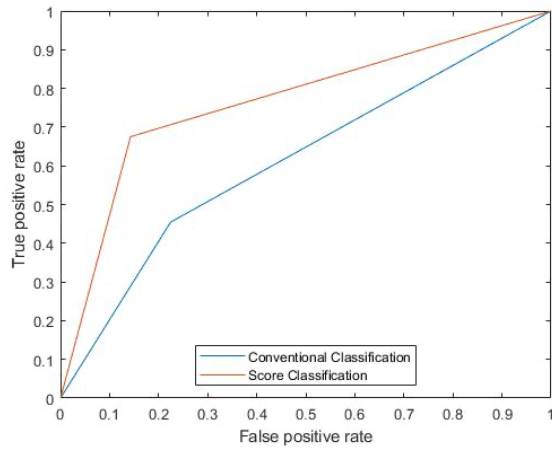
Figure 5.8. ROC curve for the performance of the conventional classification and score classification based on electrophysiological parameters
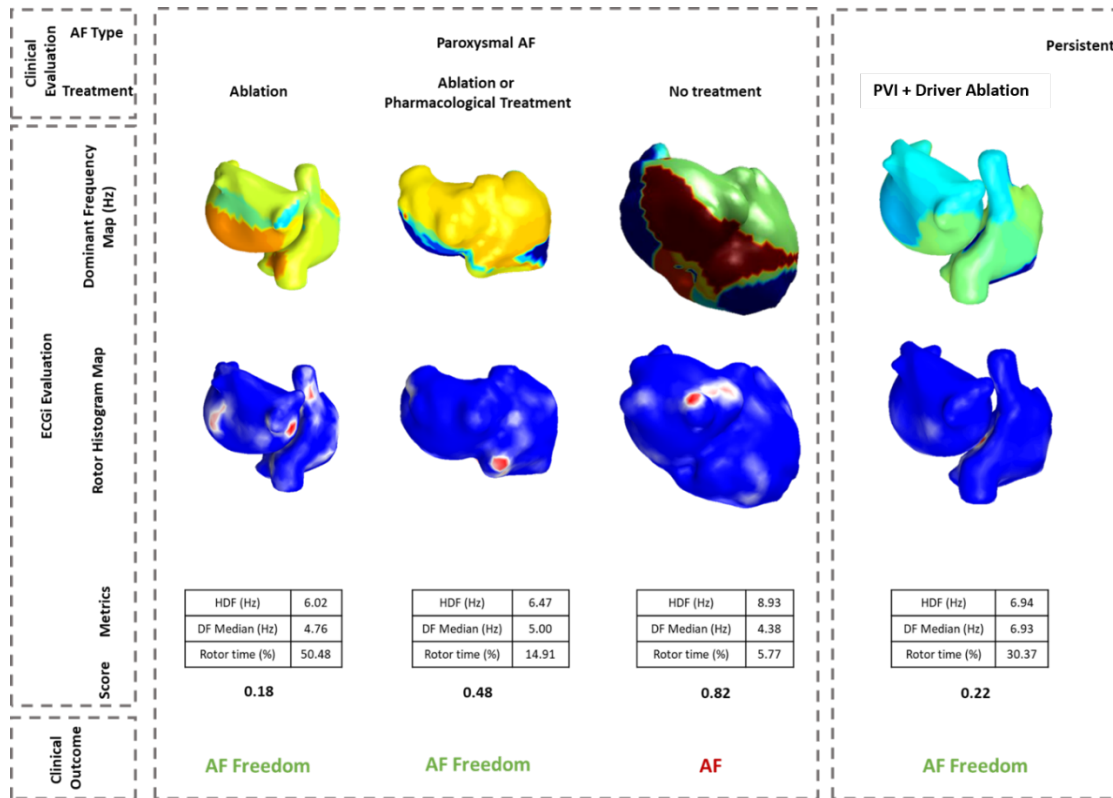
Figure 5.9. Examples of patients belonging to each of the five clusters. Panel describes the AF type, tre biomarkers for each specific patient, calculated score and clinical outcome.

95

5.4. Discussion

The present work aimed to identify AF predictive biomarkers by using the parameters obtained from the ECGi during AF episodes. From the complete patient cohort, we determined a predictive model or risk score that enable to estimate 12-month outcome prognosis based on the treatment selected according ESC guidelines. Interestingly, the use of electrophysiological information obtained from the ECGi, combined with the clinical information allowed the identification of 5 different clusters or groups that increased the performance of traditional clinical guidelines for treatment selection.

AI algorithms are being applied in multiple clinical scenarios for the automation and diagnosis (Sánchez de la Nava et al., 2021). Several scores have been previously presented for these purposes, such as the APPLE (Kornej et al., 2015), ATLAS (Mesquita et al., 2018), BASE-AF , CAAP-AF (Winkle et al., 2016), LAGO (Bisbal et al., 2018) and MB-LATER (Budzianowski et al., 2019). Although the sizes of these studies were, in some cases, larger than in this study, none of them considered different treatment approaches for the cohort in different clusters. In addition, the parameters included in the different scores or studies differ from one another due to the heterogeneity of the samples. However, all these scores recall the importance of the electrophysiological information of the heart by including data from electrophysiological tests such as the ECG or independent predictors associated with AF.

In contrast, the present study used AI technology to predict prognosis of AF patients based on electrophysiological parameters obtained from the ECGi. We developed a risk score that includes several parameters that have been already related to AF prediction, such as the highest dominant frequency and the rotor time, that is directly related to the stability of the rotor (Guillem et al., 2013; Narayan et al., 2013). In particular, HDF has been previously identified as one of the biomarkers for efficacy evaluation of patients undergoing ablation, as previously described (Rodrigo et al., 2014; Marques et al., 2020), including studies of this group using the ECGi technology. This study is in accordance with previous results obtained by the group in smaller cohorts, where we obtained a complexity algorithm in patients undergoing AF ablation where we proved that the use of paroxysmal and persistent classification in combination with electrophysiological parameters presents better prediction outcomes that standard clinical guidelines (Sanchez de la Nava et al., 2020).

In the same trend, other biomarkers have been explored presenting increased performance for long-term evolution prediction when compared

with the standard clinical guidelines. For example, Rodrigo et al. showed that lower complexity, quantified in terms of stable AF reentrant sites, was found in patients in whom AF terminated after ablation (Rodrigo et al., 2020). In addition, other studies also established a direct relation among shorter duration between time of first AF diagnosis and AF ablation procedure with better outcome results (Chew et al., 2020). Arrhythmia complexity has not only been characterized using electrophysiological parameters as in the aforementioned studies. Lankveld et al. (Lankveld et al., 2016) identified the AF termination index procedure and the mean fibrillation-wave amplitude as independent predictors, in combination with clinical information, of AF prognosis. Other studies such as the observational study presented by Meo et al (Meo et al., 2018) described complex arrhythmias as short cycle lengths and higher nondipolar component index.

Finally, the use of clinical biomarkers such as the AF type and the type of treatment, that have been present in the AF management clinical guidelines, also describe persistent patients as more complex. Interestingly, our developed score associated persistent patients with more complex scenarios, as the threshold for the score that indicated a successful ablation was lower in this case than in the case of paroxysmal patients. However, this is in agreement with previous studies that documented worse ablation results in patients with persistent AF (Rottner et al., 2020).

5.4.1. Limitations

The present work has several limitations. The cohort was recruited in a single hospital and a wider sample from different hospitals will ensure robustness of the risk score. In addition, the cohort presented imbalanced datasets, with the ablation subgroup including more patients. As the difference was not significantly high, we assumed that balancing group methods were not necessary for the development of the score but further studies should confirm this. AF complexity could only be analyzed in patients presenting AF during the outpatient visit or during the electrophysiologic procedure, potentially excluding patients with lower AF burden. However, we are currently aiming to analyze these features during sinus rhythm in ongoing protocols.

5.4.2. Conclusions

Patient evaluation and stratification prior to treatment decision is key to improve success rate of current AF patient management. With this study, we were able to predict 12-month prognosis by using AI algorithms that combined clinical information with ECGi biomarkers and identified the most suitable treatment for each patient, attending to clinical guidelines recommendations.

Supplementary Tables

Supplementary information depicts the information, by groups, of the clinical baseline characteristics of both groups included in the observational study. As it can be observed, no significant differences were found at clinical level between the AF Freedom and AF group in any case except for the age in the ablation group. The rest of the differences have been already discussed in the main body of the article.

Outpatient group baseline characteristics

	All patients	AF Freedom	AF	p-value
	84	33	51	
Gender	32 female	18 female	14 female	0.99
Age (yrs)	65.37 ± 11.00	64.72 ± 12.51	65.80 ± 10.01	0.67

Table 5.6. Description of patients included in the study attending to sex (Female/Male) and age.

	Complete cohort	AF Freedom	AF	p-value
Pathology *	84	33	51	
Arterial Hypertension	40 (47.62%)	17 (34.34%)	23 (45.10%)	0.79
Obesity	**9 (10.71%)**	**1 (3.03%)**	**8 (15.69%)**	**0.07**
Ischemic Cardiac Condition	2 (2.38%)	2 (6.06%)	0 (0.0%)	1.00
Cardiac Insufficiency	3 (3.57%)	1 (3.03%)	2 (3.92%)	0.66
Mitral Insufficiency	3 (3.57%)	2 (6.06%)	1 (1.96%)	0.94
Atrial/Ventricular Dilation	2 (2.38%)	1 (3.03%)	1 (1.96%)	0.85
Previous Valvuloplasty	3 (3.57%)	0 (0.0%)	3 (5.88%)	0.22
Infarct	3 (3.57%)	2 (6.06%)	1 (1.96%)	0.94
Ictus	5 (5.95%)	3 (6.06%)	2 (3.92%)	0.92
Diabetes	13 (15.48%)	5 (10.10%)	8 (15.67%)	0.60
Alcohol	2 (2.38%)	2 (4.04%)	0 (0.0%)	1.00
Smoking	24 (28.57%)	10 (20.20%)	14 (27.45%)	0.70
Dyslipidemia	33 (39.29%)	17 (34.34%)	16 (31.37%)	0.98
Hypothyroidism	4 (4.76%)	1 (3.03%)	3 (5.88%)	0.49
Renal Transplant	1 (1.19%)	1 (3.03%)	0 (0.0%)	1.00
Gout	1 (1.19%)	0 (0.0%)	1 (1.96%)	0.61

Psoriasis	1 (1.19%)	1 (3.03%)	0 (0.0%)	1.00
Osteoporosis	1 (1.19%)	0 (0.0%)	1 (1.96%)	0.61
Rhinitis	1 (1.19%)	0 (0.0%)	1 (1.96%)	0.61
Oncological treatment	2 (2.38%)	2 (6.06%)	0 (0.0%)	1.00

Table 5.7. Description of concomitant pathologies of the consultation group.

	Complete cohort	AF Freedom	AF	p-value
AF Type	84	33	51	
Flutter	6	4	2	
Paroxysmal	24	9	15	0.40
Persistent	53	20	33	

Table 5.8. Cohort classification depending on AF type.

As it can be observed, no significant differences were found among AF Freedom and AF patients in the consultation group, except for obesity, that presented a significantly higher rate in the AF group.

Ablation group baseline characteristics

	All patients	AF Freedom	AF	p-value
	120	80	40	
Gender	42 female	27 female	15 female	0.417
Age	60.90 ± 9.27	59.13 ± 9.50	64.45 ± 7.77	0.003

Table 5.9. Description of patients included in the study attending to sex (Female/Male) and age.

	Complete cohort	AF Freedom	AF	p-value
AF Type	120	80	40	
Flutter	12	8	4	
Paroxysmal	33	26	7	0.20
Persistent	72	44	28	

Table 5.10. Cohort classification depending on AF type.

	Complete cohort	**AF Freedom**	**AF**	**p-value**
Pathology *	120	80	40	
Arterial Hypertension	34 (28.57%)	24 (30.00%)	10 (25%)	0.78
Obesity	15 (12.5%)	12 (10%)	3 (0.75%)	0.93
Ischemic Cardiac Condition	1 (0.84%)	1 (1.25%)	0 (0.0%)	1.00
DAI	1 (0.84%)	1 (1.25%)	0 (0.0%)	1.00
Cardiac Insufficiency	2 (1.68%)	2 (2.5%)	0 (0.0%)	1.00
Mitral Insufficiency	2 (1.68%)	1 (1.25%)	1 (2.5%)	0.56
Atrial/Ventricular Dilation	2 (1.68%)	2 (2.5%)	0 (0.0%)	1.00
Infarct	2 (1.68%)	0 (0.0%)	2 (5.0%)	0.11
Angina	1 (0.84%)	1 (1.25%)	0 (0.0%)	1.00
Ictus	1 (0.84%)	0 (0.0%)	1 (2.5%)	0.33
Long QT	1 (0.84%)	0 (0.0%)	1 (2.5%)	0.33
Diabetes	11 (9.16%)	10 (12.5%)	1 (2.5%)	0.99
Smoking	11 (9.16%)	8 (10%)	3 (7.5%)	0.78
Asthma	2 (1.68%)	1 (1.25%)	1 (2.5%)	0.56
EPOC	1 (0.84%)	0 (0.0%)	1 (2.5%)	0.33
Bradycardia	1 (0.84%)	0 (0.0%)	1 (2.5%)	0.33
Pulmonary Emphysema	1 (0.84%)	1 (1.25%)	0 (0.0%)	1.00
Dyslipidemia	2 (1.68%)	1 (1.25%)	1 (2.5%)	0.56
Hypothyroidism	6 (5.00%)	5 (6.25%)	1 (2.5%)	0.92
Depression	2 (1.68%)	1 (1.25%)	1 (2.5%)	0.56
Epilepsy	2 (1.68%)	1 (1.25%)	1 (2.5%)	0.56

Table 5.11. Description of concomitant pathologies of the consultation group.

	Complete cohort	**AF Freedom**	**AF**	**p-value**
Ablation strategy	120	80	40	
PVI	49	37	12	
PVI + rotors	67	40	27	0.11
Valvuloplasty	3	3	0	

Table 5.12. Cohort classification depending on ablation strategy. P-value obtained from two-tailed Fisher exact test.

	Complete cohort	AF Freedom	AF	p-value
Ablation type	120	80	40	
Radiofrequency ablation	97	60	37	0.02
Cryoablation	23	20	3	

Table 5.13. Cohort classification depending on ablation type. P-value obtained from two-tailed Fisher exact test.

Pharmacological changes after ablation

	Complete cohort	AF Freedom	AF	p-value
Ablation type	120	80	40	
Changes in strategy after ablation	73	48	25	0.48
No changes in strategy	47	32	15	

Table 5.14. Changes registered after the ablation procedure on the patient cohort. P-value obtained from two-tailed exact test.

	Complete cohort	AF Freedom	AF	p-value
Ablation type	120	80	40	
Changes in strategy after ablation	73	48	25	
Pharmacological changes	54	42	12	1.00
Adding/Increase	32	30	2	0.99
Eliminate/decrease	22	12	10	
Interventional changes	20	6	14	
Ablation/CVE	18	4	14	0.08
Pacemaker	2	2	0	

Table 5.15. Pharmacological and interventional changes registered after the ablation procedure on the patient cohort. P-value obtained from two-tailed exact test.

Chapter 6. Conclusions and Discussion

In this chapter, a global conclusion of the results given in this dissertation is presented. First, the main conclusions of this thesis are listed by assessing the resolution of the objectives. The chapter is closed with a guideline for future work, highlighting aspects of this thesis that can be improved and the range of future lines of this research.

6.1. Main Findings

Although the most common treatment for AF patients is the pharmacological therapy, ablation has acquired more relevance due to its ability to eradicate the arrhythmia in many patients, especially when the ablation is conducted at its earliest stage (Hindricks et al., 2020). In addition, it has been reported that ablative therapies present higher rates of efficacy when a patient-tailored approach based on the characterization of the fibrillatory process in each patient is used (Seitz et al., 2017; Jungen et al., 2020). Therefore, different methods to locate the atrial drivers maintaining the arrhythmia have been used in the clinical practice, mainly based on the analysis of the intracavitary signal recorded with catheters (Ramirez et al., 2017). However, these characterization methods are only available for patients already in the laboratory and thus this analysis does not allow to select patients nor to plan the ablation procedure. In order to solve such problems, non-invasive methods for atrial driver identification have been developed, such as BSPM or ECGi. Nevertheless, the novelty of these systems together with the controversy regarding the underlying mechanisms in which they rely on are delaying their introduction into the clinical practice. This thesis broadens the scientific and technical knowledge about the non-invasive identification and localization of atrial drivers.

This Doctoral Thesis describes the multidisplinary research project aimed at deciphering one of the most critical macromolecular ion channel interactions in the normal and the diseased heart.
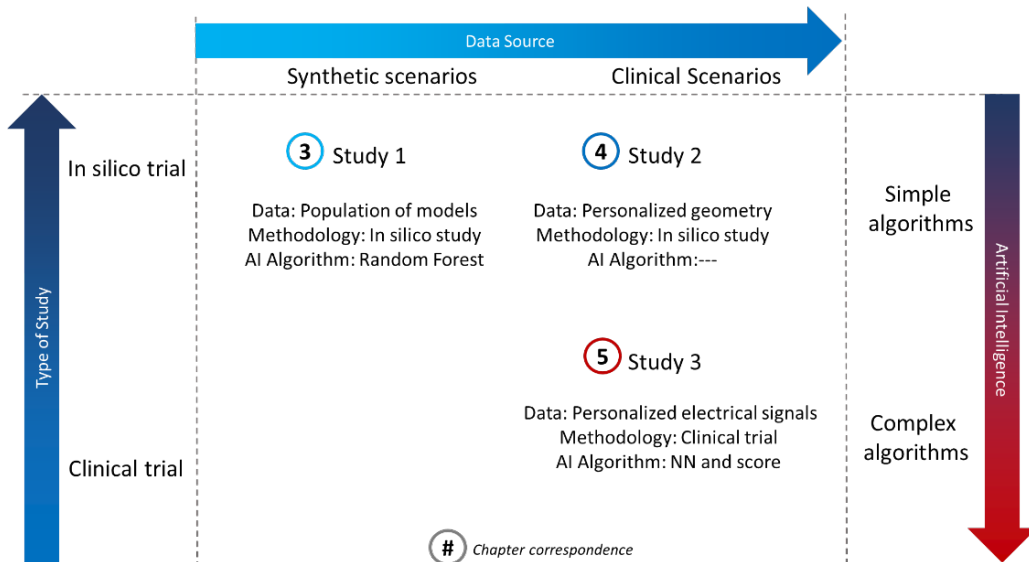
Figure 6.1. Main discussion and contributions of the thesis

All this information has been included in Figure 6.1, where the overall contributions of the thesis are illustrated. As it can be observed, the dissertation covers three different key areas that have been explored throughout the thesis. These key areas are identified as: type of study (divided into *in silico* trial or clinical trial), data source (identified as synthetic scenarios or clinical scenarios) and artificial intelligence (including simple algorithm, a neural network approach and the development of a new score).

The first study presented in this thesis (Chapter 3) is framed in the context of *in silico* trials using synthetic data and simple algorithms. In particular, we showed that the use of processing algorithms that enable the identification of patterns from a large database can be useful for AF screening and understanding. In this first study, we proved, using data from simulations calibrated with a real AF population, that the patterns identified at clinical level can also be identified with low cost computational trained algorithms.

In silico simulations were combined with clinical information using atrial anatomies from 30 patients in the second study of this thesis (Chapter 4). At simulation level, simple algorithms were implemented to lower the computational cost of the experiments and to identify a biomarker that could describe atrial complexity.

Finally, the last study of the thesis (Chapter 5) includes the Stratify-AF observational study in which AF recordings from 204 patients were characterized using complex algorithmic ECGi calculation in a clinical scenario to identify prognosis of patients depending on the treatment.

6.2. Comparison with Previous Studies

The analysis of arrhythmia complexity has been key for the identification of new biomarkers and treatment of the arrhythmia. More specifically, several studies have presented different biomarkers to evaluate and predict the effect of the ablation, including rotational driver characterization, DF ablation or eliminating the frequency gradients that promote sinus rhythm maintenance(Atienza et al., 2009; Kocyigit et al., 2015; Alarcón et al., 2020).

Clinical data from patients that presented AF episodes recorded with the ECGi system developed by the group in collaboration with other institutions was evaluated, as reflected in Chapter 4 and Chapter 5. ECGi technology has been used in the last years to non-invasively characterize atrial (Graham et al., 2020; Salinet et al., 2021) and ventricular activity during irregular both regular and irregular rhythms (Betancourt et al., 2019; Graham et al., 2020; Rehorn et al., 2020). At the atrial level, this technology enables to estimate the dominant frequencies that have been identified as a potential trigger for the arrhythmia maintenance.

In silico scenarios have also been important in the study of AF and more recently, in the process of characterization at clinical level for ablation strategy and complexity evaluation (Hwang et al., 2016; Lim et al., 2020). Several approaches have been tested to design the ablation strategy (Arevalo et al., 2016; Kim et al., 2020) demonstrating its translational approach. In addition, the latest studies demonstrate the importance of incorporating clinical relevant information in the simulations, such as population of models calibrated with patch clamp data from human biopsies (Britton et al., 2013; Liberos et al., 2016; Bai et al., 2021) and personalized anatomy models (Fastl et al., 2018; Heijman et al., 2021). In line with these studies, the present thesis has included simulations using population of models in Chapter 3 and personalized anatomies in Chapter 4, using different approaches that enabled the characterization of atrial complexity. More specifically, the study shown in Chapter 4 presents a workflow with direct translation into the clinical scenario, although prior validation of the methodology is needed.

Digital Health, and specifically Artificial Intelligence, have been applied the cardiology field in the last years, obtaining impressive results. Recordings from electronic devices such as smartwatch have enabled the identification of arrhythmic episodes in patients (Wasserlauf et al., 2019; Dagher et al., 2020), With new powerful equipment that are able to process longer

and more complex signals, studies including all the ECG derivations have also been published, with the main objective of predicting patient prognosis and evolution (Dretzke et al., 2019; Sanz-García et al., 2021). The work described in Chapter 5 belongs, therefore, to this new field that has arisen in which complex algorithmic equations are combined with clinical and digital information to evaluate patients and personalize their treatments.

Finally, one of the most important contributions of this thesis is the overall technology developed at different scales to evaluate complexity, that allows, from different perspectives, to study and categorize specific characteristics of the patients in each of the studies, demonstrating its translational approach.

6.3. Limitations

As usually occurs in most scientific studies, there are several limitations that were present during the development of this thesis. Although the current limitations have been already commented in the individual chapters concerning each study, there are some additional key points that should be commented.

As depicted in Figure 6.1., from the three different scenarios considered, a total of three different studies were performed. However, we were unable to perform a clinical trial in which only synthetic scenarios were evaluated with complex algorithms. This was motivated due to previous studies that present *in silico* scenarios with poor translation into the clinical scenario (Peirlinck et al., 2021). As it is already known, *in silico* scenarios usually present controlled environments that do not correspond to clinical complex scenarios and that, in the absence of personalized data from the patients, the results of these studies lack of translational approaches but rather scientific explanations of patterns or behaviors. Therefore, we considered that the best option in this case was to focus on the fields that enabled a direct translation into the clinical practice as the translational approach is key in a clinical environment.

In addition to those clinical applications of the developed technology, technological advances are required to increase the quality of research models and to continue improving the efficacy of characterization techniques. Those efforts are only being possible thanks to the multidisciplinary collaboration between clinicians, engineers, biologists, etc. that the team of the Laboratory for Research on Translational Cardiology of Hospital Gregorio Marañón in Madrid has been able to set-up.

6.4. Conclusions

The main objective of this thesis was to explore the application of Artificial Intelligence in the Cardiology Field, in particular in AF. Along the different chapters of this thesis, this objective has been achieved through the study of diverse approaches in non-invasive electrocardiography. This objective was broken down in the following points:

1. *To study and evaluate AF maintenance under the effect of different drugs, implementing in silico models in two different plane sizes using an electrophysiological model that includes ionic level description.*
   We presented a population of models approach in which arrhythmia induction was evaluated by modifications in tissue size and drug administration. Higher probability of induction was observed in larger tissue and, interestingly antagonistic effects were observed for some of the profiles, showing that for a minority of cases, the drugs may present adverse or non-desired effects.

2. *To study and evaluate the pulmonary vein ablation efficacy implementing in silico models in 3D personalized geometries using an activation pattern model.*
   We presented personalized in silico simulations in a cohort of 30 patients that underwent pulmonary vein ablation and in which different arrhythmia scenarios were evaluated at computational level. From these experiments, we concluded that ablation success was associated with patients that, at computational level, presented low number of high entropy foci located in the pulmonary vein area whereas patients with multiple high entropy foci outside of this area were associate to unsuccessful ablations.

3. *To identify a predictive biomarker or a combination of them from the in silico data obtained in the aforementioned objectives that enable to predict AF maintenance or termination and that relate to clinical scenarios.*
   From the data obtained in the aforementioned objectives, we identified multiple variables as potential predictive biomarkers of AF maintenance.
   First, two important patterns associated with AF maintenance at clinical level were identified as a result of the calibration of the algorithm in Chapter 3: the first one directly related to hyperkalemia and the second one directly related to hypokalemic scenarios.

Secondly, the ACB was identified in Chapter 4 as a descriptor of the rotational activity on the pulmonary vein area and as a potential predictor of ablation efficacy, showing that patients with higher rotational activity in this area presented also better outcomes after the ablation.

4. *To evaluate the performance of clinical data from the Stratify AF study to train clustering algorithms that allow to identify similar groups of patients with similar outcome.*

    Clinical and electrophysiological data were analyzed in the Stratify observational study. The electrophysiological characterization obtained from the ECGi was used to build a score for AF complexity estimation that identified highest dominant frequency, median dominant frequency and mean rotor time as predictors of treatment efficacy. Later, this score was combined with clinical data in a clustering algorithm to evaluate individual prognosis in a cohort of AF patients. This algorithm presented higher accuracy than the conventional guideline approaches in the same patient set, showing that the personalized electrophysiological data analysis from patients can be critical to evaluate the complexity of the arrhythmia.

5. *To asses and define the biomarkers that describe the sensitivity profile by analyzing the overall results of the experiments performed from a translational point of view, that combines in silico computational data and clinical data to explore the electrophysiological biomarkers that characterize AF maintenance.*

    Finally, the three studies combined together aim to present a translational platform that characterizes and evaluates AF complexity at different levels including 2D and 3D in silico scenarios that contemplate pharmacological and ablation therapies (Chapter 3 and Chapter 4) and clinical scenarios including the Stratify AF observational study (Chapter 5). The identification of all the biomarkers at different levels aim to define and characterize the sensitivity profile in AF management.

Everything above discussed has facilitated a better understanding of the physical and technical mechanisms involved in AF complexity evaluation. The better understanding of arrhythmia complexity can help to personalize patient's treatment using technologies as non-invasive systems for atrial driver location, as described in Chapter 5.

The combination of personalized *in silico* simulations with clinical relevant biomarkers can be used to benefit both patients and health systems,

that has been growing and gaining applicability at practical level and whose use is expected to increase as Digital Health enters the healthcare systems (Heijman et al., 2021).

6.5. Guidelines for future works

The methodological aspects and results presented in this thesis have concluded with three different methods for identifying and characterizing arrhythmia complexity: first, in Chapter 3 using a population of models, second in Chapter 4 using specific atrial anatomies from patients and lastly in Chapter 5 using BSPM recordings and the posterior ECGi calculation to evaluate AF prognosis depending on the treatment. Although, this characterization at three different levels have allowed an extensive evaluation of different methodologies, there are some further experiments that would help to validate all the methodology.

Future studies should include more patients to validate and characterize the already presented results. For example, the study in Chapter 3 includes a calibrated population of models that contained 127 profiles. In order to test intersubject variability, the population could be expanded to consider new profiles and to study arrhythmia inducibility in them. In addition, it would also be interesting to include simulation of more complex structures associated with proarrhythmicity such as pulmonary veins or the atrial appendage.

Regarding the simulations performed in Chapter 4, a wider range of atrial anatomies could be segmented from AF patients to validate ACB developed during the simulation study. Currently, our group at Hospital General Universitario Gregorio Marañón is carrying new observational studies (Paper-AF Study) that will enable to enlarge the anatomical database and to validate the biomarker.

Finally, the study in Chapter 5 would highly benefit from a larger patient cohort in which more parameters and algorithms could be tested and validated. In addition, other processing techniques could be explored such as evaluating AF prognosis directly from the BSPM recordings and comparing its performance with the algorithms developed from the ECGi technology.

Chapter 7. Contributions

7.1. Main contributions of this thesis

7.1.1. Journal papers

- **Sánchez de la Nava, A. M.**, Atienza, F., Bermejo, J., & Fernández-Avilés, F. (2021). Artificial Intelligence for a Personalized Diagnosis and Treatment of Atrial Fibrillation. American Journal of Physiology-Heart and Circulatory Physiology. https://doi.org/10.1152/ajpheart.00764.2020

- **Sánchez de la Nava, A.M.;** González Mansilla, A.; González-Torrecilla, E.; Ávila, P.; Datino, T.; Bermejo, J.; Arenal, Á.; Fernández-Avilés, F.; Atienza, F. Personalized Evaluation of Atrial Complexity of Patients Undergoing Atrial Fibrillation Ablation: A Clinical Computational Study. *Biology* 2021, *10*, 838. https://doi.org/10.3390/biology10090838

- **Sanchez de la Nava, A. M**., Arenal, Á., Fernández-Avilés, F., & Atienza, F. (2021). Artificial Intelligence-Driven Algorithm for Drug Effect Prediction on Atrial Fibrillation: An in silico Population of Models Approach. Frontiers in Physiology, 0, 2079. https://doi.org/10.3389/FPHYS.2021.768468

7.1.2. International conferences

- **Sanchez de la Nava, A.M.;** Soto, N.; López, J.; Datino, T.; Ávila, P.; Gonzalez-Torrecilla, E.; Maiz, A.A.; Fernández-Avilés, F.; Atienza, F. B-PO02-023 Artificial Intelligence Platform for Stratification of Atrial Fibrillation prior to Ablation.Hear. Rhythm 2021, 18, S104, doi:10.1016/J.HRTHM.2021.06.280.

- **AM Sanchez De La Nava**, E Gonzalez-Torrecilla, A Gonzalez-Mansilla, N Soto, P Avila, T Datino, J Bermejo, A Arenal, F Fernandez-Aviles, F Atienza, Evaluation of atrial complexity of patients undergoing atrial fibrillation ablation: a clinical computational study, EP Europace, Volume 23, Issue Supplement_3, May 2021, euab116.236, https://doi.org/10.1093/europace/euab116.236
- **Sanchez de la Nava, A.** ., Climent, A., Hernandez, I., Lopez, J., Bermejo, J., Arenal, A., … Atienza, F. (2020). Atrial Fibrillation Complexity Score Predicts Patient Outcome after Pulmonary Vein Ablation. Heart Rhythm, 17(5), Suppl (S1-S762): D-PO01-169. Heart Rhythm.
- **AS. De la Nava**, MC. Fabregat, M. Rodrigo, I. Hernández-Romero, A. Liberos, F. Fernández-Avilés, F.Atienza, MS. Guillem, A.M. Climent. Non-invasive Electrophysiologycal Mapping Entropy Predicts Atrial Fibrillation Ablation Efficacy Better than Clinical Characteristics. Computing in Cardiology Conference,September 2019.
- **AS. De la Nava**, A.Liberos, I. Hernández-Romero, F. Fernández-Avilés, F. Atienza, MS. Guillem, AM. Climent. Antiarrhythmic Drug Treatment for Atrial Dibrillation: Effectiveness of Drug Depends on Electrophysiological Profile. Computing in Cardiology Conference, September 2019.
- A. Dominguez-Sobrino, **AS. De la Nava**, I. Hernández-Romero, M. Rodrigo, MS. Guillem, F. Atienza, F.Fernández-Avilés, AM. Climent. In-silico 2D Atrial Tissue Modelling on a Population: Impact of Fibrosis in Arrhythmogenesis. Computing in Cardiology, September 2019.
- **AS. de la Nav**a, A. Liberos, I. Hernández-Romero, MS Guillem, F. Atienza, F. Fernández-Avilés, AM Climent. In-silico Safety Pharmacology on Intersubject Variability Population of Models: A Regression Model Approach. Computing in Cardiology Conference 2018
- A. Liberos, AM. Climent, **AS. De la Nava**, M Rodrigo, I. Hernández-Romero, F. Fernández-Avilés, F. Atienza, MS. Guillem. Atrial Flutter Re-entrant Circuit Identification based on Body Surface Phase Mapping. VPH 2018
- **AS. De la Nava**, I. Hernández-Romero, MS. Guillem, F. Atienza, F. Fernández-Avilés, A. Liberos, AM. Climent. Automatic Atrial Fibrillation Initiation for the Evaluation of Proarrhythmic Risk at Tissue In-Silico Models. VPH

7.1.3. National conferences

- A.M. Sánchez de la Nava et al, "A Novel Translational Stratification System for Electrophysioilogical Characterization: Evaluating Arrhythmia Complexity from the Lab to the Clinic", TerCel, 2021.

7.1.4. Awards

- First award in the Young Investigators Award of the Computing in Cardiology conference in 2018, Maastricht, The Netherlands.
- Travel Scholarship for 2020 Heart Rhythm Scientific Sessions
- First award in the IV Health Hackathon 2019, Madrid, Spain.
- Computing in Cardiology Travel Grant 2019
- Heart Rhythm Travel Grant 2020
- Finalist in TerCel Young Investigators Award 2021

7.1.5. Courses Attended

- Image-Based Biomedical Modeling (IBBM) Summer Course (2018 Edition)
- Summer School in Computational Physiology held by Simula Research Laboratory and University California San Diego (2019 Edition)
- EHRA Webinar: Rise of the machines: the role of artificial intelligence and machine learning in arrhythmia diagnosis and management

7.1.6. Courses and presentations

- Simposio Médico sobre Medicina Regenerativa de Vanguardia, Pamplona, Spain. Organized by Clínica Universidad de Navarra and CIMA Universidad de Navarra. November 2021.

7.2. Contributions related to this thesis

7.2.1. Journal papers

- Gómez-Cid, L., Grigorian-Shamagian, L., Sanz-Ruiz, R., **de la Nava, A. S**., Fernández, A. I., Fernández-Santos, M. E., & Fernández-Avilés, F. (2021). The Essential Need for a Validated Potency Assay for Cell-Based Therapies in Cardiac Regenerative and Reparative Medicine. A Practical Approach to Test Development. Stem Cell Reviews and Reports 2021, 1, 1–10. https://doi.org/10.1007/S12015-021-10244-5
- Carvajal-Vergara, X.; López-Muneta, L.; Linares, J.; Casis, O.;

Martínez-Ibáñez, L.; Gonzalez Miqueo, A.; Bezunartea, J.; **Sanchez De La Nava, A.M.;** Gallego, M.; Fernández-Santos, M.E.; et al. Generation of NKX2.5GFP reporter human iPSCs and differentiation into functional cardiac fibroblasts. Front. Cell Dev. Biol. 1AD, 0, 3669, doi:10.3389/FCELL.2021.797927.

- Gómez-Cid, L., Moro-López, M., **de la Nava, A. S**., Hernández-Romero, I., Fernández, A. I., Suárez-Sancho, S., … Fernández-Avilés, F. (2020). Electrophysiological effects of extracellular vesicles secreted by cardiosphere-derived cells: Unraveling the antiarrhythmic properties of cell therapies. Processes, 8(8), 924. https://doi.org/10.3390/PR8080924

7.2.2. International conferences

- **A. M. Sanchez et al.,** "Influence of highest dominant frequency area on fibrillation dynamics and frequency spectrum on electrograms." ESC 2021.
- G. R. Rios-Munoz et al., "Unveiling the impact of fibrosis presence in fibrillatory electrograms," Eur. Heart J., vol. 42, no. Supplement_1, Oct. 2021.
- Diez-Del-Hoyo, F.; Sanz, R.; **Sanchez De La Nava, A.**.; Torrecilla, E.; Datino, T.; Avila, P.; Bermejo, J.; Arenal, A.; Atienza, F.; Fernandez-Aviles, F. Reverse remodeling of the atria in patients with rheumatic mitral stenosis: impact of balloon mitral commissurotomy plus atrial fibrillation ablation. Eur. Heart J. 2020, 41, doi:10.1093/EHJCI/EHAA946.0458.

7.2.3. National conferences

- **A.M. Sánchez de la Nava** et al. "Electrophysiological Characterization Based on Frequency and Rotor Biomarkers of Cardiac Constructs:; A Critical Step Towards the Evaluation of Regenerative Products", in TerCel, 2021.
- **A. M. Sánchez de la Nava** et al., "Influencia del área de la frecuencia dominante en las dinámicas de firbilación y el espectro de frecuencia en los electrogramas," in Rev Esp Cardiol, 2021, vol. 74, p. 1046.
- G. Ricardo Ríos Muñoz et al., "Desvelando el impacto de la fibrosis en electrogramas de fibrilación auricular," in Rev Esp Cardiol, 2021, vol. 74, p. 134.
- Moro-López, M.; Gómez-Cid, L.; **de la Nava, A.S.**; Férnandez Santos, M.E.; Grigorian-Shamagian, L.; Fernandez-Aviles, F. Effect of cardiac stem cell derived extracellular vesicles on

cardiomyocytes. In Proceedings of the XXXVIII Congreso Anual de la Sociedad Española de Ingeniería Biomédica.; 2020; pp. 161–164.

- P. Montero, M. Flandes-Iparaguirre, **AS. De la Nava**, S. Zaballa, AM. Climent, F. Fernández-Avilés, F. Prosper, M. Mazo. Towards Mature Cardiac Tissue by Additive Manufacturing with Melt Electrospinning Writing. TECAM 2019

7.2.4. Conducted bachelor thesis

- "Automatic deposistion techniques for the development of realistic cardiac in vitro models" David Sanz Gutiérrez, June 2018. Universidad Carlos III de Madrid.
- "Effect of cardiomyocyte-fibroblast coupling on arrhythmogenesis" Alonso Fomínguez Sobrino. July 2019. Universidad Carlos III de Madrid.
- "Automatic deposition and characterization of hydrogel bioprinter cardiac structures". José Joaquin Casado Garrido. July 2020. Universidad Carlos III de Madrid.

7.3. Participation in research projects

This work has been developed within the framework of several research projects. The interest and relevance of the research activity carried out by our group has been acknowledged by public administrations by means of the following research project in which the author has participated:

- Proyectos de Investigación en Salud
  Estratificación y tratamiento de la fibrilación auricular basada en los mecanismos de perpetuación de la arritmia (STRATIFY-AF)
  IP: Felipe Atienza Fernández
  Identification code: PI17/01059

- Proyectos de Investigación en Salud
  Electrophysiological Substrate Characterization on Paroxysmal and Persistent Atrial Fibrillation Patients (PAPER-AF)
  IP: Felipe Atienza Fernández
  Identification code: PI20/01618

- European Institute of Technology Health (EIT Health) Funded Project
  Artificial Intelligence driven platform for atrial fibrillation stratification (AF-FINE)

IP: Felipe Atienza Fernández

- European Union's Horizon Reseach Project
Computational biomechanics and bioengineering 3D printing to develop a personalized regenerative biological ventricular assist device to provide lasting functional support to damaged hearts (BRAV3).
IP: Felipe Prósper Cardoso
Identification code: Grant agrreement 874827

7.4. Author contribution

The hypothesis consideration of this thesis and their development were carried out by the author under the guidance of Dr. Felipe Atienza, Prof. Dr. Fernández-Avilés and Prof. María de la Salud Guillem. The author implemented all simulations from the mathematical model dataset and accomplished the data analysis from both models and patient's dataset under the guidance of Prof. María de la Salud Guillem.

Dr. Felipe Atienza, Prof. Dr. Francisco Fernández-Avilés and the team at Hospital General Universitario Gregorio Marañón carried out the patient recordings used in this thesis.

Dr. Felipe Atienza, Prof. Dr. Francisco Fernández-Avilés and Prof. María de la Salud Guillem Sánchez supervised the final version of this thesis.

References

Akar, F. G., Laurita, K. R., and Rosenbaum, D. S. (2000). Cellular basis for dispersion of repolarization underlying reentrant arrhythmias. *J. Electrocardiol.* 33, 23–31. doi:10.1054/jelc.2000.20313.

Al'Aref, S. J., Anchouche, K., Singh, G., Slomka, P. J., Kolli, K. K., Kumar, A., et al. (2019). Clinical applications of machine learning in cardiovascular disease and its relevance to cardiac imaging. *Eur. Heart J.* 40, 1975–1986. doi:10.1093/eurheartj/ehy404.

Alarcón, F., Atienza, F., and Mont, L. (2020). Atrial fibrillation drivers mapping: should I burn or should I go? *EP Eur.* 22, 843–844. doi:10.1093/EUROPACE/EUAA064.

Alonso-Atienza, F., Carrión, R., Alberola, G., and Álvarez, L. R. (2005). A RRHYTHMIAS A Probabilistic Model of Cardiac Electrical Activity Based on a Cellular Automata System. 58, 41–47.

Alpaydin, E. (2014). *Introduction to Machine Learning*. doi:10.4018/978-1-7998-0414-7.ch003.

Althoff, T. F., and Mont, L. (2021). Novel concepts in atrial fibrillation ablation-breaking the trade-off between efficacy and safety. *J. arrhythmia* 37, 904–911. doi:10.1002/JOA3.12592.

Aparna, P., and Sharma, K. M. (2020). Detection of A Fib and its Classification using SVM. in *2020 2nd International Conference on Innovative Mechanisms for Industry Applications (ICIMIA)* (IEEE), 116–120. doi:10.1109/ICIMIA48430.2020.9074888.

Arevalo, H. J., Vadakkumpadan, F., Guallar, E., Jebb, A., Malamas, P., Wu, K. C., et al. (2016). Arrhythmia risk stratification of patients after myocardial infarction using personalized heart models. *Nat. Commun.* 7. doi:10.1038/ncomms11437.

Aronis, K. N., Ali, R. L., Liang, J. A., Zhou, S., and Trayanova, N. A. (2019).

Understanding AF mechanisms through computational modelling and simulations. *Arrhythmia Electrophysiol. Rev.* 8, 210–219. doi:10.15420/aer.2019.28.2.

Ashihara, T., Haraguchi, R., Nakazawa, K., Namba, T., Ikeda, T., Nakazawa, Y., et al. (2012). The Role of Fibroblasts in Complex Fractionated Electrograms During Persistent/Permanent Atrial Fibrillation. *Circ. Res.* 110, 275–284. doi:10.1161/CIRCRESAHA.111.255026.

Aslanidi, O. V, Colman, M. A., Stott, J., Dobrzynski, H., Boyett, M. R., Holden, A. V, et al. (2011). 3D virtual human atria: A computational platform for studying clinical atrial fibrillation. *Prog. Biophys. Mol. Biol.* 107, 156–68. doi:10.1016/j.pbiomolbio.2011.06.011.

Atienza, F., Almendral, J. J., Moreno, J., Vaidyanathan, R., Talkachou, A., Kalifa, J. J., et al. (2006). Activation of Inward Rectifier Potassium Channels Accelerates Atrial Fibrillation in Humans. *Circulation* 114, 2434–2442. doi:10.1161/CIRCULATIONAHA.106.633735.

Atienza, F., Almendral, J., Jalife, J., Zlochiver, S., Ploutz-Snyder, R., Torrecilla, E. G., et al. (2009). Real-time dominant frequency mapping and ablation of dominant frequency sites in atrial fibrillation with left-to-right frequency gradients predicts long-term maintenance of sinus rhythm. *Hear. Rhythm* 6, 33–40. doi:10.1016/j.hrthm.2008.10.024.

Atienza, F., Almendral, J., Ormaetxe, J. M., Moya, Á., Martínez-Alday, J. D., Hernández-Madrid, A., et al. (2014). Comparison of radiofrequency catheter ablation of drivers and circumferential pulmonary vein isolation in atrial fibrillation: A noninferiority randomized multicenter RADAR-AF trial. *J. Am. Coll. Cardiol.* 64, 2455–2467. doi:10.1016/j.jacc.2014.09.053.

Atienza, F., Martinez-Alzamora, N., De Velasco, J. A., Dreiseitl, S., and Ohno-Machado, L. (2000). Risk stratification in heart failure using artificial neural networks. *Proc. AMIA Symp.*, 32–36.

Atienza, F., Martins, R. P., and Jalife, J. (2012). Translational research in atrial fibrillation: A quest for mechanistically based diagnosis and therapy. *Circ. Arrhythmia Electrophysiol.* 5, 1207–1215. doi:10.1161/CIRCEP.111.970335.

Atienza, F., Rodrigo, M., Climent, A., Guillem, M., F, A., M, R., et al. (2021). "Non-invasive Frequency-Phase Mapping of Atrial Fibrillation," in *Cardiac Electrophysiology: From Cell to Bedside*.

Atrial fibrillation: Overview (2017). Available at: https://www.ncbi.nlm.nih.gov/books/NBK464171/ [Accessed September 20, 2021].

Attia, Z. I., Friedman, P. A., Noseworthy, P. A., Lopez-Jimenez, F., Ladewig, D. J., Satam, G., et al. (2019). Age and Sex Estimation Using Artificial Intelligence from Standard 12-Lead ECGs. *Circ. Arrhythmia Electrophysiol.* 12. doi:10.1161/CIRCEP.119.007284.

Ávila, P., Calvo, D., Tamargo, M., Uribarri, A., Datino, T., Arenal, A., et al. (2021). Association of age with clinical features and ablation outcomes of paroxysmal supraventricular tachycardias. *Heart*, heartjnl-2021-319685. doi:10.1136/HEARTJNL-2021-319685.

Aydın, S., Melih, H., Lu, S. ̆, and Kara, S. Log Energy Entropy-Based EEG

Classification with Multilayer Neural Networks in Seizure. doi:10.1007/s10439-009-9795-x.

Badano, A. (2021). In silico imaging clinical trials: cheaper, faster, better, safer, and more scalable. *Trials* 22, 64. doi:10.1186/s13063-020-05002-w.

Bai, J., Lu, Y., and Zhang, H. (2020). In silico study of the effects of anti-arrhythmic drug treatment on sinoatrial node function for patients with atrial fibrillation. *Sci. Reports 2020 101* 10, 1–14. doi:10.1038/s41598-019-57246-5.

Bai, J., Zhu, Y., Lo, A., Gao, M., Lu, Y., Zhao, J., et al. (2021). In Silico Assessment of Class I Antiarrhythmic Drug Effects on Pitx2-Induced Atrial Fibrillation: Insights from Populations of Electrophysiological Models of Human Atrial Cells and Tissues. *Int. J. Mol. Sci. 2021, Vol. 22, Page 1265* 22, 1265. doi:10.3390/IJMS22031265.

Bai, W., Sinclair, M., Tarroni, G., Oktay, O., Rajchl, M., Vaillant, G., et al. (2018). Automated cardiovascular magnetic resonance image analysis with fully convolutional networks. *J. Cardiovasc. Magn. Reson.* 20, 65. doi:10.1186/s12968-018-0471-x.

Bassett, A. L., Chakko, S., and Epstein, M. (1997). Are calcium antagonists proarrhythmic? *J. Hypertens.* 15, 915–923. doi:10.1097/00004872-199715090-00001.

Bello, G. A., Dawes, T. J. W., Duan, J., Biffi, C., de Marvao, A., Howard, L. S. G. E., et al. (2019). Deep-learning cardiac motion analysis for human survival prediction. *Nat. Mach. Intell.* 1, 95–104. doi:10.1038/s42256-019-0019-2.

Berenfeld, O., Wellner, M., Jalife, J., and Pertsov, A. M. (2001). Shaping of a scroll wave filament by cardiac fibers. *Phys. Rev. E* 63, 061901. doi:10.1103/PhysRevE.63.061901.

Betancourt, J. E., Noheria, A., Cooper, D., Orme, G., Sodhi, S., Steyers, C., et al. (2019). Accuracy of Cardioinsight NonInvasive Electrocardiographic Imaging Compared with Invasive Mapping for Determining Location of Ventricular Arrhythmias. *J. Am. Coll. Cardiol.* 73, 458. doi:10.1016/S0735-1097(19)31066-6.

Bezzina, C. R., Rook, M. B., and Wilde, A. A. . (2001). Cardiac sodium channel and inherited arrhythmia syndromes. *Cardiovasc. Res.* 49, 257–271. doi:10.1016/S0008-6363(00)00272-8.

Bisbal, F., Alarcón, F., Ferrero-De-Loma-Osorio, A., González-Ferrer, J. J., Alonso, C., Pachón, M., et al. (2018). Left atrial geometry and outcome of atrial fibrillation ablation: results from the multicentre LAGO-AF study. *Eur. Hear. J. - Cardiovasc. Imaging* 19, 1002–1009. doi:10.1093/EHJCI/JEY060.

Blanc, O., Virag, N., Vesin, J.-M., and Kappenberger, L. (2001). A computer model of human atria with reasonable computation load and realistic anatomical properties. *IEEE Trans. Biomed. Eng.* 48, 1229–1237. doi:10.1109/10.959315.

Boon, K. H., Khalil-Hani, M., and Malarvili, M. B. (2018). Paroxysmal atrial fibrillation prediction based on HRV analysis and non-dominated sorting genetic algorithm III. *Comput. Methods Programs Biomed.* 153, 171–184.

doi:10.1016/j.cmpb.2017.10.012.

Boyle, P. M., Zghaib, T., Zahid, S., Ali, R. L., Deng, D., Franceschi, W. H., et al. (2019). Computationally guided personalized targeted ablation of persistent atrial fibrillation. *Nat. Biomed. Eng.* 3, 870–879. doi:10.1038/s41551-019-0437-9.

Britton, O. J., Bueno-Orovio, A., Van Ammel, K., Lu, H. R., Towart, R., Gallacher, D. J., et al. (2013). Experimentally calibrated population of models predicts and explains intersubject variability in cardiac cellular electrophysiology. *Proc. Natl. Acad. Sci.* 110, E2098–E2105. doi:10.1073/pnas.1304382110.

Brundel, B. J. J. ., Van Gelder, I. C., Henning, R. H., Tuinenburg, A. E., Wietses, M., Grandjean, J. G., et al. (2001). Alterations in potassium channel gene expression in atria of patients with persistent and paroxysmal atrial fibrillation: differential regulation of protein and mRNA levels for K+channels. *J. Am. Coll. Cardiol.* 37, 926–932. doi:10.1016/S0735-1097(00)01195-5.

Budzianowski, J., Hiczkiewicz, J., Burchardt, P., Pieszko, K., Rzeźniczak, J., Budzianowski, P., et al. (2019). Predictors of atrial fibrillation early recurrence following cryoballoon ablation of pulmonary veins using statistical assessment and machine learning algorithms. 34, 352–359. doi:10.1007/s00380-018-1244-z.

Burdumy, M., Luik, A., Neher, P., Hanna, R., Krueger, M. W., Schilling, C., et al. (2012). Comparing measured and simulated wave directions in the left atrium - a workflow for model personalization and validation. *Biomed. Tech. (Berl).* 57, 79–87. doi:10.1515/bmt-2011-0059.

Calvo, C. J., Deo, M., Zlochiver, S., Millet, J., and Berenfeld, O. (2014). Attraction of Rotors to the Pulmonary Veins in Paroxysmal Atrial Fibrillation: A Modeling Study. *Biophys. J.* 106, 1811–1821. doi:10.1016/J.BPJ.2014.02.030.

Carro, J., Rodríguez-Matas, J. F., Monasterio, V., and Pueyo, E. (2017). Limitations in electrophysiological model development and validation caused by differences between simulations and experimental protocols. *Prog. Biophys. Mol. Biol.* 129, 53–64. doi:10.1016/J.PBIOMOLBIO.2016.11.006.

Cerrone, M., Noujaim, S. F., Tolkacheva, E. G., Talkachou, A., O'Connell, R., Berenfeld, O., et al. (2007). Arrhythmogenic Mechanisms in a Mouse Model of Catecholaminergic Polymorphic Ventricular Tachycardia. *Circ. Res.* 101, 1039–1048. doi:10.1161/CIRCRESAHA.107.148064.

Charitos, E. I., Pürerfellner, H., Glotzer, T. V., and Ziegler, P. D. (2014). Clinical Classifications of Atrial Fibrillation Poorly Reflect Its Temporal Persistence. *J. Am. Coll. Cardiol.* 63, 2840–2848. doi:10.1016/j.jacc.2014.04.019.

Chen, S.-A., Hsieh, M.-H., Tai, C.-T., Tsai, C.-F., Prakash, V. S., Yu, W.-C., et al. (1999). Initiation of Atrial Fibrillation by Ectopic Beats Originating From the Pulmonary Veins. *Circulation* 100, 1879–1886. doi:10.1161/01.CIR.100.18.1879.

Cheniti, G., Puyo, S., Martin, C. A., Frontera, A., Vlachos, K., Takigawa, M., et al. (2019). Non-invasive Mapping and ECGI in Atrial and Ventricular

Arrhythmias (CardioInsight).

Chew, D. S., Black-Maier, E., Loring, Z., Noseworthy, P. A., Packer, D. L., Exner, D. V., et al. (2020). Diagnosis-to-Ablation Time and Recurrence of Atrial Fibrillation following Catheter Ablation: A Systematic Review and Meta-Analysis of Observational Studies. *Circ. Arrhythmia Electrophysiol.* 13, 350–357. doi:10.1161/CIRCEP.119.008128.

Chua, W., Di Biase, L., Bayes De Luna, A., David, C., Haase, D., Hindricks, G., et al. (2021). Dynamic changes of cardiovascular biomarkers after ablation for atrial fibrillation: observations from AXAFA-AFNET5. *Eur. Heart J.* 42. doi:10.1093/EURHEARTJ/EHAB724.0538.

Chugh, S. S., Havmoeller, R., Narayanan, K., Singh, D., Rienstra, M., Benjamin, E. J., et al. (2014). Worldwide epidemiology of atrial fibrillation: A global burden of disease 2010 study. *Circulation* 129, 837–847. doi:10.1161/CIRCULATIONAHA.113.005119.

Clayton, R. H., Bernus, O., Cherry, E. M., Dierckx, H., Fenton, F. H., Mirabella, L., et al. (2010). Models of cardiac tissue electrophysiology : Progress , challenges and open questions. doi:10.1016/j.pbiomolbio.2010.05.008.

Clayton, R. H., and Panfilov, A. V. (2008). A guide to modelling cardiac electrical activity in anatomically detailed ventricles. *Prog. Biophys. Mol. Biol.* 96, 19–43. doi:10.1016/j.pbiomolbio.2007.07.004.

Clayton, R. H., Zhuchkova, E. A., and Panfilov, A. V (2006). Phase singularities and filaments: simplifying complexity in computational models of ventricular fibrillation. *Prog. Biophys. Mol. Biol.* 90, 378–98. doi:10.1016/j.pbiomolbio.2005.06.011.

Colman, M. A., Aslanidi, O. V., Kharche, S., Boyett, M. R., Garratt, C., Hancox, J. C., et al. (2013). Pro-arrhythmogenic effects of atrial fibrillation-induced electrical remodelling: insights from the three-dimensional virtual human atria. *J. Physiol.* 591, 4249–4272. doi:10.1113/jphysiol.2013.254987.

Corradi, D., Callegari, S., Maestri, R., Ferrara, D., Mangieri, D., Alinovi, R., et al. (2012). Differential structural remodeling of the left-atrial posterior wall in patients affected by mitral regurgitation with or without persistent atrial fibrillation: A morphological and molecular study. *J. Cardiovasc. Electrophysiol.* 23, 271–279. doi:10.1111/j.1540-8167.2011.02187.x.

Corral-Acero, J., Margara, F., Marciniak, M., Rodero, C., Loncaric, F., Feng, Y., et al. (2020). The "Digital Twin" to enable the vision of precision cardiology. *Eur. Heart J.* 41, 4556-4564B. doi:10.1093/EURHEARTJ/EHAA159.

Costoya-Sánchez, A., Climent, A. M., Hernández-Romero, I., Liberos, A., Fernández-Avilés, F., Narayan, S. M., et al. (2020). Automatic quality electrogram assessment improves phase-based reentrant activity identification in atrial fibrillation. *Comput. Biol. Med.* 117. doi:10.1016/J.COMPBIOMED.2019.103593.

Courtemanche, M., Ramirez, R. J., and Nattel, S. (1998). Ionic mechanisms underlying human atrial action potential properties: insights from a mathematical model. *Am. J. Physiol. Circ. Physiol.* 275, H301–H321. doi:10.1152/ajpheart.1998.275.1.H301.

Crumb, W. J., Vicente, J., Johannesen, L., and Strauss, D. G. (2016). An

evaluation of 30 clinical drugs against the comprehensive in vitro proarrhythmia assay (CiPA) proposed ion channel panel. *J. Pharmacol. Toxicol. Methods* 81, 251–262. doi:10.1016/j.vascn.2016.03.009.

Dagher, L., Shi, H., Zhao, Y., and Marrouche, N. F. (2020). Wearables in cardiology: Here to stay. *Hear. Rhythm* 17, 889–895. doi:10.1016/j.hrthm.2020.02.023.

Dang, L., Virag, N., Ihara, Z., Jacquemet, V., Vesin, J.-M., Schlaepfer, J., et al. (2005). Evaluation of Ablation Patterns Using a Biophysical Model of Atrial Fibrillation. *Ann. Biomed. Eng.* 33, 465–474. doi:10.1007/s10439-005-2502-7.

Davies, M. R., Mistry, H. B., Hussein, L., Pollard, C. E., Valentin, J., and Swinton, J. (2019). An in silico canine cardiac midmyocardial action potential duration model as a tool for early drug safety assessment. 1466–1480. doi:10.1152/ajpheart.00808.2011.

Davis, J., and Goadrich, M. (2006). The relationship between precision-recall and ROC curves. in *ACM International Conference Proceeding Series* (New York, New York, USA: ACM Press), 233–240. doi:10.1145/1143844.1143874.

Dempsey, C. E., Wright, D., Colenso, C. K., Sessions, R. B., and Hancox, J. C. (2014). Assessing hERG Pore Models As Templates for Drug DockingUsing Published Experimental Constraints: The Inactivated State inthe Context of Drug Block. *J. Chem. Inf. Model.* 54, 601. doi:10.1021/CI400707H.

Deng, L., and Yu, D. (2014). Deep Learning: Methods and Applications. Available at: https://www.microsoft.com/en-us/research/publication/deep-learning-methods-and-applications/.

Di Biase, L., Natale, A., and Romero, J. (2018). Thrombogenic and Arrhythmogenic Roles of the Left Atrial Appendage in Atrial Fibrillation. *Circulation* 138, 2036–2050. doi:10.1161/CIRCULATIONAHA.118.034187.

DiFrancesco, D., and Noble, D. (1985). A model of cardiac electrical activity incorporating ionic pumps and concentration changes. *Philos. Trans. R. Soc. Lond. B. Biol. Sci.* 307, 353–398. doi:10.1098/rstb.1985.0001.

Dobrev, D., Voigt, N., and Wehrens, X. H. T. (2011). The ryanodine receptor channel as a molecular motif in atrial fibrillation : pathophysiological and therapeutic implications. 734–743. doi:10.1093/cvr/cvq324.

Donnelly, R. (2004). Characterizing variability in cardiovascular drug responses. *Br. J. Clin. Pharmacol.* 57, 535–537. doi:10.1111/j.1365-2125.2004.02148.x.

Dössel, O., Krueger, M. W., Weber, F. M., Wilhelms, M., and Seemann, G. (2012). Computational modeling of the human atrial anatomy and electrophysiology. *Med. Biol. Eng. Comput.* 50, 773–799. doi:10.1007/s11517-012-0924-6.

Dretzke, J., Chuchu, N., Chua, W., Fabritz, L., Bayliss, S., Kotecha, D., et al. (2019). Prognostic models for predicting incident or recurrent atrial fibrillation: Protocol for a systematic review. *Syst. Rev.* 8, 221. doi:10.1186/s13643-019-1128-z.

Echt, D. S., and Ruskin, J. N. (2020). Use of Flecainide for the Treatment of Atrial Fibrillation. *Am. J. Cardiol.* 125, 1123–1133. doi:10.1016/j.amjcard.2019.12.041.

Eckstein, J., Zeemering, S., Linz, D., Maesen, B., Verheule, S., van Hunnik, A., et al. (2013). Transmural Conduction Is the Predominant Mechanism of Breakthrough During Atrial Fibrillation. *Circ. Arrhythmia Electrophysiol.* 6, 334–341. doi:10.1161/CIRCEP.113.000342.

Ellinwood, N., Dobrev, D., Morotti, S., and Grandi, E. (2017). In Silico Assessment of Efficacy and Safety of IKur Inhibitors in Chronic Atrial Fibrillation: Role of Kinetics and State-Dependence of Drug Binding. *Front. Pharmacol.* 0, 799. doi:10.3389/FPHAR.2017.00799.

Engineering, B. (2011). Position paper on the European Commission Green Paper From Challenges to Opportunities : Towards a Common Strategic Framework for EU Research and Innovation funding. 1–4.

Faes, L., Nollo, G., Kirchner, M., Olivetti, E., Gaita, F., Riccardi, R., et al. (2001). Principal component analysis and cluster analysis for measuring the local organisation of human atrial fibrillation. *Med. Biol. Eng. Comput.* 39, 656–663. doi:10.1007/BF02345438.

Fahmy, A. S., Neisius, U., Chan, R. H., Rowin, E. J., Manning, W. J., Maron, M. S., et al. (2020). Three-dimensional deep convolutional neural networks for automated myocardial scar quantification in hypertrophic cardiomyopathy: A multicenter multivendor study. *Radiology* 294, 52–60. doi:10.1148/radiol.2019190737.

Falk, R. H. (1989). Flecainide-Induced Ventricular Tachycardia and Fibrillation in Patients Treated for Atrial Fibrillation. *Ann. Intern. Med.* 111, 107–111. doi:10.7326/0003-4819-111-2-107.

Fastl, T. E., Tobon-Gomez, C., Crozier, A., Whitaker, J., Rajani, R., Mccarthy, K. P., et al. (2018). Personalized computational modeling of left atrial geometry and transmural myofiber architecture. *Med. Image Anal.* 47, 180–190. doi:10.1016/j.media.2018.04.001.

Faust, O., Shenfield, A., Kareem, M., San, T. R., Fujita, H., and Acharya, U. R. (2018). Automated detection of atrial fibrillation using long short-term memory network with RR interval signals. *Comput. Biol. Med.* 102, 327–335. doi:10.1016/j.compbiomed.2018.07.001.

Feeny, A. K., Chung, M. K., Madabhushi, A., Attia, Z. I., Cikes, M., Firouznia, M., et al. (2020). Artificial Intelligence and Machine Learning in Arrhythmias and Cardiac Electrophysiology. *Circ. Arrhythmia Electrophysiol.* 13. doi:10.1161/CIRCEP.119.007952.

Ferrer, A., Sebastián, R., Sánchez-Quintana, D., Rodríguez, J. F., Godoy, E. J., Martínez, L., et al. (2015). Detailed Anatomical and Electrophysiological Models of Human Atria and Torso for the Simulation of Atrial Activation. *PLoS One* 10, e0141573. doi:10.1371/journal.pone.0141573.

Ghanem, R. N., Jia, P., Ramanathan, C., Ryu, K., Markowitz, A., and Rudy, Y. (2005). Noninvasive Electrocardiographic Imaging (ECGI): Comparison to intraoperative mapping in patients. *Hear. Rhythm* 2, 339–354. doi:10.1016/j.hrthm.2004.12.022.

References

Gharaviri, A., Pezzuto, S., Potse, M., Verheule, S., Conte, G., Krause, R., et al. (2021). Left Atrial Appendage Electrical Isolation Reduces Atrial Fibrillation Recurrences. *Circ. Arrhythmia Electrophysiol.*, 105–107. doi:10.1161/CIRCEP.120.009230.

Gosai, J., Purva, M., and Gunn, J. (2015). Simulation in cardiology: state of the art. *Eur. Heart J.* 36, 777–783. doi:10.1093/EURHEARTJ/EHU527.

Gottesman, O., Johansson, F., Komorowski, M., Faisal, A., Sontag, D., Doshi-Velez, F., et al. (2019). Guidelines for reinforcement learning in healthcare. *Nat. Med.* 25, 16–18. doi:10.1038/s41591-018-0310-5.

Graham, A. J., Orini, M., Zacur, E., Dhillon, G., Daw, H., Srinivasan, N. T., et al. (2020). Evaluation of ECG Imaging to Map Hemodynamically Stable and Unstable Ventricular Arrhythmias. *Circ. Arrhythmia Electrophysiol.* 13, 155–165. doi:10.1161/CIRCEP.119.007377.

Grandi, E., Pandit, S. V., Voigt, N., Workman, A. J., Dobrev, D., Jalife, J., et al. (2011). Human atrial action potential and Ca 2+ model: Sinus rhythm and chronic atrial fibrillation. *Circ. Res.* 109, 1055–1066. doi:10.1161/CIRCRESAHA.111.253955.

Guillem, M. S., Climent, A. M., Millet, J., Arenal, Á., Fernández-Avilés, F., Jalife, J., et al. (2013). Noninvasive Localization of Maximal Frequency Sites of Atrial Fibrillation by Body Surface Potential Mapping. *Circ. Arrhythmia Electrophysiol.* 6, 294–301. doi:10.1161/CIRCEP.112.000167.

Guillem, M. S., Climent, A. M., Rodrigo, M., Fernández-Avilés, F., Atienza, F., Berenfeld, O., et al. (2016). Presence and stability of rotors in atrial fibrillation: evidence and therapeutic implications. *Cardiovasc. Res.* 109, 480–92. doi:10.1093/cvr/cvw011.

Guo, J., Massaeli, H., Xu, J., Jia, Z., Wigle, J., Mesaeli, N., et al. (2009). Extracellular K+ concentration controls cell surface density of IKr in rabbit hearts and of the HERG channel in human cell lines. *J. Clin. Invest.* 119, 2745–2757. doi:10.1172/JCI39027.

Haissaguerre, M., Hocini, M., Denis, A., Shah, A. J., Komatsu, Y., Yamashita, S., et al. (2014). Driver domains in persistent atrial fibrillation. *Circulation* 130, 530–538. doi:10.1161/CIRCULATIONAHA.113.005421.

Haïssaguerre, M., Jaïs, P., Shah, D. C., Takahashi, A., Hocini, M., Quiniou, G., et al. (1998). Spontaneous initiation of atrial fibrillation by ectopic beats originating in the pulmonary veins. 339, 659–666. doi:10.1056/NEJM199809033391003.

Haissaguerre, M., Lim, K. T., Jacquemet, V., Rotter, M., Dang, L., Hocini, M., et al. (2007). Atrial fibrillatory cycle length: computer simulation and potential clinical importance. *Europace* 9 Suppl 6. doi:10.1093/EUROPACE/EUM208.

Halfar, R., Lawson, B. A. J., dos Santos, R. W., and Burrage, K. (2021). Machine Learning Identification of Pro-arrhythmic Structures in Cardiac Fibrosis. *Front. Physiol.* 0, 1145. doi:10.3389/FPHYS.2021.709485.

Hannun, A. Y., Rajpurkar, P., Haghpanahi, M., Tison, G. H., Bourn, C., Turakhia, M. P., et al. (2019). Cardiologist-level arrhythmia detection and classification in ambulatory electrocardiograms using a deep neural network. *Nat. Med.* 25, 65–69. doi:10.1038/s41591-018-0268-3.

Heijman, J., Sutanto, H., Crijns, H. J. G. M., Nattel, S., and Trayanova, N. A. (2021). Computational models of atrial fibrillation: achievements, challenges, and perspectives for improving clinical care. *Cardiovasc. Res.* 117, 1682–1699. doi:10.1093/cvr/cvab138.

Helms, T. M., Duong, G., Zippel-Schultz, B., Tilz, R. R., Kuck, K. H., and Karle, C. A. (2014). Prediction and personalised treatment of atrial fibrillation-stroke prevention: Consolidated position paper of CVD professionals. *EPMA J.* 5, 15. doi:10.1186/1878-5085-5-15.

Herlin, A., and Jacquemet, V. (2011). Eikonal-based initiation of fibrillatory activity in thin-walled cardiac propagation models. *Chaos* 21, 043136. doi:10.1063/1.3670060.

Herlin, A., Jacquemet, V., Herlin, A., and Jacquemet, V. (2013). Eikonal-based initiation of fibrillatory activity in thin-walled cardiac propagation models Eikonal-based initiation of fibrillatory activity in thin-walled cardiac propagation models. 043136. doi:10.1063/1.3670060.

Hill, N. R., Ayoubkhani, D., McEwan, P., Sugrue, D. M., Farooqui, U., Lister, S., et al. (2019). Predicting atrial fibrillation in primary care using machine learning. *PLoS One* 14. doi:10.1371/journal.pone.0224582.

Hindricks, G., Potpara, T., Dagres, N., Arbelo, E., Bax, J. J., Blomström-Lundqvist, C., et al. (2020). 2020 ESC Guidelines for the diagnosis and management of atrial fibrillation developed in collaboration with the European Association of Cardio-Thoracic Surgery (EACTS). *Eur. Heart J.*, 1–126. doi:10.1093/eurheartj/ehaa612.

Hodgkin, A. L., and Huxley, A. F. (1952). Currents carried by sodium and potassium ions through the membrane of the giant axon of Loligo. *J. Physiol.* 116, 449–472. Available at: http://www.ncbi.nlm.nih.gov/pmc/articles/PMC1392213/.

Horáček, B. M., and Clements, J. C. (1997). The inverse problem of electrocardiography: A solution in terms of single- and double-layer sources on the epicardial surface. *Math. Biosci.* 144, 119–154. doi:10.1016/S0025-5564(97)00024-2.

How the Heart Pumps Blood Available at: https://www.news-medical.net/health/How-the-Heart-Pumps-Blood.aspx [Accessed September 20, 2021].

Hwang, M., Song, J.-S., Lee, Y.-S., Li, C., Shim, E. B., and Pak, H.-N. (2016). Electrophysiological Rotor Ablation in In-Silico Modeling of Atrial Fibrillation: Comparisons with Dominant Frequency, Shannon Entropy, and Phase Singularity. *PLoS One* 11, e0149695. doi:10.1371/journal.pone.0149695.

Iyer, A. N., and Gray, R. A. (2001). An experimentalist's approach to accurate localization of phase singularities during reentry. *Ann. Biomed. Eng.* 29, 47–59. doi:10.1114/1.1335538.

Iyer, V., Mazhari, R., and Winslow, R. L. (2004). A Computational Model of the Human Left-Ventricular Epicardial Myocyte. *Biophys. J.* 87, 1507. doi:10.1529/BIOPHYSJ.104.043299.

Jacquemet, V., van Oosterom, A., Vesin, J.-M., and Kappenberger, L. (2006). Analysis of electrocardiograms during atrial fibrillation. A biophysical

model approach. *IEEE Eng. Med. Biol. Mag.* 25, 79–88. doi:10.1109/emb-m.2006.250511.

Jalife, J. (2011). Déjà vu in the theories of atrial fibrillation dynamics. *Cardiovasc. Res.* 89, 766–75. doi:10.1093/cvr/cvq364.

Jalife, J., and Berenfeld, O. (2004). Molecular mechanisms and global dynamics of fibrillation: an integrative approach to the underlying basis of vortex-like reentry. *J. Theor. Biol.* 230, 475–87. doi:10.1016/j.jtbi.2004.02.024.

Jalife, J., Delmar, M., Anumonwo, J., Berenfeld, O., and Kalifa, J. (2009). *Basic Cardiac Electrophysiology for the Clinician: Second Edition*. Wiley-Blackwell doi:10.1002/9781444316940.

Jiang, Y., Hou, H., Yang, Q., Liu, X., and He, G. (2017). Chloride Channels are Involved in the Development of Atrial Fibrillation – A Transcriptomic and proteomic Study. *Sci. Rep.*, 1–12. doi:10.1038/s41598-017-10590-w.

Johnson, K. W., Torres Soto, J., Glicksberg, B. S., Shameer, K., Miotto, R., Ali, M., et al. (2018). Artificial Intelligence in Cardiology. *J. Am. Coll. Cardiol.* 71, 2668–2679. doi:10.1016/j.jacc.2018.03.521.

Jungen, C., Akbulak, R., Kahle, A. K., Eickholt, C., Schaeffer, B., Scherschel, K., et al. (2020). Outcome after tailored catheter ablation of atrial tachycardia using ultra-high-density mapping. *J. Cardiovasc. Electrophysiol.* 31, 2645–2652. doi:10.1111/JCE.14703.

Kashoki, M., Hanaizi, Z., Yordanova, S., Veselý, R., Bouygues, C., Llinares, J., et al. (2020). A Comparison of EMA and FDA Decisions for New Drug Marketing Applications 2014–2016: Concordance, Discordance, and Why. *Clin. Pharmacol. Ther.* 107, 195. doi:10.1002/CPT.1565.

Kharche, S., Seemann, G., Margetts, L., Leng, J., Holden, A. V., and Zhang, H. (2008). Simulation of clinical electrophysiology in 3D human atria: A high-performance computing and high-performance visualization application. in *Concurrency Computation Practice and Experience* (John Wiley & Sons, Ltd), 1317–1328. doi:10.1002/cpe.1332.

Khorovets, A. (2000). What Is An Electrocardiogram (ECG)? *Internet J. Heal.* 1. doi:10.5580/297e.

Kim, I.-S., Lim, B., Shim, J., Hwang, M., Yu, H. T., Kim, T.-H., et al. (2020). Clinical Usefulness of Simulation-Guided Catheter Ablation of Atrial Fibrillation: Updated Outcome of a Multicenter Prospective Randomized Study. *SSRN Electron. J.* doi:10.2139/ssrn.3361174.

King, J. H., Huang, C. L.-H., and Fraser, J. A. (2013). Determinants of myocardial conduction velocity: implications for arrhythmogenesis. *Front. Physiol.* 4. doi:10.3389/FPHYS.2013.00154.

Kirchhof, P., Breithardt, G., Aliot, E., Al Khatib, S., Apostolakis, S., Auricchio, A., et al. (2013). Personalized management of atrial fibrillation: Proceedings from the fourth Atrial Fibrillation competence NETwork/European Heart Rhythm Association consensus conference. *Europace* 15, 1540–56. doi:10.1093/europace/eut232.

Kirchhof, P., Camm, A. J., Goette, A., Brandes, A., Eckardt, L., Elvan, A., et al. (2020). Early Rhythm-Control Therapy in Patients with Atrial Fibrillation. *N. Engl. J. Med.* 383, 1305–1316. doi:10.1056/NEJMoa2019422.

Klein, H. O., Pauzner, H., Segni, E., David, D., and Kaplinsky, E. (1979). The Beneficial Effects of Verapamil in Chronic Atrial Fibrillation. *Arch. Intern. Med.* 139, 747–749. doi:10.1001/archinte.1979.03630440017009.

Kocyigit, D., Canpolat, U., and Aytemir, K. (2015). Atrial fibrillation - Who needs catheter ablation and which approach? *J. Atr. Fibrillation* 8. doi:10.4022/jafib.1335.

Koivumäki, J. T., Korhonen, T., and Tavi, P. (2011). Impact of Sarcoplasmic Reticulum Calcium Release on Calcium Dynamics and Action Potential Morphology in Human Atrial Myocytes: A Computational Study. *PLOS Comput. Biol.* 7, e1001067. doi:10.1371/JOURNAL.PCBI.1001067.

Koivumäki, J. T., Seemann, G., Maleckar, M. M., Tavi, P., Koivumaki, J. T., Seemann, G., et al. (2014). In silico screening of the key cellular remodeling targets in chronic atrial fibrillation. *PLOS Comput. Biol.* 10, e1003620. doi:10.1371/journal.pcbi.1003620.

Kornej, J., Hindricks, G., Shoemaker, M. B., Husser, D., Arya, A., Sommer, P., et al. (2015). The APPLE score: a novel and simple score for the prediction of rhythm outcomes after catheter ablation of atrial fibrillation. 104, 871–876. Available at: https://pubmed.ncbi.nlm.nih.gov/25876528/ [Accessed May 4, 2020].

Kou, S., Caballero, L., Dulgheru, R., Voilliot, D., De Sousa, C., Kacharava, G., et al. (2014). Echocardiographic reference ranges for normal cardiac chamber size: Results from the NORRE study. *Eur. Heart J. Cardiovasc. Imaging* 15, 680–690. doi:10.1093/ehjci/jet284.

Kraushaar, U., Meyer, T., Hess, D., Gepstein, L., L Mummery, C., R Braam, S., et al. (2012). Cardiac safety pharmacology: from human ether-a-gogo related gene channel block towards induced pluripotent stem cell based disease models. *Expert Opin. Drug Saf.* 11, 285–298. doi:10.1517/14740338.2012.639358.

Krijthe, B. P., Heeringa, J., Kors, J. A., Hofman, A., Franco, O. H., Witteman, J. C. M., et al. (2013). Serum potassium levels and the risk of atrial fibrillation: The Rotterdam Study. *Int. J. Cardiol.* 168, 5411–5415. doi:10.1016/j.ijcard.2013.08.048.

Krittanawong, C., Johnson, K. W., Rosenson, R. S., Wang, Z., Aydar, M., Baber, U., et al. (2019). Deep learning for cardiovascular medicine: a practical primer. *Eur. Heart J.* 40, 2058–2073. doi:10.1093/eurheartj/ehz056.

Krittanawong, C., Zhang, H. J., Wang, Z., Aydar, M., and Kitai, T. (2017). Artificial Intelligence in Precision Cardiovascular Medicine. *J. Am. Coll. Cardiol.* 69, 2657–2664. doi:10.1016/j.jacc.2017.03.571.

Krueger, M. W., Schmidt, V., Tobón, C., Weber, F. M., Lorenz, C., Keller, D. U. J., et al. (2011). Modeling Atrial Fiber Orientation in Patient-Specific Geometries: A Semi-automatic Rule-Based Approach. *Lect. Notes Comput. Sci. (including Subser. Lect. Notes Artif. Intell. Lect. Notes Bioinformatics)* 6666 LNCS, 223–232. doi:10.1007/978-3-642-21028-0_28.

Krueger, M. W., Seemann, G., Rhode, K., Keller, D. U. J., Schilling, C., Arujuna, A., et al. (2013). Personalization of atrial anatomy and electrophysiology as a basis for clinical modeling of radio-frequency ablation of atrial

fibrillation. *IEEE Trans. Med. Imaging* 32, 73–84. doi:10.1109/TMI.2012.2201948.

Kuck, K.-H., Brugada, J., Fürnkranz, A., Metzner, A., Ouyang, F., Chun, K. R. J., et al. (2016). Cryoballoon or Radiofrequency Ablation for Paroxysmal Atrial Fibrillation. Available at: https://www.nejm.org/doi/full/10.1056/NEJMoa1602014 [Accessed January 8, 2021].

Kügler, P. (2020). Modelling and Simulation for Preclinical Cardiac Safety Assessment of Drugs with Human iPSC-Derived Cardiomyocytes. *Jahresbericht der Dtsch. Math.* 122, 209–257. doi:10.1365/s13291-020-00218-w.

Lankveld, T., Zeemering, S., Scherr, D., Kuklik, P., Hoffmann, B. A., Willems, S., et al. (2016). Atrial Fibrillation Complexity Parameters Derived From Surface ECGs Predict Procedural Outcome and Long-Term Follow-Up of Stepwise Catheter Ablation for Atrial Fibrillation. *Circ. Arrhythmia Electrophysiol.* 9, e003354. doi:10.1161/CIRCEP.115.003354.

Le, T. A., Günes, A., Günes¸baydin, G., Zinkov, R., and Wood, F. (2017). Using Synthetic Data to Train Neural Networks is Model-Based Reasoning. Available at: https://probprog.github.io/inference-compilation/ [Accessed August 20, 2020].

Leef, G., Shenasa, F., Bhatia, N. K., Rogers, A. J., Sauer, W., Miller, J. M., et al. (2019). Wavefront Field Mapping Reveals a Physiologic Network Between Drivers Where Ablation Terminates Atrial Fibrillation. 12. doi:10.1161/CIRCEP.118.006835.

Lefebvre, C., and Hoekstra, J. (2007). Early detection and diagnosis of acute myocardial infarction: the potential for improved care with next-generation, user-friendly electrocardiographic body surface mapping. *Am. J. Emerg. Med.* 25, 1063–1072. doi:10.1016/j.ajem.2007.06.011.

Li, S., Harner, E. J., and Adjeroh, D. A. (2011). Random KNN feature selection - a fast and stable alternative to Random Forests. *BMC Bioinformatics* 12. doi:10.1186/1471-2105-12-450.

Li, T., and Zhou, M. (2016). ECG classification usingwavelet packet entropy and random forests. *Entropy* 18, 285. doi:10.3390/e18080285.

Li, Z., Dutta, S., Sheng, J., Tran, P. N., Wu, W., Chang, K., et al. (2017). Improving the in silico assessment of proarrhythmia risk by combining hERG (Human Ether-à-go-go-Related Gene) channel-drug binding kinetics and multichannel pharmacology. *Circ. Arrhythmia Electrophysiol.* 10. doi:10.1161/CIRCEP.116.004628.

Liberos, A., Bueno-Orovio, A., Rodrigo, M., Ravens, U., Hernandez-Romero, I., Fernandez-Aviles, F., et al. (2016). Balance between sodium and calcium currents underlying chronic atrial fibrillation termination: An in silico intersubject variability study. *Hear. Rhythm* 13, 2358–2365. doi:10.1016/j.hrthm.2016.08.028.

Liberos, A., Rodrigo, M., Hernandez-Romero, I., Quesada, A., Fernandez-Aviles, F., Atienza, F., et al. Phase singularity point tracking for the identification of typical and atypical flutter patients: A clinical-computational study. *Comput. Biol. Med.* 104, 319–328. Available at: https://doi.org/10.1016/j.compbiomed.2018.11.020 [Accessed March 12,

2021].

Lim, B., Kim, J., Hwang, M., Song, J. S., Lee, J. K., Yu, H. T., et al. (2020). In situ procedure for high-efficiency computational modeling of atrial fibrillation reflecting personal anatomy, fiber orientation, fibrosis, and electrophysiology. *Sci. Rep.* 10, 1–10. doi:10.1038/s41598-020-59372-x.

Lim, H. S., Hocini, M., Dubois, R., Denis, A., Derval, N., Zellerhoff, S., et al. (2017). Complexity and Distribution of Drivers in Relation to Duration of Persistent Atrial Fibrillation. *J. Am. Coll. Cardiol.* 69, 1257–1269. doi:10.1016/j.jacc.2017.01.014.

Lin, W.-S., Tai, C.-T., Hsieh, M.-H., Tsai, C.-F., Lin, Y.-K., Tsao, H.-M., et al. (2003). Catheter Ablation of Paroxysmal Atrial Fibrillation Initiated by Non–Pulmonary Vein Ectopy. *Circulation* 107, 3176–3183. doi:10.1161/01.CIR.0000074206.52056.2D.

Luo, C. H., and Rudy, Y. (1991). A model of the ventricular cardiac action potential. Depolarization, repolarization, and their interaction. *Circ. Res.* 68, 1501–1526. doi:10.1161/01.RES.68.6.1501.

Macdonald, G. (2008). Harrison's Internal Medicine, 17th edition. - by A. S. Fauci, D. L. Kasper, D. L. Longo, E. Braunwald, S. L. Hauser, J. L. Jameson and J. Loscalzo. *Intern. Med. J.* 38, 932–932. doi:10.1111/j.1445-5994.2008.01837.x.

Macfarlane, P., Oosterom, A., Janse, M., Kligfield, P., Camm, J., and Pahlm, O. (2011). *Cardiac Arrhythmias and Mapping Techniques*. 1st Editio. Springer.

Makridakis, S. (2017). The forthcoming Artificial Intelligence (AI) revolution: Its impact on society and firms. *Futures* 90, 46–60. doi:10.1016/j.futures.2017.03.006.

Maleckar, M. M., Greenstein, J. L., Giles, W. R., and Trayanova, N. A. (2009). Electrotonic coupling between human atrial myocytes and fibroblasts alters myocyte excitability and repolarization. *Biophys. J.* 97, 2179–2190. doi:10.1016/j.bpj.2009.07.054.

Maleckar, M. M., Greenstein, J. L., Trayanova, N. A., and Giles, W. R. (2008). Mathematical simulations of ligand-gated and cell-type specific effects on the action potential of human atrium. *Prog. Biophys. Mol. Biol.* 98, 161–170. doi:10.1016/j.pbiomolbio.2009.01.010.

Mamoshina, P., Bueno-Orovio, A., and Rodriguez, B. (2020). Dual Transcriptomic and Molecular Machine Learning Predicts all Major Clinical Forms of Drug Cardiotoxicity. *Front. Pharmacol.* 11, 639. doi:10.3389/fphar.2020.00639.

Margeta, J., Criminisi, A., Cabrera Lozoya, R., Lee, D. C., and Ayache, N. (2017). Fine-tuned convolutional neural nets for cardiac MRI acquisition plane recognition. *Comput. Methods Biomech. Biomed. Eng. Imaging Vis.* 5, 339–349. doi:10.1080/21681163.2015.1061448.

Marques, V. G., Rodrigo, M., Guillem, M. de la S., and Salinet, J. (2020). Characterization of atrial arrhythmias in body surface potential mapping: A computational study. *Comput. Biol. Med.* 127, 103904. doi:10.1016/j.compbiomed.2020.103904.

Marrouche, N. F., Greene, T., Dean, J. M., Kholmovski, E. G., Boer, L. M.,

Mansour, M., et al. (2021). Efficacy of LGE-MRI-Guided Fibrosis Ablation vs. Conventional Catheter Ablation of Atrial Fibrillation: The DECAAF II Trial: Study Design. *J. Cardiovasc. Electrophysiol.*, jce.14957. doi:10.1111/jce.14957.

Marrouche, N. F., Wilber, D., Hindricks, G., Jais, P., Akoum, N., Marchlinski, F., et al. (2014). Association of atrial tissue fibrosis identified by delayed enhancement MRI and atrial fibrillation catheter ablation: The DECAAF study. *JAMA - J. Am. Med. Assoc.* 311, 498–506. doi:10.1001/jama.2014.3.

McAllister, R. E., Noble, D., and Tsien, R. W. (1975). Reconstruction of the electrical activity of cardiac Purkinje fibres. *J. Physiol.* 251, 1–59. doi:10.1113/JPHYSIOL.1975.SP011080.

McAlpine, W. A. (1975). *Heart and Coronary Arteries*. 1st ed. Berlin, Heidelberg: Springer Berlin Heidelberg doi:10.1007/978-3-642-65983-6.

McDowell, K. S., Vadakkumpadan, F., Blake, R., Blauer, J., Plank, G., MacLeod, R. S., et al. (2012). Methodology for patient-specific modeling of atrial fibrosis as a substrate for atrial fibrillation. *J. Electrocardiol.* 45, 640–645. doi:10.1016/j.jelectrocard.2012.08.005.

McKay, M. D., Beckman, R. J., and Conover, W. J. (1979). A Comparison of Three Methods for Selecting Values of Input Variables in the Analysis of Output from a Computer Code. *Technometrics* 21, 239–245. doi:10.2307/1268522.

Meo, M., Pambrun, T., Derval, N., Dumas-Pomier, C., Puyo, S., Duchâteau, J., et al. (2018). Noninvasive assessment of atrial fibrillation complexity in relation to ablation characteristics and outcome. *Front. Physiol.* 9, 929. doi:10.3389/FPHYS.2018.00929/BIBTEX.

Mesquita, J., Ferreira, A. M., Cavaco, D., Moscoso Costa, F., Carmo, P., Marques, H., et al. (2018). Development and validation of a risk score for predicting atrial fibrillation recurrence after a first catheter ablation procedure - ATLAS score. *Europace* 20, f428–f435. doi:10.1093/EUROPACE/EUX265.

Milstein, M. L., Musa, H., Balbuena, D. P., Anumonwo, J. M. B., Auerbach, D. S., Furspan, P. B., et al. (2012). Dynamic reciprocity of sodium and potassium channel expression in a macromolecular complex controls cardiac excitability and arrhythmia. *Proc. Natl. Acad. Sci.* 109. doi:10.1073/PNAS.1109370109.

Mirams, G. R., Davies, M. R., Cui, Y., Kohl, P., and Noble, D. (2012). Application of cardiac electrophysiology simulations to pro- arrhythmic safety testing. doi:10.1111/j.1476-5381.2012.02020.x.

Mitchel, T. (1997). *Machine Learning*. McGraw Hill.

Moe, G. K., and Abildskov, J. A. (1959). Atrial fibrillation as a self-sustaining arrhythmia independent of focal discharge. *Am. Heart J.* 58, 59–70. doi:10.1016/0002-8703(59)90274-1.

Moe, G. K., Rheinboldt, W. C., and Abildskov, J. . (1964). A computer model of atrial fibrillation. *Am. Heart J.* 67, 200–220. doi:10.1016/0002-8703(64)90371-0.

Molero, R., Soler Torro, J. M., Martínez Alzamora, N., M. Climent, A., and

Guillem, M. S. (2021). Higher reproducibility of phase derived metrics from electrocardiographic imaging during atrial fibrillation in patients remaining in sinus rhythm after pulmonary vein isolation. *Comput. Biol. Med.* 139, 104934. doi:10.1016/J.COMPBIOMED.2021.104934.

Morin, D. P., Bernard, M. L., Madias, C., Rogers, P. A., Thihalolipavan, S., Mark, N. A., et al. (2016). The State of the Art: Atrial Fibrillation Epidemiology, Prevention, and Treatment. *Mayo Clin Proc*, 1778–1810. doi:10.1016/j.mayocp.2016.08.022.

Muffoletto, M., Qureshi, A., Zeidan, A., Muizniece, L., Fu, X., Zhao, J., et al. (2021). Toward Patient-Specific Prediction of Ablation Strategies for Atrial Fibrillation Using Deep Learning. *Front. Physiol.* 0, 717. doi:10.3389/FPHYS.2021.674106.

Musuamba, F. T., Skottheim Rusten, I., Lesage, R., Russo, G., Bursi, R., Emili, L., et al. (2021). Scientific and regulatory evaluation of mechanistic in silico drug and disease models in drug development: Building model credibility. *CPT Pharmacometrics Syst. Pharmacol.* 10, 804–825. doi:10.1002/psp4.12669.

Muszkiewicz, A., Britton, O. J., Gemmell, P., Passini, E., Sanchez, C., Zhou, X., et al. (2016). Variability in cardiac electrophysiology: Using experimentally-calibrated populations of models to move beyond the single virtual physiological human paradigm. *Prog. Biophys. Mol. Biol.* 120, 115–127. doi:10.1016/j.pbiomolbio.2015.12.002.

Narayan, S. M., Krummen, D. E., Clopton, P., Shivkumar, K., and Miller, J. M. (2013). Direct or coincidental elimination of stable rotors or focal sources may explain successful atrial fibrillation ablation: on-treatment analysis of the CONFIRM trial (Conventional ablation for AF with or without focal impulse and rotor modulation). *J. Am. Coll. Cardiol.* 62, 138–147. doi:10.1016/J.JACC.2013.03.021.

Narayan, S. M., Krummen, D. E., Shivkumar, K., Clopton, P., Rappel, W.-J., and Miller, J. M. (2012). Treatment of Atrial Fibrillation by the Ablation of Localized Sources. *J. Am. Coll. Cardiol.* 60, 628–636. doi:10.1016/j.jacc.2012.05.022.

Nattel, S., Burstein, B., and Dobrev, D. (2008). Atrial Remodeling and Atrial Fibrillation. *Circ. Arrhythmia Electrophysiol.* 1, 62–73. doi:10.1161/CIRCEP.107.754564.

Nattel, S., and Dobrev, D. (2012). The multidimensional role of calcium in atrial fibrillation pathophysiology: mechanistic insights and therapeutic opportunities. *Eur. Heart J.* 33, 1870–1877. doi:10.1093/EURHEARTJ/EHS079.

Nava, A. M. S. de la, Soto, N., López, J., Datino, T., Ávila, P., Gonzalez-Torrecilla, E., et al. (2021). B-PO02-023 ARTIFICIAL INTELLIGENCE PLATFORM FOR STRATIFICATION OF ATRIAL FIBRILLATION PRIOR TO ABLATION. *Hear. Rhythm* 18, S104. doi:10.1016/J.HRTHM.2021.06.280.

Nicholson Price, W. (2018). Big data and black-box medical algorithms. *Sci. Transl. Med.* 10. doi:10.1126/scitranslmed.aao5333.

Noble, D. (1962). A modification of the Hodgkin--Huxley equations applicable to Purkinje fibre action and pace-maker potentials. *J. Physiol.* 160, 317–

352. doi:10.1113/jphysiol.1962.sp006849.

Nogales Asensio, J. M., Moreno Sánchez, N., Doncel Vecino, L. J., Villar Mariscal, C., López-Mínguez, J. R., and Merchán Herrera, A. (2007). Torsade-de-pointes in a patient under flecainide treatment, an unusual case of proarrhythmicity. *Int. J. Cardiol.* 114, E65–E67. doi:10.1016/j.ijcard.2006.07.124.

Noujaim, S., Pandit, S., Berenfeld, O., Vikstrom, K., Cerrone, M., Mironov, S., et al. (2007). Up-regulation of the inward rectifier K+ current (I K1) in the mouse heart accelerates and stabilizes rotors. *J. Physiol.* 578, 315–326. doi:10.1113/JPHYSIOL.2006.121475.

Novig, S. J. R. and P. (1995). *Artificial Intelligence: A Modern Approach.* Prentince Hall, Engleworrd Cliffs.

Nygren, A., Fiset, C., Firek, L., Clark, J. W., Lindblad, D. S., Clark, R. B., et al. (1998). Mathematical Model of an Adult Human Atrial Cell. *Circ. Res.* 82, 63–81. doi:10.1161/01.RES.82.1.63.

Oral, H., Crawford, T., Frederick, M., Gadeela, N., Wimmer, A., Dey, S., et al. (2008). Inducibility of paroxysmal atrial fibrillation by isoproterenol and its relation to the mode of onset of atrial fibrillation. *J. Cardiovasc. Electrophysiol.* 19, 466–470. doi:10.1111/j.1540-8167.2007.01089.x.

Oster, H. S., Taccardi, B., Lux, R. L., Ershler, P. R., and Rudy, Y. (1997). Noninvasive Electrocardiographic Imaging. *Circulation* 96, 1012–1024. doi:10.1161/01.CIR.96.3.1012.

Palacio, L. C., Ugarte, J. P., Saiz, J., and Tobón, C. (2021). The effects of fibrotic cell type and its density on atrial fibrillation dynamics: An in silico study. *Cells* 10. doi:10.3390/CELLS10102769/S1.

Pandit, S., Zlochiver, S., Filgueiras-Rama, D., Mironov, S., Yamazaki, M., Ennis, S., et al. (2011). Targeting atrioventricular differences in ion channel properties for terminating acute atrial fibrillation in pigs. *Cardiovasc. Res.* 89, 843–851. doi:10.1093/CVR/CVQ359.

Pandit, S. V, Berenfeld, O., Anumonwo, J. M. B., Zaritski, R. M., Kneller, J., Nattel, S., et al. (2005). Ionic determinants of functional reentry in a 2-D model of human atrial cells during simulated chronic atrial fibrillation. *Biophys. J.* 88, 3806–3821. doi:10.1529/biophysj.105.060459.

Pandit, S. V, and Jalife, J. (2013). Rotors and the dynamics of cardiac fibrillation. *Circ. Res.* 112, 849–62. doi:10.1161/CIRCRESAHA.111.300158.

Park, J., Lee, S., and Jeon, M. (2009). Atrial fibrillation detection by heart rate variability in Poincare plot. *Biomed. Eng. Online* 8, 1–12. doi:10.1186/1475-925X-8-38.

Passini, E., Britton, O. J., Lu, H. R., Rohrbacher, J., Hermans, A. N., Gallacher, D. J., et al. (2017). Human In Silico Drug Trials Demonstrate Higher Accuracy than Animal Models in Predicting Clinical Pro-Arrhythmic Cardiotoxicity. *Front. Physiol.* 8, 668. doi:10.3389/fphys.2017.00668.

Patel, D., Stohlman, J., Dang, Q., Strauss, D. G., and Blinova, K. (2019). Assessment of Proarrhythmic Potential of Drugs in Optogenetically Paced Induced Pluripotent Stem Cell-Derived Cardiomyocytes. *Toxicol. Sci.* 170, 167–179. doi:10.1093/toxsci/kfz076.

Pedrón-Torrecilla, J., Rodrigo, M., Climent, A. M., Liberos, A., Pérez-David, E., Bermejo, J., et al. (2016). Noninvasive Estimation of Epicardial Dominant High-Frequency Regions During Atrial Fibrillation. *J. Cardiovasc. Electrophysiol.* 27, 435–442. doi:10.1111/JCE.12931.

Peirlinck, M., Costabal, F. S., Yao, J., Guccione, J. M., Tripathy, S., Wang, Y., et al. (2021). Precision medicine in human heart modeling: Perspectives, challenges, and opportunities. *Biomech. Model. Mechanobiol.* 20, 803. doi:10.1007/S10237-021-01421-Z.

Ponce-Balbuena, D., Guerrero-Serna, G., Valdivia, C. R., Caballero, R., Diez-Guerra, F. J., Jiménez-Vázquez, E. N., et al. (2018). Cardiac Kir2.1 and NaV1.5 Channels Traffic Together to the Sarcolemma to Control Excitability. *Circ. Res.* 122, 1501. doi:10.1161/CIRCRESAHA.117.311872.

Pourbabaee, B., Roshtkhari, M. J., and Khorasani, K. (2018). Deep Convolutional Neural Networks and Learning ECG Features for Screening Paroxysmal Atrial Fibrillation Patients. *IEEE Trans. Syst. Man, Cybern. Syst.* 48, 2095–2104. doi:10.1109/TSMC.2017.2705582.

Qureshi, W., Soliman, E. Z., Solomon, S. D., Alonso, A., Arking, D. E., Shah, A., et al. (2014). Risk factors for atrial fibrillation in patients with normal versus dilated left atrium (from the Atherosclerosis Risk in Communities Study). *Am. J. Cardiol.* 114, 1368–1372. doi:10.1016/j.amjcard.2014.07.073.

Rakisheva, A., Marketou, M., Klimenko, A., Troyanova-Shchutskaia, T., and Vardas, P. (2020). Hyperkalemia in heart failure: Foe or friend? *Clin. Cardiol.* 43, 666–675. doi:10.1002/clc.23392.

Ramirez, F. D., Birnie, D. H., Nair, G. M., Szczotka, A., Redpath, C. J., Sadek, M. M., et al. (2017). Efficacy and safety of driver-guided catheter ablation for atrial fibrillation: A systematic review and meta-analysis. *J. Cardiovasc. Electrophysiol.* 28, 1371–1378. doi:10.1111/JCE.13313.

Rappel, W.-J., Zaman, J. A. B., and Narayan, S. M. (2015). Mechanisms for the Termination of Atrial Fibrillation by Localized Ablation: Computational and Clinical Studies. *Circ. Arrhythm. Electrophysiol.* 8, 1325–33. doi:10.1161/CIRCEP.115.002956.

Rehorn, M. R., Koontz, J., Barnett, A. S., Black-Maier, E., Piccini, J. P., Loring, Z., et al. (2020). Noninvasive electrocardiographic mapping of ventricular tachycardia in a patient with a left ventricular assist device. *Hear. Case Reports* 6, 398–401. doi:10.1016/J.HRCR.2020.03.015.

Reumann, M., Bohnert, J., Seemann, G., Osswald, B., and Dossel, O. (2008). Preventive Ablation Strategies in a Biophysical Model of Atrial Fibrillation Based on Realistic Anatomical Data. *IEEE Trans. Biomed. Eng.* 55, 399–406. doi:10.1109/TBME.2007.912672.

Reychav, I., Zhu, L., McHaney, R., Zhang, D., Shacham, Y., and Arbel, Y. (2019). Real-time survival prediction in emergency situations with unbalanced cardiac patient data. *Health Technol. (Berl).* 9, 277–287. doi:10.1007/s12553-019-00307-6.

Rivera-Juárez, A., Hernández-Romero, I., Puertas, C., Zhang-Wang, S., Sánchez-Álamo, B., Martins, R., et al. (2019). Clinical Characteristics and Electrophysiological Mechanisms Underlying Brugada ECG in Patients

With Severe Hyperkalemia. *J. Am. Hear. Assoc. Cardiovasc. Cerebrovasc. Dis.* 8. doi:10.1161/JAHA.118.010115.

Rodrigo, M., Climent, A. M., Hernández-Romero, I., Liberos, A., Baykaner, T., Rogers, A. J., et al. (2020). Noninvasive Assessment of Complexity of Atrial Fibrillation: Correlation With Contact Mapping and Impact of Ablation. *Circ. Arrhythm. Electrophysiol.* 13, e007700. doi:10.1161/CIRCEP.119.007700.

Rodrigo, M., Climent, A. M., Liberos, A., Calvo, D., Fernández-Avilés, F., Berenfeld, O., et al. (2016). Identification of Dominant Excitation Patterns and Sources of Atrial Fibrillation by Causality Analysis. *Ann. Biomed. Eng.* 44, 2364–2376. doi:10.1007/s10439-015-1534-x.

Rodrigo, M., Climent, A. M., Liberos, A., Fernández-Aviles, F., Atienza, F., Guillem, M. S., et al. (2017). Minimal configuration of body surface potential mapping for discrimination of left versus right dominant frequencies during atrial fibrillation. *Pacing Clin. Electrophysiol.* 40, 940–946. doi:10.1111/PACE.13133.

Rodrigo, M., Climent, A. M., Liberos, A., Hernández-Romero, I., Arenal, Á., Bermejo, J., et al. (2018). Solving Inaccuracies in Anatomical Models for Electrocardiographic Inverse Problem Resolution by Maximizing Reconstruction Quality. *IEEE Trans. Med. Imaging* 37, 733–740. doi:10.1109/TMI.2017.2707413.

Rodrigo, M., Guillem, M. S., Climent, A. M., Pedrón-Torrecilla, J., Liberos, A., Millet, J., et al. (2014). Body surface localization of left and right atrial high-frequency rotors in atrial fibrillation patients: A clinical-computational study. *Hear. Rhythm* 11, 1584–1591. doi:10.1016/j.hrthm.2014.05.013.

Roney, C. H., Williams, S. E., Cochet, H., Mukherjee, R. K., O'neill, L., Sim, I., et al. Patient-specific simulations predict efficacy of ablation of interatrial connections for treatment of persistent atrial fibrillation. doi:10.1093/europace/euy232.

Rosenblueth, A., and Ramos, J. G. (1947). Studies on flutter and fibrillation. *Am. Heart J.* 33, 677–684. doi:10.1016/0002-8703(47)90084-7.

Rottner, L., Bellmann, B., Lin, T., Reissmann, B., Tönnis, T., Schleberger, R., et al. (2020). Catheter Ablation of Atrial Fibrillation: State of the Art and Future Perspectives. *Cardiol. Ther.*, 1–14. doi:10.1007/s40119-019-00158-2.

Sachetto Oliveira, R., Martins Rocha, B., Burgarelli, D., Meira, W., Constantinides, C., and Weber dos Santos, R. (2018). Performance evaluation of GPU parallelization, space-time adaptive algorithms, and their combination for simulating cardiac electrophysiology. *Int. j. numer. method. biomed. eng.* 34, e2913. doi:10.1002/cnm.2913.

Salinet, J., Molero, R., Schlindwein, F. S., Karel, J., Rodrigo, M., Rojo-Álvarez, J. L., et al. (2021). Electrocardiographic Imaging for Atrial Fibrillation: A Perspective From Computer Models and Animal Experiments to Clinical Value. *Front. Physiol.* 12. doi:10.3389/fphys.2021.653013.

Sampedro-Gómez, J., Dorado-Díaz, P. I., Vicente-Palacios, V., Sánchez-Puente, A., Jiménez-Navarro, M., San Roman, J. A., et al. (2020). Machine Learning to Predict Stent Restenosis Based on Daily Demographic, Clinical, and Angiographic Characteristics. *Can. J. Cardiol.*

36, 1624–1632. doi:10.1016/j.cjca.2020.01.027.

Sánchez, C., Bueno-Orovio, A., Wettwer, E., Loose, S., Simon, J., Ravens, U., et al. (2014). Inter-subject variability in human atrial action potential in sinus rhythm versus chronic atrial fibrillation. *PLoS One* 9. doi:10.1371/journal.pone.0105897.

Sanchez de la Nava, A. ., Climent, A., Hernandez, I., Lopez, J., Bermejo, J., Arenal, A., et al. (2020). Atrial Fibrillation Complexity Score Predicts Patient Outcome after Pulmonary Vein Ablation. in *Heart Rhythm* (Heart Rhythm), Suppl (S1-S762): D-PO01-169.

Sanchez De La Nava, A. M., Arenal, Á., Fernández-Avilés, F., and Atienza, F. (1AD). Artificial Intelligence-Driven Algorithm for Drug Effect Prediction on Atrial Fibrillation: An In Silico Population of Models Approach. *Front. Physiol.* 0, 2079. doi:10.3389/FPHYS.2021.768468.

Sánchez de la Nava, A. M., Atienza, F., Bermejo, J., and Fernández-Avilés, F. (2021). Artificial Intelligence for a Personalized Diagnosis and Treatment of Atrial Fibrillation. *Am. J. Physiol. Circ. Physiol.* doi:10.1152/ajpheart.00764.2020.

Sánchez, J., Trenor, B., Saiz, J., Dössel, O., and Loewe, A. (2021). Fibrotic Remodeling during Persistent Atrial Fibrillation: In Silico Investigation of the Role of Calcium for Human Atrial Myofibroblast Electrophysiology. *Cells* 10. doi:10.3390/CELLS10112852.

Sanz-García, A., Cecconi, A., Vera, A., Camarasaltas, J. M., Alfonso, F., Ortega, G. J., et al. (2021). Electrocardiographic biomarkers to predict atrial fibrillation in sinus rhythm electrocardiograms. *Heart*. doi:10.1136/HEARTJNL-2021-319120.

Scherf, D., Romano, F. J., and Terranova, R. (1948). Experimental studies on auricular flutter and auricular fibrillation. *Am. Heart J.* 36, 241–251. doi:10.1016/0002-8703(48)90403-7.

Schotten, U. (2002). Atrial fibrillation-induced atrial contractile dysfunction: a tachycardiomyopathy of a different sort. *Cardiovasc. Res.* 53, 192–201. doi:10.1016/S0008-6363(01)00453-9.

Schotten, U., Ausma, J., Stellbrink, C., Sabatschus, I., Vogel, M., Frechen, D., et al. (2001). Cellular Mechanisms of Depressed Atrial Contractility in Patients With Chronic Atrial Fibrillation. *Circulation* 103, 691–698. doi:10.1161/01.CIR.103.5.691.

Seitz, J., Bars, C., Théodore, G., Beurtheret, S., Lellouche, N., Bremondy, M., et al. (2017). Wholly Patient-tailored Ablation of Atrial Fibrillation Guided by Spatio-Temporal Dispersion of Electrograms in the Absence of Pulmonary Veins Isolation. *J. Am. Coll. Cardiol.* 69, 303. doi:10.1016/J.JACC.2016.10.065.

Shao, M., Bin, G., Wu, S., Bin, G., Huang, J., and Zhou, Z. (2018). Detection of atrial fibrillation from ECG recordings using decision tree ensemble with multi-level features. *Physiol. Meas.* 39. doi:10.1088/1361-6579/aadf48.

Simon, A., Liberos, A., Hernandez-Romero, I., Bueno Orovio, A., Rodrigo, M., Guillem S�nchez, M. de la S., et al. (2017). Electrophysiological Parameters in the Electrical Propagation During Atrial Fibrillation: a Population of Models Study. 1–4. doi:10.22489/CinC.2017.018-358.

References

Siontis, K. C., and Friedman, P. A. (2021). The Role of Artificial Intelligence in Arrhythmia Monitoring. *Card. Electrophysiol. Clin.* 13, 543–554. doi:10.1016/j.ccep.2021.04.011.

Skasa, M., Jüngling, E., Picht, E., Schöndube, F., and Lückhoff, A. (2001). L-type calcium currents in atrial myocytes from patients with persistent and non-persistent atrial fibrillation. *Basic Res. Cardiol.* 96, 151–159. doi:10.1007/s003950170065.

Skibsbye, L., Jespersen, T., Christ, T., Maleckar, M. M., van den Brink, J., Tavi, P., et al. (2016). Refractoriness in human atria: Time and voltage dependence of sodium channel availability. *J. Mol. Cell. Cardiol.* 101, 26–34. doi:10.1016/j.yjmcc.2016.10.009.

Skogestad, J., and Aronsen, J. M. (2018). Hypokalemia-induced arrhythmias and heart failure: New insights and implications for therapy. *Front. Physiol.* 9, 1500. doi:10.3389/fphys.2018.01500.

Stockbridge, N. CIPA - Comprehensive In Vitro Proarrhythmia Assay. Available at: https://www.ilsiextra.org/hesi/science/cardiac/cipa/SitePages/Home.aspx .

Tarakji, K. G., Silva, J., Chen, L. Y., Turakhia, M. P., Perez, M., Attia, Z. I., et al. (2020). Digital Health and the Care of the Patient With Arrhythmia: What Every Electrophysiologist Needs to Know. *Circ. Arrhythm. Electrophysiol.* 13, e007953. doi:10.1161/CIRCEP.120.007953.

ten Tusscher, K. H. W. J., Noble, D., Noble, P. J., and Panfilov, A. V. (2004). A model for human ventricular tissue. *Am. J. Physiol. Circ. Physiol.* 286, H1573–H1589. doi:10.1152/ajpheart.00794.2003.

Tenti, E., Simonetti, G., Bochicchio, M. T., and Martinelli, G. (2018). Main changes in European Clinical Trials Regulation (No 536/2014). *Contemp. Clin. Trials Commun.* 11, 99. doi:10.1016/J.CONCTC.2018.05.014.

Thrun, S., and Pratt, L. (1998). *Learning to Learn*. Springer US.

Tkachenko, R., Doroshenko, A., Izonin, I., Tsymbal, Y., and Havrysh, B. (2019). Imbalance Data Classification via Neural-Like Structures of Geometric Transformations Model: Local and Global Approaches BT - Advances in Computer Science for Engineering and Education. in *Advances in Intelligent Systems and Computing*, eds. Z. Hu, S. Petoukhov, I. Dychka, and M. He (Cham: Springer International Publishing), 112–122. doi:10.1007/978-3-319-91008-6_12.

Tobón, C., Cardona, K., Rodríguez, J., Hornero, F., Ferrero, J., and Sáiz, J. (2010). A biophysical model of atrial fibrillation to simulate the Maze III ablation pattern. in *Computing in Cardiology*.

Trayanova, N. (2006). Defibrillation of the heart: insights into mechanisms from modelling studies. *Exp. Physiol.* 91, 323–337. doi:10.1113/expphysiol.2005.030973.

Tsai, C.-F., Tai, C.-T., Hsieh, M.-H., Lin, W.-S., Yu, W.-C., Ueng, K.-C., et al. (2000). Initiation of Atrial Fibrillation by Ectopic Beats Originating From the Superior Vena Cava. *Circulation* 102, 67–74. doi:10.1161/01.CIR.102.1.67.

Umscheid, C. A., Margolis, D. J., and Grossman, C. E. (2011). Key Concepts

of Clinical Trials: A Narrative Review. *Postgrad. Med.* 123, 194–204. doi:10.3810/pgm.2011.09.2475.

van Dam, P. M., and van Oosterom, A. (2003). Atrial excitation assuming uniform propagation. *J. Cardiovasc. Electrophysiol.* 14, S166-71. doi:10.1046/j.1540.8167.90307.x.

Varela, M., Bisbal, F., Zacur, E., Berruezo, A., Aslanidi, O. V., Mont, L., et al. (2017). Novel Computational Analysis of Left Atrial Anatomy Improves Prediction of Atrial Fibrillation Recurrence after Ablation. *Front. Physiol.* 0, 68. doi:10.3389/FPHYS.2017.00068.

Varela, M., Colman, M. A., Hancox, J. C., and Aslanidi, O. V. (2016). Atrial Heterogeneity Generates Re-entrant Substrate during Atrial Fibrillation and Anti-arrhythmic Drug Action: Mechanistic Insights from Canine Atrial Models. *PLOS Comput. Biol.* 12, e1005245. doi:10.1371/JOURNAL.PCBI.1005245.

Venkatesan, C., Karthigaikumar, P., and Varatharajan, R. (2018). A novel LMS algorithm for ECG signal preprocessing and KNN classifier based abnormality detection. *Multimed. Tools Appl.* 77, 10365–10374. doi:10.1007/s11042-018-5762-6.

Vesal, S., Ravikumar, N., and Maier, A. (2019). Dilated Convolutions in Neural Networks for Left Atrial Segmentation in 3D Gadolinium Enhanced-MRI. in *Lecture Notes in Computer Science (including subseries Lecture Notes in Artificial Intelligence and Lecture Notes in Bioinformatics)* (Springer Verlag), 319–328. doi:10.1007/978-3-030-12029-0_35.

Vescovo, G., Jones, S. M., Harding, S. E., and Poole-Wilson, P. A. (1989). Isoproterenol sensitivity of isolated cardiac myocytes from rats with monocrotaline-induced right-sided hypertrophy and heart failure. *J. Mol. Cell. Cardiol.* 21, 1047–1061. doi:10.1016/0022-2828(89)90803-1.

Vicente, J., Johannesen, L., Hosseini, M., Mason, J. W., Sager, P. T., Pueyo, E., et al. (2016). Electrocardiographic Biomarkers for Detection of Drug-Induced Late Sodium Current Block. *PLoS One* 11. doi:10.1371/JOURNAL.PONE.0163619.

Vicente, J., Zusterzeel, R., Johannesen, L., Ochoa-Jimenez, R., Mason, J. W., Sanabria, C., et al. (2019). Assessment of Multi-Ion Channel Block in a Phase I Randomized Study Design: Results of the CiPA Phase I ECG Biomarker Validation Study. *Clin. Pharmacol. Ther.* doi:10.1002/cpt.1303.

Vigmond, E., Vadakkumpadan, F., Gurev, V., Arevalo, H., Deo, M., Plank, G., et al. (2009). Towards predictive modelling of the electrophysiology of the heart. *Exp. Physiol.* 94, 563–577. doi:10.1113/expphysiol.2008.044073.

Virag, N., Jacquemet, V., Henriquez, C. S., Zozor, S., Blanc, O., Vesin, J.-M., et al. (2002). Study of atrial arrhythmias in a computer model based on magnetic resonance images of human atria. *Chaos An Interdiscip. J. Nonlinear Sci.* 12, 754–763. doi:10.1063/1.1483935.

Walters, T. E., and Kalman, J. M. (2015). Human Persistent Atrial Fibrillation Is Maintained by Rotors. *Circ. Arrhythmia Electrophysiol.* 8, 517–519. doi:10.1161/CIRCEP.115.003089.

Wasserlauf, J., You, C., Patel, R., Valys, A., Albert, D., and Passman, R. (2019). Smartwatch Performance for the Detection and Quantification of

Atrial Fibrillation. *Circ. Arrhythmia Electrophysiol.* 12. doi:10.1161/CIRCEP.118.006834.

Wellner, M., Berenfeld, O., Jalife, J., and Pertsov, A. M. (2002). Minimal principle for rotor filaments. *Proc. Natl. Acad. Sci. U. S. A.* 99, 8015–8. doi:10.1073/pnas.112026199.

Wettwer, E., Christ, T., Endig, S., Rozmaritsa, N., Matschke, K., Lynch, J. J., et al. (2013). The new antiarrhythmic drug vernakalant: ex vivo study of human atrial tissue from sinus rhythm and chronic atrial fibrillation. *Cardiovasc. Res.* 98, 145–154. doi:10.1093/CVR/CVT006.

Winkle, R. A., Julian, †, Jarman, W. E., Mead, R. H., Engel, G., Kong, M. H., et al. (2016). Predicting atrial fibrillation ablation outcome: The CAAP-AF score. 13, 2119–2125. Available at: https://pubmed.ncbi.nlm.nih.gov/27435586/ [Accessed April 13, 2020].

Winters, J., Zeemering, S., Isaacs, A., Casadei, B., Fabritz, L., Guasch, E., et al. (2021). Female sex, atrial fibrillation, and heart failure, but not ageing, are associated with endomysial fibrosis in atrial myocardium: results from the CATCH ME consortium. *EP Eur.* 23. doi:10.1093/EUROPACE/EUAB116.554.

Workman, A. (2001). The contribution of ionic currents to changes in refractoriness of human atrial myocytes associated with chronic atrial fibrillation. *Cardiovasc. Res.* 52, 226–235. doi:10.1016/S0008-6363(01)00380-7.

Xia, Y., Wulan, N., Wang, K., and Zhang, H. (2018). Detecting atrial fibrillation by deep convolutional neural networks. *Comput. Biol. Med.* 93, 84–92. doi:10.1016/j.compbiomed.2017.12.007.

Xiong, Z., Nalar, A., Jamart, K., Stiles, M. K. ., Fedorov, V. V., and Zhao, J. (2020). Fully Automatic 3D Bi-Atria Segmentation from Late Gadolinium-Enhanced MRIs Using Double Convolutional Neural Networks. in *Lecture Notes in Computer Science (including subseries Lecture Notes in Artificial Intelligence and Lecture Notes in Bioinformatics)* (Springer), 63–71. doi:10.1007/978-3-030-39074-7_7.

Xiong, Z., Nash, M. P., Cheng, E., Fedorov, V. V, Stiles, M. K., and Zhao, J. (2018). ECG signal classification for the detection of cardiac arrhythmias using a convolutional recurrent neural network. *Physiol. Meas.* 39, 094006. doi:10.1088/1361-6579/aad9ed.

Yamazaki, M., Vaquero, L. M., Hou, L., Campbell, K., Zlochiver, S., Klos, M., et al. (2009). Mechanisms of stretch-induced atrial fibrillation in the presence and the absence of adrenocholinergic stimulation: Interplay between rotors and focal discharges. *Hear. Rhythm* 6, 1009–1017. doi:10.1016/j.hrthm.2009.03.029.

Yan, L., Jiang, T., Yang, X., and Xu, M. (2018). Spontaneous conversion of atrial fibrillation caused by severe hyperkalemia: A case report. *Medicine (Baltimore).* 97. doi:10.1097/MD.0000000000010442.

Yang, G., Zhuang, X., Khan, H., Haldar, S., Nyktari, E., Ye, X., et al. (2017). Segmenting Atrial Fibrosis from Late Gadolinium-Enhanced Cardiac MRI by Deep-Learned Features with Stacked Sparse Auto-Encoders BT - Medical Image Understanding and Analysis. in *Communications in Computer and Information Science*, eds. M. Valdés Hernández and V.

González-Castro (Cham: Springer International Publishing), 195–206. doi:10.1007/978-3-319-60964-5_17.

Yang, P. C., Demarco, K. R., Aghasafari, P., Jeng, M. T., Dawson, J. R. D., Bekker, S., et al. (2020). A Computational Pipeline to Predict Cardiotoxicity: From the Atom to the Rhythm. 126, 947–964. doi:10.1161/CIRCRESAHA.119.316404.

Yıldırım, Ö., Pławiak, P., Tan, R. S., and Acharya, U. R. (2018). Arrhythmia detection using deep convolutional neural network with long duration ECG signals. *Comput. Biol. Med.* 102, 411–420. doi:10.1016/j.compbiomed.2018.09.009.

Yushkevich, P. A., Piven, J., Hazlett, H. C., Smith, R. G., Ho, S., Gee, J. C., et al. (2006). User-guided 3D active contour segmentation of anatomical structures: Significantly improved efficiency and reliability. *Neuroimage* 31, 1116–1128. doi:10.1016/j.neuroimage.2006.01.015.

Zaman, J. A. B., Rogers, A. J., and Narayan, S. M. (2017). Rotational Drivers in Atrial Fibrillation. *Circ. Arrhythmia Electrophysiol.* 10, 6022. doi:10.1161/CIRCEP.117.006022.

Zolotarev, A. M., Hansen, B. J., Ivanova, E. A., Helfrich, K. M., Li, N., Janssen, P. M. L., et al. (2020). *Optical Mapping-Validated Machine Learning Improves Atrial Fibrillation Driver Detection by Multi-Electrode Mapping*. doi:10.1161/circep.119.008249.

Zou, R., Kneller, J., Leon, L. J., and Nattel, S. (2005). Substrate size as a determinant of fibrillatory activity maintenance in a mathematical model of canine atrium. *Am. J. Physiol. Circ. Physiol.* 289, H1002–H1012. doi:10.1152/ajpheart.00252.2005.